personal buildup for

Force Motors Limited Library

MTZ worldwide 11/2012
http://www.mtz-worldwide.com

content:

www.MTZonline.com

MTZ WORLDWIDE

11 November 2012 | Volume 73

VEHICLE Integration of a Range Extender Engine

MODULAR Charge Air Cooling for Combustion Engines

PRESSURE Pulsation Dampers for Injectors

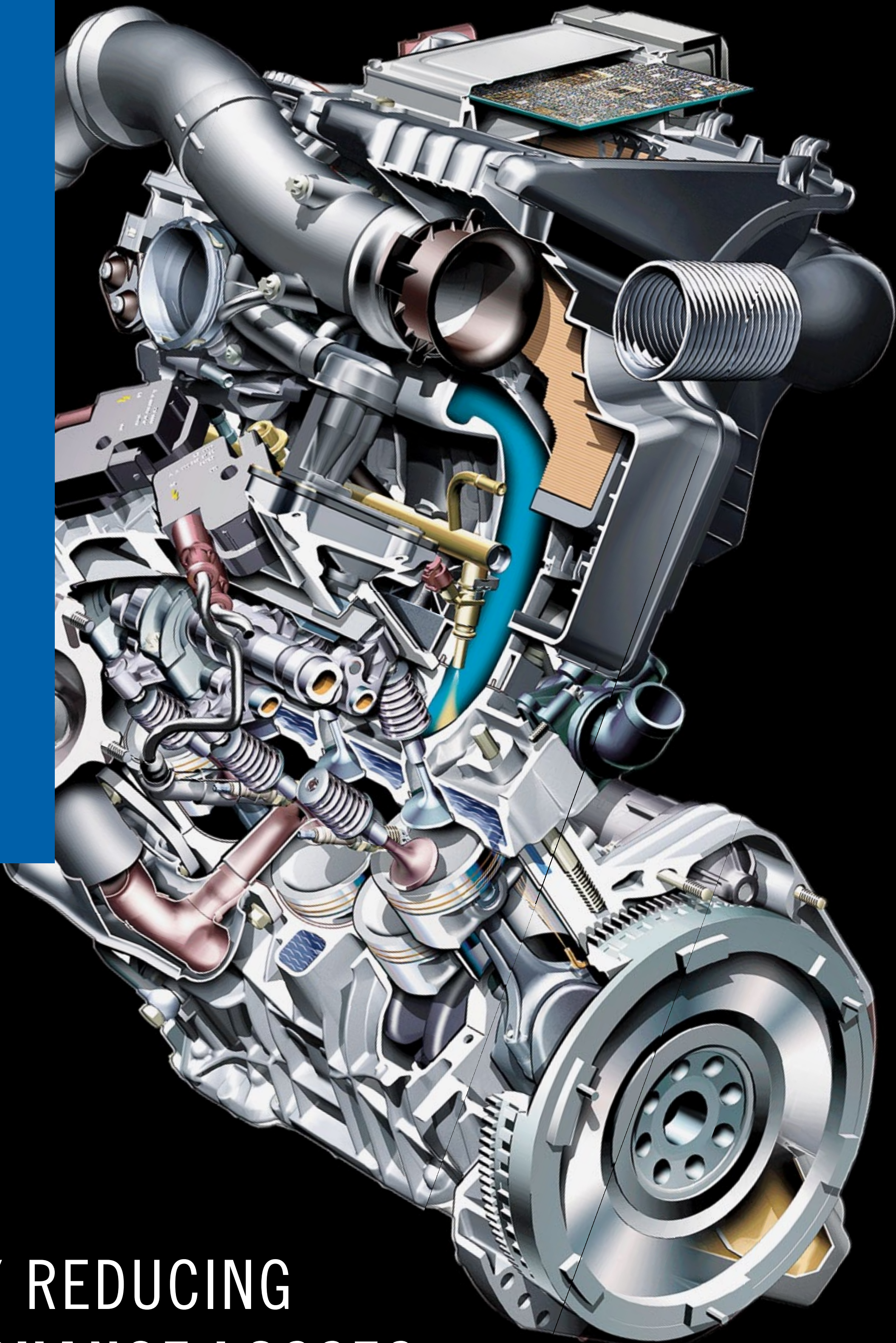

EFFECTIVELY REDUCING CHARGE EXCHANGE LOSSES

Springer Vieweg

COVER STORY

EFFECTIVELY REDUCING CHARGE EXCHANGE LOSSES

4, 10 I The charge exchange process has a decisive influence on the efficiency and therefore the fuel consumption and CO_2 emissions of an internal combustion engine. Throttling and flow losses in particular can take on considerable dimensions, which means that a system-wide consideration of all components involved in the charge exchange process will become even more important in the future than it already is today. MTZ takes a look at those system developments that can help to further reduce charge exchange work. Ricardo presents a new jet-guided direct fuel injection process that allows spark-ignition engines to run almost completely without throttling, thus exploiting the benefits of lean combustion over an unusually large area of the engine map. Schaeffler and IAV have examined the potentials of cylinder-selective multiple valve lift changeover for a typical turbocharged four-cylinder gasoline engine. They give an insight into the findings gained from engine simulation models.

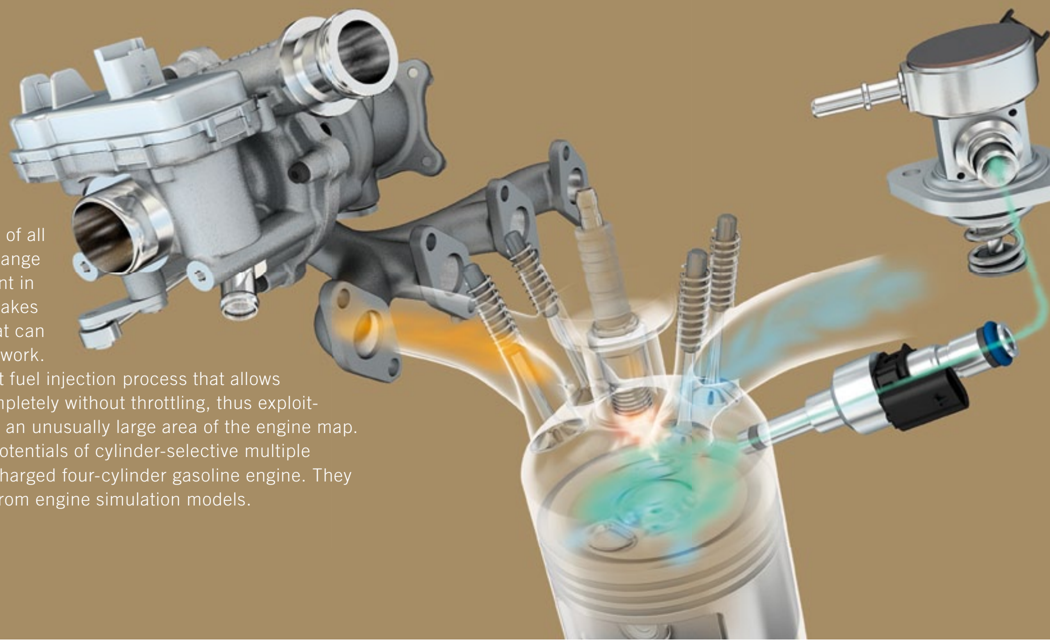

COVER FIGURE © Daimler **FIGURE ABOVE** © Continental

QUALITY

Dear Reader,

Almost every week, I receive enquiries from creative inventors wishing to publish an article in MTZ about a new engine concept. Many of them have invested a huge amount of time, energy and money in their invention, which they claim will revolutionise engine technology. However, these exotic creations usually exist only as graphics or colourful presentations or, at best, as a prototype engine made from old engine components that has managed to shown signs of life in the form of the odd detonation. And that is exactly the problem: MTZ has an obligation to you, its readers. Over a period of 73 years, we have earned a worldwide reputation as a technical-scientific journal – a reputation that we strive to maintain. Therefore, when it comes to new engine concepts in particular, we make every effort to ensure that there are not only simulation results available but also findings from test bench tests on real engines. These tests must at least validate power output, fuel consumption and emissions figures, and if necessary be supplemented by further measurements, such as NVH characteristics. Above all, it is about serious evidence of the potential of a new engine concept, and not about technocracy for its own sake. I am convinced that this proven practice is a key component of the high quality of the articles published in MTZ.

What is more, for many years we have had a transparent and fair procedure for selecting the articles for our family of specialist magazines. On the basis of an abstract, we decide in an editorial conference whether a proposed article is suitable for MTZ. In addition to the innovative value and expected technical depth of the article, other criteria include its relevance to current issues being debated in our industry. These assessment criteria serve as a measure for all article proposals, no matter whether they come from the above-mentioned amateur inventors or from the R&D department of a major company.

Our mission is to provide serious and substantial engineering documentation that is far remote from advertising-based marketing journalism. Would you like to support us in this undertaking? There are bound to be some new developments in your company that are worth being published in MTZ. I would therefore like to invite you to submit proposals for articles in the form of a short abstract. Please send your proposals or let me know your opinion on quality journalism in an e-mail to Richard.Backhaus@springer.com.

With best regards

Richard Backhaus

RICHARD BACKHAUS,
Vice-Editor in Chief
Wiesbaden, 10 September 2012

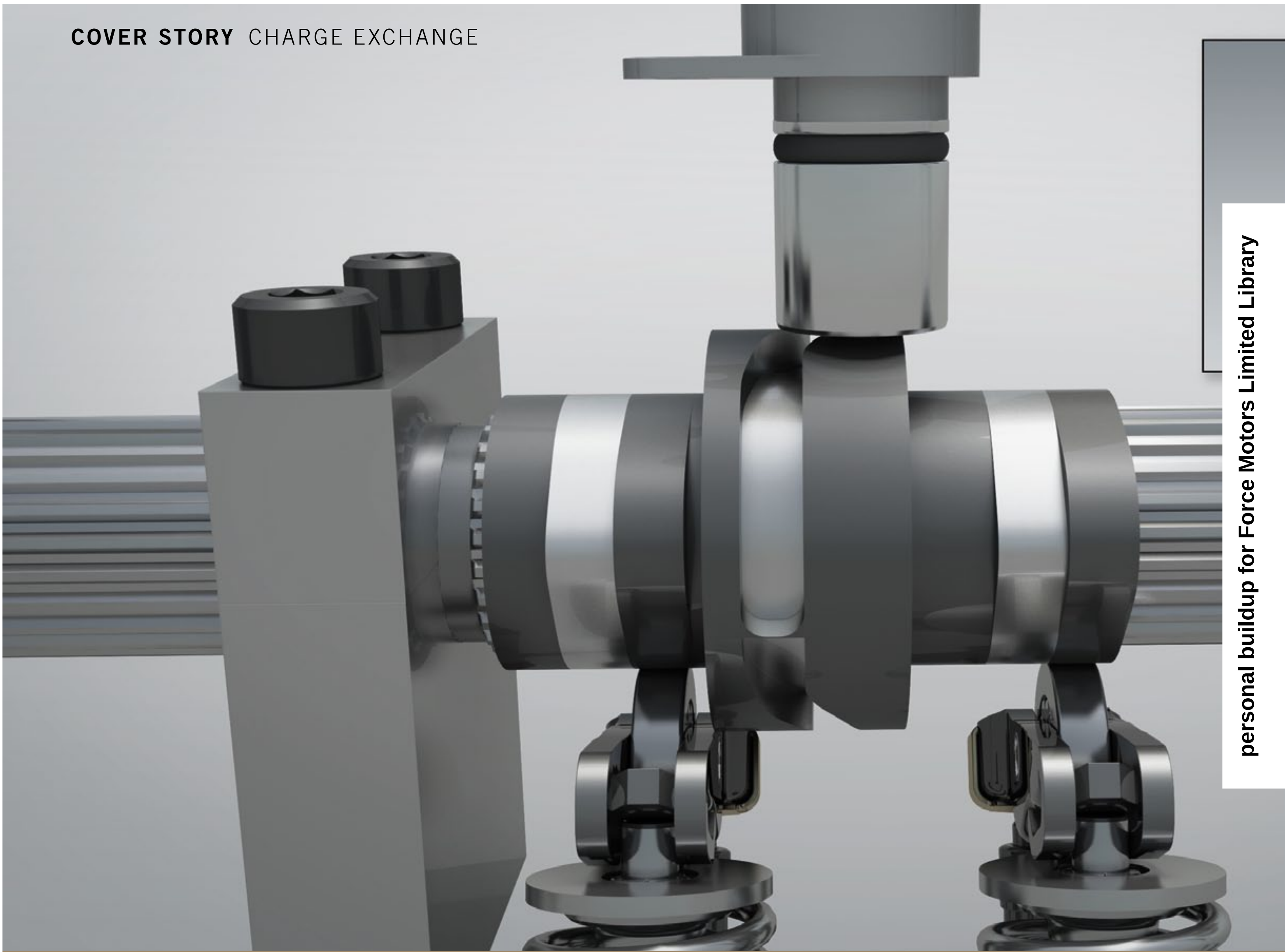

SELECTIVE VALVE-LIFTING IN GASOLINE ENGINES

In gasoline engines, the combination of flexible valve lift design and downsizing promises significant reductions in fuel consumption. In a joint project, Schaeffler and IAV have examined the potentials of cylinder-selective multiple valve lift changeover for a typical four-cylinder turbocharged gasoline engine on the basis of engine simulation models.

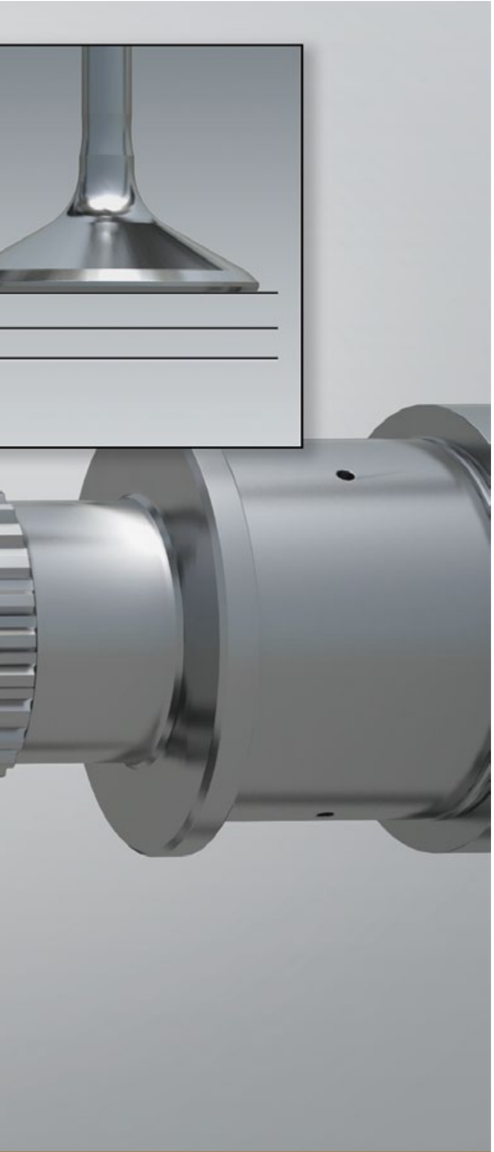

AUTHORS

PROF. DR.-ING. KURT KIRSTEN
is Senior Vice President R&D in the Business Division Engine Systems at the Schaeffler Technologies AG & Co. KG in Herzogenaurach (Germany).

DR.-ING. CHRISTOPH BRANDS
is Director Advanced Engineering Analysis R&D in the Business Division Engine Systems at the Schaeffler Technologies AG & Co. KG in Herzogenaurach (Germany).

MATTHIAS KRATZSCH
is Senior Vice President Gasoline Engine Development at the IAV GmbH Ingenieurgesellschaft Auto und Verkehr in Berlin (Germany).

MICHAEL GÜNTHER
is Head of the Department Combustion/Thermodynamics SI Engines at the IAV GmbH Ingenieurgesellschaft Auto und Verkehr in Chemnitz (Germany).

MOTIVATION

In the light of climate change and the resultant demand for far lower CO_2 emissions, optimising management of the gasoline engine process to improve fuel economy continues to play an important part. Exploiting appreciable potential for reducing CO_2 significantly increases the demands on gas exchange components. Multiple valve-lift switching permits the utilisation of different potentials in various stages on a cylinder-selective basis. The combined use of up to three discrete valve lifts permits significant fuel savings in the part-load range. For the gasoline engine, the options for flexibly configuring valve lift combined with downsizing can be expected to produce fuel reductions of up to 20 % at map level and up to 10 % in the NEDC. In a joint project between Schaeffler and IAV, the potentials of cylinder-selective multiple valve-lift switching for a typical four-cylinder turbocharged gasoline engine have been worked out on the basis of test-bench-calibrated engine simulation models.

VARIABLE VALVE TIMING – REALISED SYSTEMS

Examples of systems with variable valve lift in gasoline engines can be divided into fully and partially variable systems or systems that can be switched in stages. On the intake side, fully variable systems (Valvetronic [1], Multi-Air [2]) reduce gas-exchange losses by selecting the optimum valve event for the operating point whereas the partially variable systems, e.g. two-point switching (Vario-Cam Plus [3], Audi Valvelift system [4]), represent a compromise configuration in relation to valve lift and, with this, to reducing throttle losses. Schaeffler offers an appropriate system solution with key components and actuators for most valvetrain types, ❶:

: switchable tappet (coaxial arrangement of two tappets with a locking mechanism)
: switchable pivot element (conventional element with the capability of a lost stroke movement in the pivot element)
: switchable roller finger follower (electro-hydraulically actuated cam follower for accomplishing cam profile switching, valve and cylinder deactivation)

	Switchable pivot element	Switchable tappet	Switchable roller finger follower	Cam shifting system	Uni Air
Electro-hydraulic actuated					
Electro-mechanical actuated (enlarged temperature range)					
Valve Deactivation (one valve per cylinder)	✓	✓	✓	✓	✓
Cylinder deactivation (all valves per cylinder)	✓	✓	✓	✓	✓
Internal EGR (retain)	✗	✓	✓	✓	✓
Internal EGR (re-breath)	✗	✗	✓	✓	✓
Crossing of valve events	✗	✗	✗	✓	✓
Two-step	✗	✓	✓	✓	✓
Three-step	✗	✗	✗	✓	✓
Multi lift	✗	✗	✗	✗	✓

❶ Possibilities of realisation with INA switching elements

: Schaeffler cam shifting system (flexible and future-proof solution for realising various thermodynamic concepts in the valvetrain).

SIMULATION AND OPTIMISATION OF MULTIPLE VALVE-LIFT SWITCHING

Evaluating the potentials of complex valvetrain strategies demands extended model-based approaches in simulation, ❷. Beside the dethrottling potentials, simulating the engine process in particular involves realistically simulating the effects on combustion in the model. Given the large number of combinations, heat release is predicted using a quasi-dimensional combustion model. This provides the basis for efficiently evaluating changed operating conditions, such as engine speed, load, residual-gas content, air-fuel ratio and changes in charge motion. An Arrhenius approach was applied for evaluating changes in knock tendency and resultant centre of heat release (COHR). Allowance was made for mechanical losses using a physically based approach to Fischer. This made it possible to include the geometry-related variables influencing friction (influence of the cam drive) of the valvetrain strategy under study.

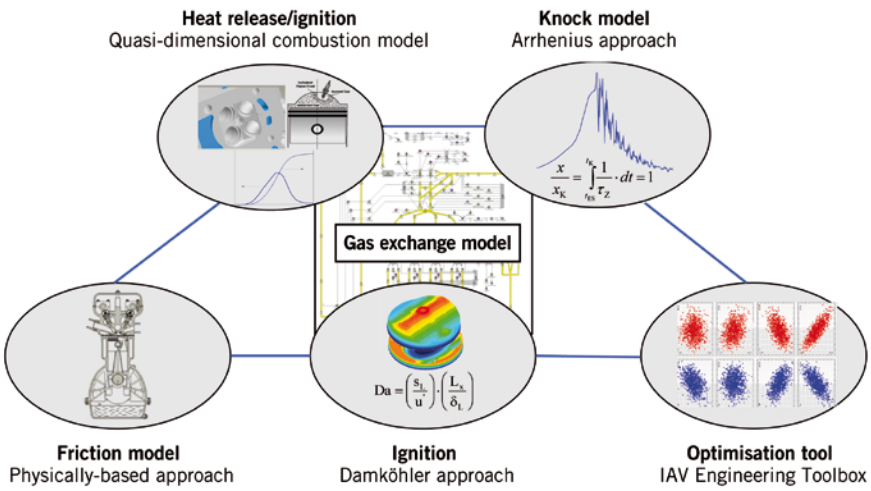

❷ Prediction models and optimisation tool

The parameters for optimising fuel consumption were in each case determined at steady-state map points produced from the frequency distribution of the engine/vehicle combination in the particular driving cycle. Supported by analogous modelling, stochastic optimisation methods were used for optimising valve-lift and timing configuration for a large number of versions in the relevant map range. Final evaluation of the different gas-exchange strategies in the engine/vehicle combination was carried out in the various driving cycles using overall-vehicle simulation.

VALVE-LIFT SWITCHING VARIANTS

The following possible combinations were examined:

: two-point valve-lift switching for all cylinders
: three-point valve-lift switching for all cylinders
: cylinder deactivation in combination with two-point valve-lift switching (two-point cylinder-selective)
: cylinder deactivation in combination with three-point valve-lift switching (three-point cylinder-selective).

TWO-POINT/THREE-POINT VALVE-LIFT SWITCHING FOR ALL CYLINDERS

The most frequently used map points depend on vehicle type and associated transmission stepping. As shown in ❸, a high share of low-load points is produced in the NEDC. To configure the best possible partial lift, a compromise cam is determined after optimising the steady-state map points on the basis of frequency distribution in the driving cycle. Timing was selected in a way that produces the maximum possible residual-gas content for all versions. The loss of charge motion or turbulence brought about by reducing valve lift and early intake closure were counteracted using appropriate measures that made it possible to leave a residual-gas content of 25 % while maintaining the engine smoothnesss demanded. As such, it was possible to verify the potentials shown in addition to the savings already familiar from valve overlap. Optimum valve lift resulted in a potential fuel saving of 5.7 % in the journey profile of the NEDC, ③.

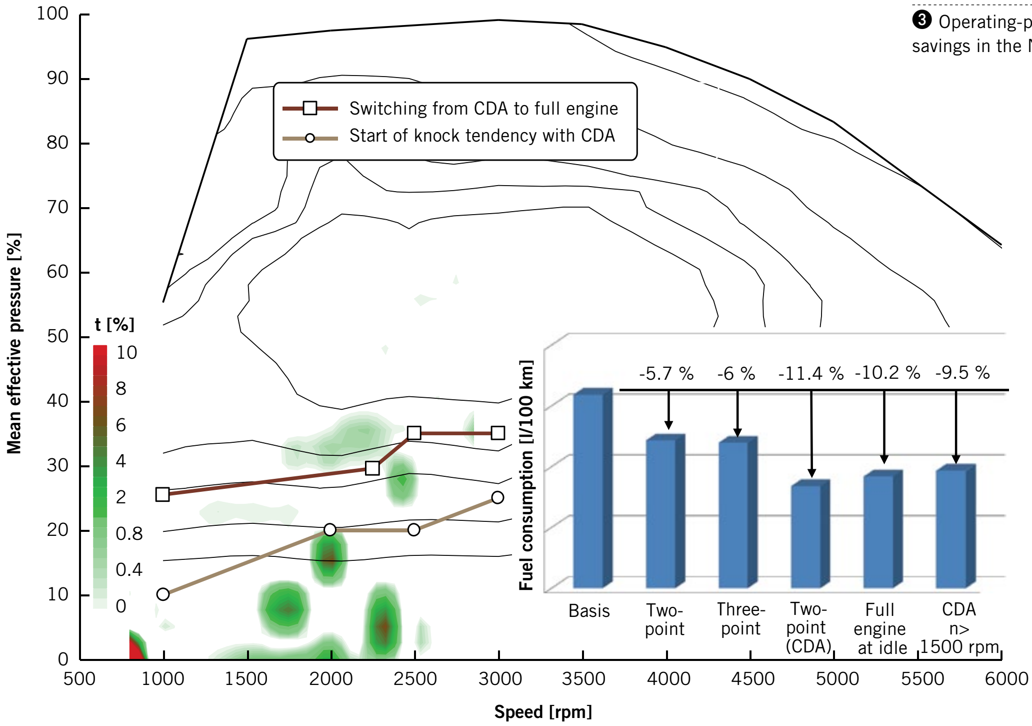

❸ Operating-point frequencies and potential fuel savings in the NEDC (CDA: cylinder deactivation)

Evaluating three-point valve-lift switching for all cylinders requires two compromise cams for the NEDC-relevant map. The resultant further improvement in fuel economy of 0.3 % was relatively low. On the one hand, the compression losses limit any further reduction in valve lift at very low loads. On the other, the potentials for further dethrottling an already downsized engine in the mid-load range are innately only slight.

CYLINDER DEACTIVATION

Using two-point valve-lift switching simultaneously on the intake and exhaust side permits cylinder deactivation. The maximum possible load at which the fired cylinders can be operated with optimum efficiency ($\alpha_{Q50}=8$ °CA ATDC) in cylinder deactivation (CDA) mode is presented in ③. As load rises, the centre of heat release must be retarded on account of knock. The correct time to switch over to full-engine operation occurs precisely at the point where the drawback of late COHR erodes the better level of efficiency from dethrottling in two-cylinder mode.

When applied to all operating points of the NEDC, cylinder deactivation produces benefits in consumption per unit of distance of up to 11.4 %. CDA in the four-cylinder engine, however, produces a deterioration in comfort at idle and in the low-speed range. Depending on concept, this makes full-engine operation necessary in this range which reduces the usable CDA potential, ③. Depending on the quality with which the switching processes are calibrated, the remaining potential for improving fuel economy may continue to fall.

CYLINDER-SELECTIVE MULTIPLE VALVE-LIFT SWITCHING

Cylinder-selective multiple valve-lift switching demands that the cams be configured on a cylinder-specific basis for each two cylinder pairs in different map ranges. The permanently fired cylinders require two-point switching (partial lift/full lift) and the deactivatable cylinders three-point switching (zero lift/partial lift/full lift), ❹. To begin with, it was necessary to optimise the partial-lift cam for the CDA case (range I). Due to the already high grade of de-throtteling in this area, valve lifts from 5.1 to 9 mm turned up. ④ shows the additional improvement in fuel economy from using a partial-lift cam for the cylinder deactivation case. To tap all potentials, further optimisations were necessary at medium and/or higher-level vehicle speeds in the NEDC. The engine must be throttled again at the load point requiring switchover to four-cylinder operation. Depending on the combustion process, the map range is produced in which the engine should be operated with a further partial-load cam in four-cylinder mode to avoid throttling losses (range III). With the engine/vehicle combination selected, this map segment produces vehicle speeds of 80 to 120 km/h. Despite the low frequency of operating points in the NEDC, a specially optimised partial lift results in an additional fuel-saving potential of 0.7 % on account of the higher fuel throughput rates.

To simplify the system, however, both partial-lift cams should be of identical design. Sharing a partial lift for two-cylinder and four-cylinder operation only slightly reduces the potential over using a valve lift optimised for each operating mode. The total potential fuel saving from cylinder-selective multiple valve-lift switching in the NEDC amounts to 11 %, with an additional potential of just 0.8 % being produced over the pure CDA operating mode.

CONSUMER-TYPICAL CONSUMPTION CYCLE

To evaluate the strategies under consumer-typical conditions, the Hyzem

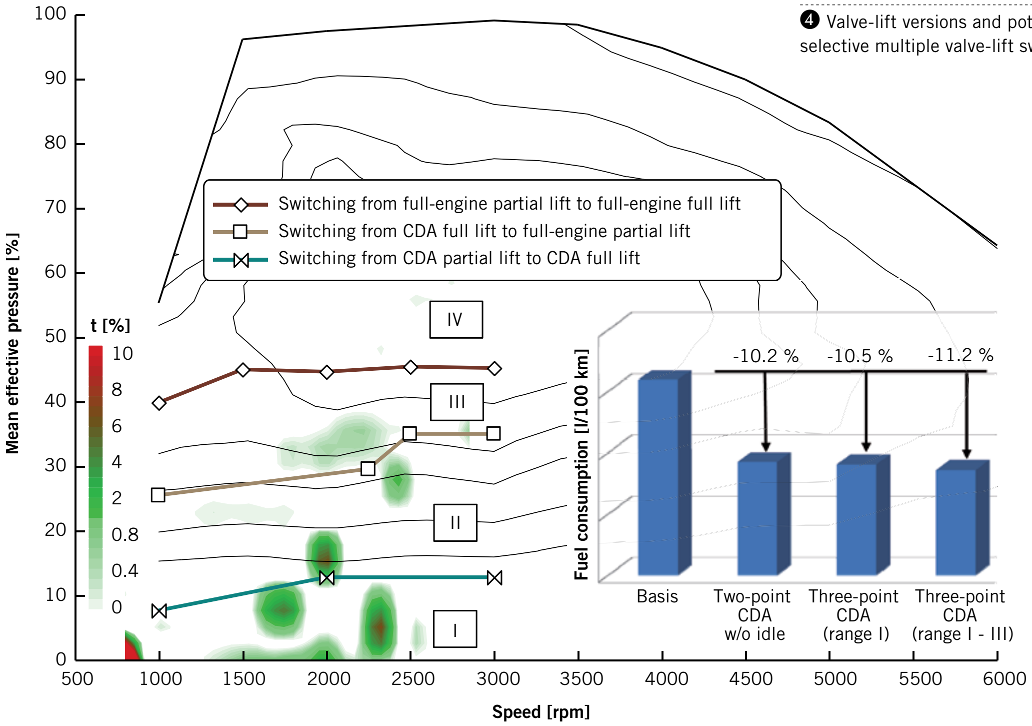

❹ Valve-lift versions and potential fuel saving from cylinder-selective multiple valve-lift switching in the NEDC

cycle – comprising an urban, extra-urban and highway cycle – was selected as an alternative driving profile, ❺. Frequent and dynamic load changes typify commuter behaviour in real-life road traffic. The resultant frequency components of the engine/vehicle combination under analysis shift toward higher loads in the Hyzem cycle. The fuel saving ascertained for the case of cylinder deactivation is compared in ❻ with the NEDC potential. It can be seen that the potential fuel saving from two-point valve-lift switching with cylinder deactivation is far lower in the Hyzem cycle. In the consumer-typical driving profile, however, a specially optimised valve lift can achieve a significantly higher cut in consumption of 4.1 % over the pure CDA operating mode, ⑥. This means cylinder-selective multiple valve-lift switching also pro-

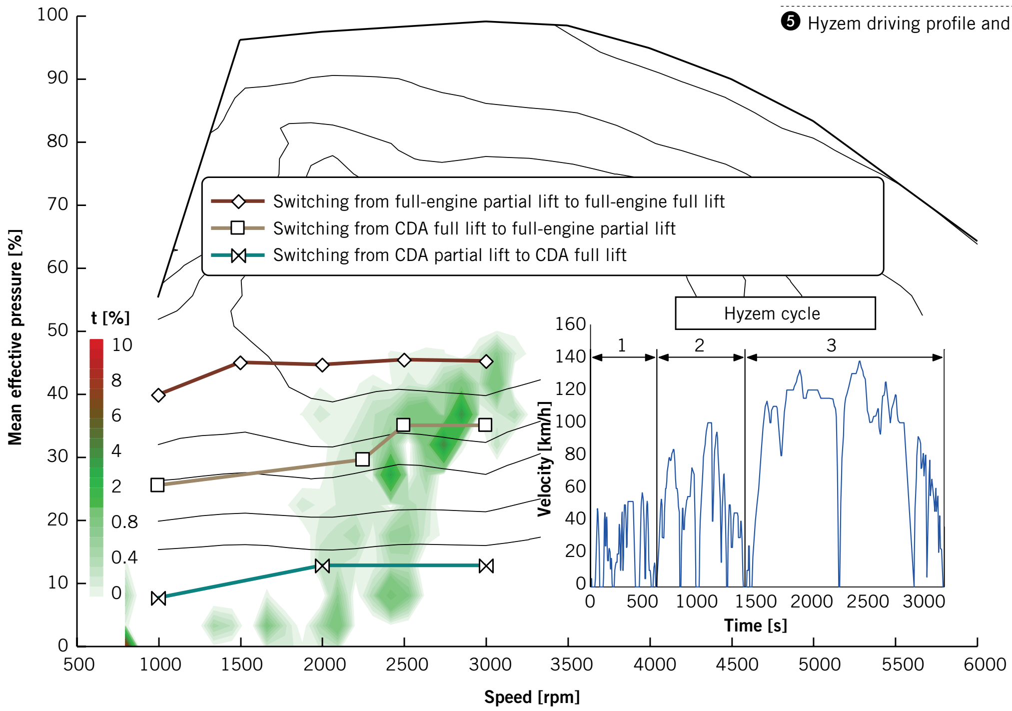

❺ Hyzem driving profile and frequency distribution

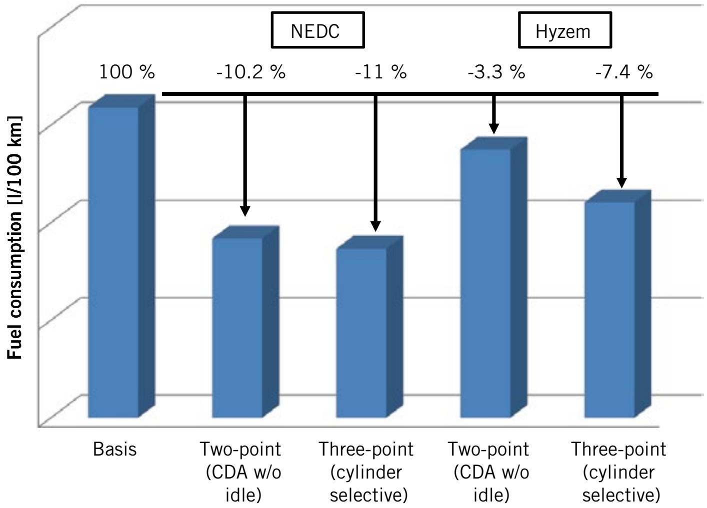

❻ Influence of the test cycle on the potential fuel savings from cylinder deactivation as well as cylinder-selective multiple valve-lift switching

vides the potential capability of improving efficiency outside the currently applicable NEDC.

SUMMARY AND OUTLOOK

Using two-point or three-point valve-lift switching for all cylinders, it is possible to tap potential fuel savings in the NEDC of 5.7 % and 6 % respectively. Far better improvements were produced with cylinder-selective multiple valve-lift switching. Combining two-point switching on one cylinder group and three-point switching on the second cylinder group makes it possible to cut fuel consumption by 11 % in the NEDC. However, at 0.8 %, the additional potential over pure cylinder deactivation is relatively slight. Applying a consumer-typical driving profile increases this advantage to 4.1 % which, in real-life driving, is a significant reduction in consumption that the consumer notices. Using cylinder-selective multiple valve-lift switching beyond here and into the full-load range creates an excellent valvetrain concept for a modern turbocharged combustion engine that is also very well suited to small four-cylinder engines in the volume segment.

REFERENCES

[1] Liebl, J.; Klüting, M.; Poggel, J.; Missy, S: Der neue BMW Vierzylinder-Ottomotor mit Valvetronic, Teil 2: Thermodynamik und funktionale Eigenschaften. In: MTZ 62 (2001), No. 7/8
[2] Bernard, L.; Ferrari, A.; Micelli, D.; Perotto, A.; Rinolfi, R.; Vattaneo, F.: Elektrohydraulische Ventilsteuerung mit dem "MultiAir"-Verfahren. In: MTZ 70 (2009), No. 12
[3] Beer, M.; Held, W.; Kerkau, M; Rehr, A.: Der neue Motor des Porsche 911 Turbo. In: MTZ 61 (2000), No. 11
[4] Wurms, R.; Dengler, S.; Budack, R.; Mendl, G.; Dicke, T.; Eiser, A.: Audi valvelift system – ein neues innovatives Ventiltriebssystem von Audi. 15. Aachener Kolloquium Fahrzeug- und Motorentechnik, 2006

THANKS

Also involved in the production of this article were Mr. Eggerath and Mr. Nitz from INA Schaeffler as well as Mr. Elsner and Mr. Spannaus from IAV in Chemnitz (Germany).

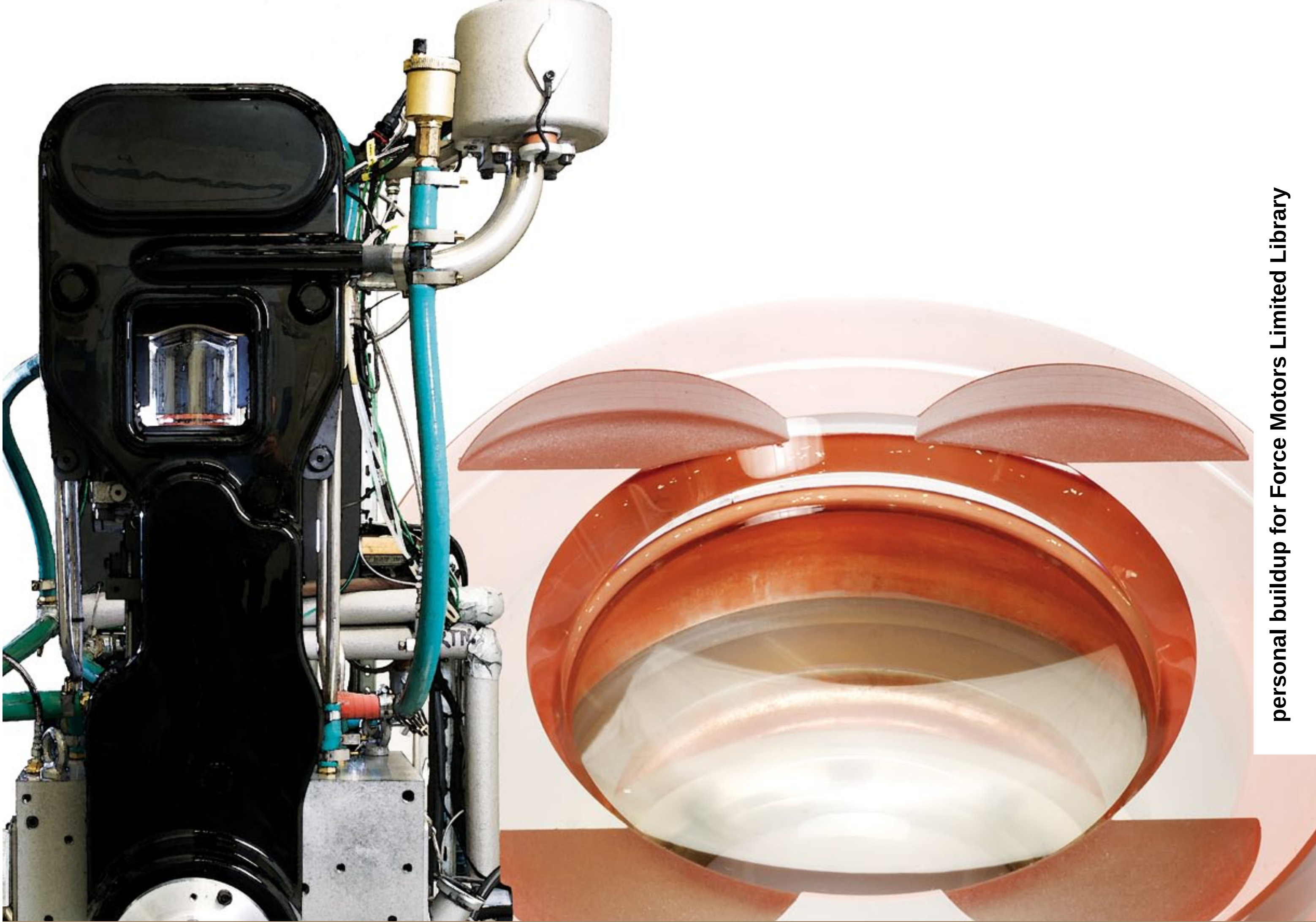

SPRAY-GUIDED DIRECT INJECTION FOR BOOSTED GASOLINE ENGINES

The combustion process continues to be highly instrumental in further improving the gasoline engine's fuel economy. Ricardo's newly developed spray-guided direct injection combustion system allows turbocharged gasoline engines to run with low fuel consumption, at some operating points even at diesel levels. Using this technology, the gasoline engine runs nearly completely unthrottled and exploits lean burn benefits throughout an exceptionally wide part of the engine map. It is also able to burn up to E85 or M40 fuels.

AUTHORS

JASON KING
is Chief Engineer Gasoline Engines at Ricardo in Shoreham-by-Sea (Great Britain).

PETER FEULNER
is Leader Research and Technology for Ricardo Germany at the Ricardo Technical Centre in Schwäbisch Gmünd (Germany).

MOTIVATION

Meeting future passenger car fuel efficiency targets remains a challenge around the globe. Further progress will depend on innovation in many fields but the combustion process will obviously have to play a key part in the industry's efforts to improve vehicle fuel economy and emission levels. Since the late 1990s, stratified injection has been used to increase the gasoline engine's fuel efficiency during part-load operation. It turned out that it is quite feasible to design a stable stratified charge and combustion process that approaches 290 g/kWh of fuel efficiency at 2000 rpm and 2 bar brake mean effective pressure (BMEP). Yet, the expected gains shown within regulated drive cycles could not be fully translated into real-world benefits. The primary reason for this was that even spray-guided stratified injection was limited to low speeds and loads.

However, the principle of using excess air and/or residual gas as a diluent in the combustion chamber, to minimise the amount of stoichiometric combustible charge, continues to offer potential. When Ricardo began to develop what ultimately resulted in the new turbocharged spray guided direct injection (T-SGDI) combustion system, the initial goal was to design an efficient, low-NO_x combustion process that would run stably under the most demanding of operating conditions. During a technology review, stratified charge was identified as the ultimate challenge, therefore the development goal was to come up with a combustion strategy that is highly tolerant to diluent across the full engine operating map.

During the subsequent work, which was carried out in collaboration with Petronas Research between 2008 and 2011, it became clear that a T-SGDI engine can overcome the previous limitations of stratified charging. In retrospect it appears that boosting was one of the missing elements of the first stratified charge combustion solutions. Applied to Ricardo's four-cylinder 2.0-l Volcano gasoline engine, the new boosted T-SGDI with utilises stratified charge at previously unachievable BMEP levels of up to 15 bar BMEP results in a remarkable fuel efficiency increase. At the "classic" 2000 rpm, 2 bar BMEP point the brake specific fuel consumption (BSFC) of the lean stratified T-SGDI engine was measured at only 277.5 g/kWh versus 370 g/kWh in homogenous lambda 1 mode, yet at 10 bar BMEP and 40 Nm torque the BSFC falls to a diesel like 206 g/kWh. At 2500 rpm the T-SGDI engine undercuts the BSFC levels of a benchmark Euro 5 four-cylinder 1.6-l diesel engine, ❶.

ENGINE AND OPERATION

A combination of benchmarking, advanced design, analysis, rig testing,

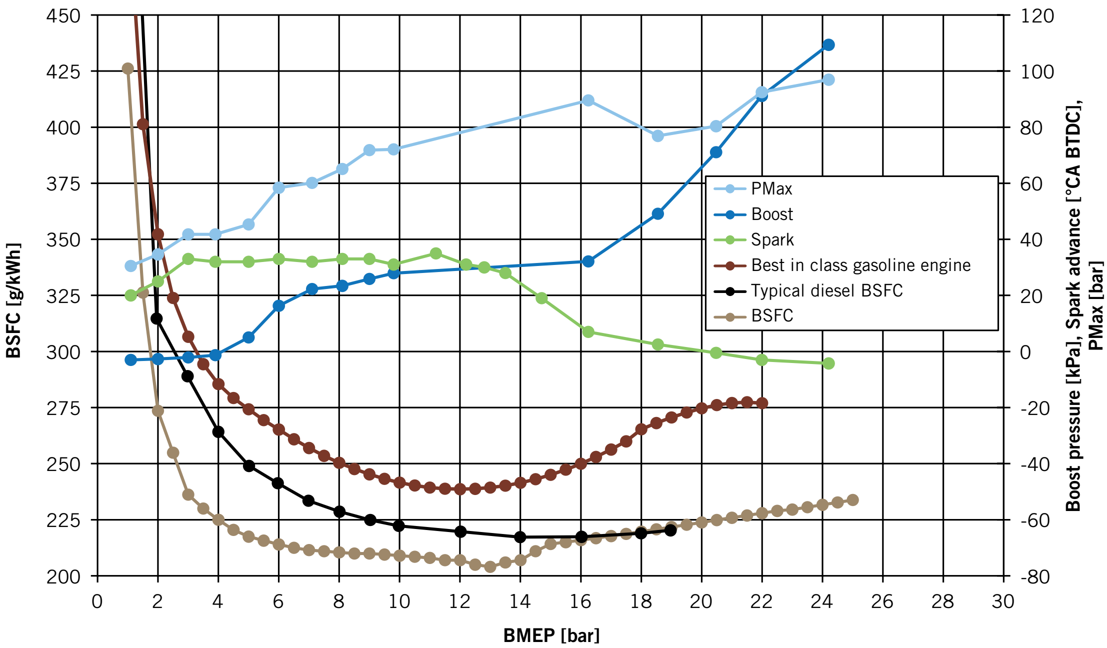

❶ Detailed T-SGDI engine data at 2500 rpm show how well BSFC can be maintained at high loads whilst not exceeding maximum pressure limits

❷ A Hydra single-cylinder optical engine was used to validate the CFD spray and combustion modelling

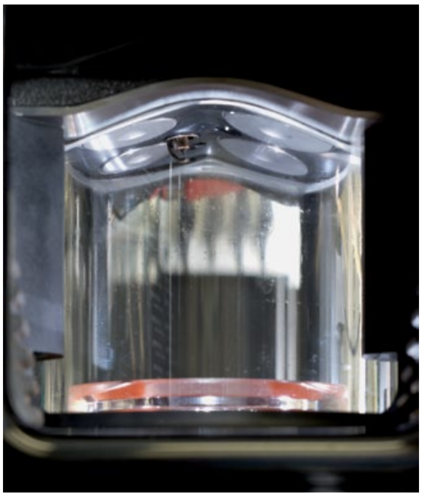

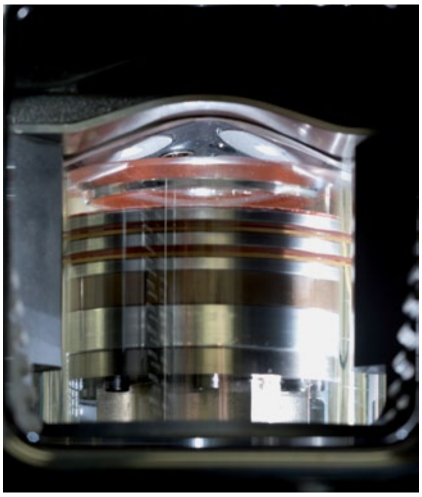

engine development plus calibration tools and techniques was utilised to realise the T-SGDI technology. An optical access single-cylinder research engine served to validate the CFD models of injection and combustion, ❷. Finally, the fully functional four-cylinder Volcano gasoline engines were used on a test bench to validate the single-cylinder engine results and undertake further emissions development. The Volcano engine is a four-cylinder in-line gasoline engine with 2.0 l displacement (86 mm bore, 86 mm stroke), with a nominal compression ratio of 10.7:1. It has twin cam phasers for variable valve timing (VVT) but the variable valve lift explored in the single-cylinder engine study was considered unnecessary for the multi-cylinder engine. A Garrett fixed geometry turbocharger was matched to the multi-cylinder engine to provide high specific performance. For the T-SGDI development four different types of injector technology were investigated in a central position within the combustion chamber, including piezo-electric and solenoid types. The engine management includes a Pectel+Drivven injector driver unit.

At 197 kW and 391 Nm of torque the engine is strong enough to offer the generous level of power for a D-segment car typically found in Europe or North America. However, the T-SGDI technol-

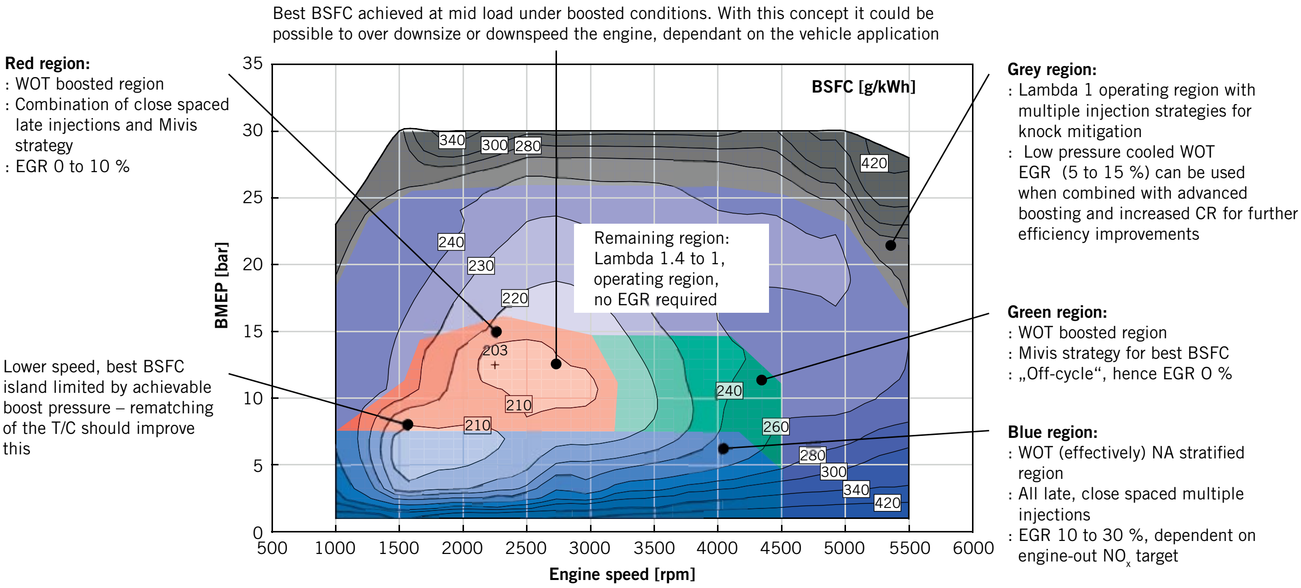

❸ Map of the BSFC of the T-SGDI engine

ogy has been developed to be scaleable down to a 72 mm bore. The standard fuel is 95 RON ULG, but the injection process also works stably with alternative fuels up to E85 and M40 blends.

Much like a diesel engine, the T-SGDI engine runs almost completely unthrottled with excess air (up to 4500 rpm): the driver's load request is directly translated into the injected fuel quantity. Depending on the load request, the size of the λ=1 air fuel mix zone is varied from stratified to a stoiciometric mix, in the whole of the combustion chamber. From stable idling at an air/fuel ratio of 160:1 (λ>10) to a boosted mid load at up to 15 bar BMEP, the stratified charge is surrounded by excess air and/or residual gas.

By expanding boosted and stratified operation, the T-SGDI engine offers the combined benefits of downsizing and minimum fuel injection. The multi-cylinder engine demonstrated that fuel consumption benefits were significantly enhanced through boosting, with a best BSFC of 203 g/kWh being achieved at 2250 rpm and 13 bar BMEP. The higher mass flow during part load, resulting from unthrottled operation also improves turbocharger response. In addition, the best BSFC engine map areas are much closer to real-world requirements than is the case with previous stratified charge solutions, ❸. Unlike a diesel engine, there is no practical smokelimited air/fuel ratio, so lambda can be instantaneously switched from lean to 1 or richer to maximise the air utilisation for maximum torque and for increased enthalpy release to the turbine to enhance run-up.

INJECTION STRATEGY

As the fuel efficiency and engine-out emission levels depend on the initial fuel spray, evaporation and mixture preparation, the injection strategy plays a central role in the T-SGDI engine. The injectors tested on the project have been capable of a minimum of four completely independent injections, and in theory one injector type is able to perform up to 15 shots per cycle. In the cold engine up to eight shots are used during catalyst light-off to minimise both particulate mass and number. When warm, the T-SGDI engine typically utilises up to five injections per working cycle, which are timed depending on the operating conditions.

At lower loads and up to around 7 bar BMEP, the engine runs effectively naturally aspirated with stratified charge. Multiple injections are closely grouped together and timed late in the compression stroke to enable phasing of the combustion to the thermodynamic optimum in order to improve fuel efficiency and to significantly reduce engine out NO_x levels. This addresses one of the previous issues of stratified charge engines which tended towards over-advanced combustion at almost all stratified points. As high NO_x levels are typically found during the combustion phase before top dead centre, retarding combustion is important to meet NO_x legislation at minimum system cost. By this strategy alone, NO_x emissions were almost halved in the T-SGDI engine.

At mid load (1250 to 4500 rpm and typically 8 up to 15 bar BMEP) the T-SGDI engine is run in boosted stratified mode. The individual injection shots are separated from each other and stretched out over a longer time-span to improve thermal efficiency when combined with the lower heat losses achieved by leaner operation thanks to boosting. This mode is called Multiple Injection Variable Injection Separation (Mivis). In both fully stratified and Mivis modes the injection strategies enable optimum mixing but also control charge turbulent kinetic energy to ensure good ignitability and optimum heat release after spark.

From mid to full load the combustion chamber is charged with either a lean or homogenous λ=1 mixture depending upon fuel economy or emissions control priorities. Fuel is injected during both the intake and compression stroke to mitigate knock.

NO_x EMISSIONS

The most challenging aspect of the project was to reduce part load engine out NO_x levels to those suitable for a lowest cost aftertreatment solution for Euro 6 and beyond, including proposed stringent LEV 3 US legislation. This was

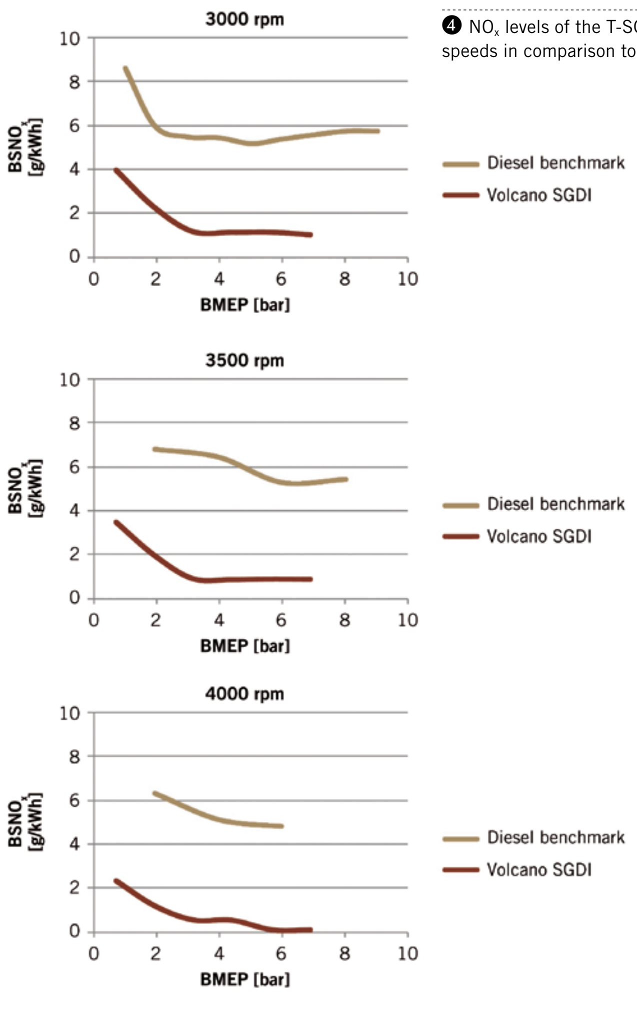

❹ NO_x levels of the T-SGDI engine at various speeds in comparison to a benchmark diesel engine

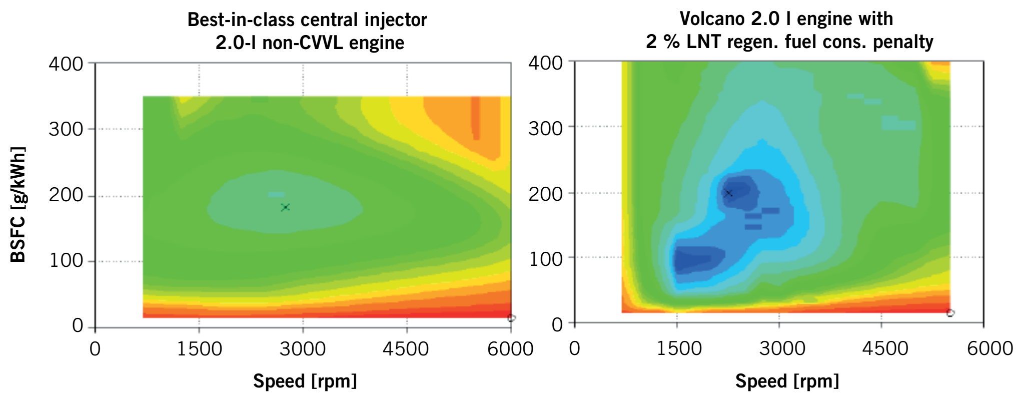

* Stop/start and upgraded thermal systems benefit included

❺ A vehicle simulation shows that the T-SGDI engine would reduce the BSFC of a conventional D-segment saloon with 3.0-l NA engine by 40 %, and the BSFC of a downsized turbocharged 2.0-l λ=1 engine by 15 %

achieved through the optimised combustion phasing enabled by multiple injections and external EGR. In the boosted mode the T-SGDI engine uses up to 30 % of low pressure EGR. In the non-boosted mode both low and high pressure EGR are feasible.

External EGR can also be used under high load conditions, but here it is for knock mitigation rather than NO_x reduction. ❹ shows that NO_x levels in the region of 0.5 to 2 g/kWh have achieved with the T-SGDI engine when fully stratified. By combining Mivis and EGR, the engine-out NO_x is between a fifth and a tenth of a conventional homogenous gasoline engine. The figures suggest that a small NO_x trap would suffice for the T-SGDI engine to meet future NO_x legislation.

SUMMARY AND OUTLOOK

The T-SGDI engine is based on a new, robust, boosted stratified charge combustion system that runs successfully in extreme modes. The combustion process is very tolerant to diluent but works equally well with a homogenous stoichiometric charge. Even at high loads the combustion process shows little degradation in fuel consumption. At the same time the concept is based around in production or near production technologies. The T-SGDI engine's best efficiency is typically approached at around mid load, which on the boosted engine is 10 to 13 bar BMEP, where the BSFC approaches 200 g/kWh.

The multiple injection strategy, which is optimised for individual operating modes, improves combustion efficiency and brings down NO_x levels. Together with the gains from low pumping and heat losses, this gives T-SGDI a good potential to improve fuel economy, ❺. Challenges, such as the US passenger car target of 54.5 mpg (US) by 2025 and other similarly stringent regulations on fuel economy and CO_2, are already resulting in a lot of interest in stratified charge. The combined effects of stratified charge and boosting can be used to achieve better fuel efficiency without excessive downsizing. Driveability, for instance, could benefit from the torque reserve that a slightly bigger engine has to offer.

Potential future concept progress appears possible by further improving the robustness to even more diluent. Recent work with a re-optimised single-cylinder research engine with a revised ignition system has shown a brake specific fuel consumption of less than 200 g/kWh but the challenge will be maintaining this high level of efficiency whilst meeting future US LEV 3 emission requirements. By applying a Miller cycle to reduce compression temperatures and increase the expansion ratio, there may be additional potential to increase the tolerance to knocking.

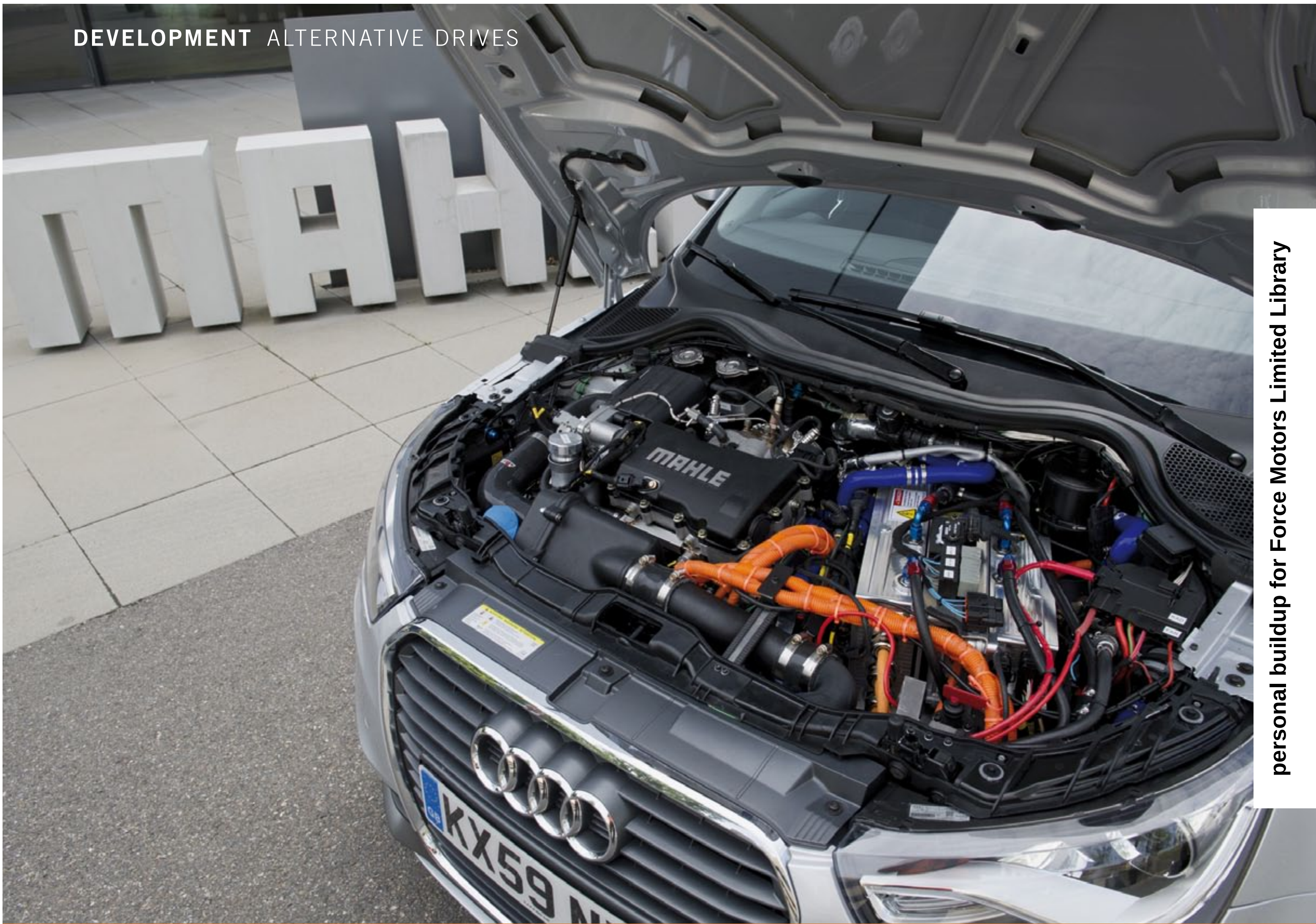

VEHICLE INTEGRATION OF A RANGE EXTENDER ENGINE

Range extenders might play a key role for the future success of electric vehicles. Mahle has developed a range extended electric powertrain for the small and compact car segment, suitable for everyday use with very low fuel consumption, full system integration and flexible vehicle installation. In the following, the implementation of the range extended electric powertrain into the car is spotlighted.

AUTHORS

DR. MIKE BASSETT
is Head of Product Group Hybrid at Mahle Powertrain Ltd. in Northampton (Great Britain).

JONATHAN HALL
is Senior Project Manager at Mahle Powertrain Ltd. in Northampton (Great Britain).

TONY CAINS
is Senior Principal Engineer at Mahle Powertrain Ltd. in Northampton (Great Britain).

DR. MARCO WARTH
is Engineering Director at Mahle Powertrain Ltd. in Northampton (Great Britain).

MOTIVATION

Range Extended Electric Vehicles (REEVs) offer significantly different vehicle integration opportunities and pose new noise, vibration and harshness (NVH) challenges in comparison to conventional vehicles. The elimination of a mechanical coupling between the engine and the driven wheels enables more flexible positioning within the vehicle. However, the intermittent engine operation, in an otherwise silent vehicle, leads to new requirements in terms of noise and vibration development of the vehicle. Mahle Powertrain has integrated the range extender (RE) in a conventional compact class vehicle [1]. The development of this included the conversion to a pure electric vehicle as well as the REEV system integration and implementation of the appropriate drive system. The demonstrator vehicle enables comprehensive testing of the range extender concept.

RANGE EXTENDER DRIVE

The Mahle range extender engine, a 0.9-l twin-cylinder with a maximum power output of 30 kW, is a targeted solution for a compact class REEV. The design is strongly focused towards minimal package size, weight and cost. The noise and vibration development takes on particular significance within an REEV due to the fact that the engine is not operating for large periods of time, and should not be noticeable over electric-only operation.

The 38 kW generator is fully integrated into the engine, with the rotor mounted directly to the crankshaft. The generator is also used to start the engine, thus no separate starter motor is required and engine starting is achieved in very short timescales (measured at less than 0.2 s), and the engine can be motored up to full running speed before combustion is enabled. This has benefits for clean starting and improvements to NVH at engine start.

Further measures to improve the noise and vibration performance of the engine operation include, amongst others, the dynamic control of the generator. The non-symmetric, 180°/540°, firing interval provides primary balance, and thus enables the omission of balancer shafts, giving direct cost, weight and package benefits. However, the uneven firing order is detrimental to the intra-cycle torque profile of the engine and hence intra-cycle speed fluctuation of the engine. The resulting total engine cyclic torque profile is shown in ❶ for 2000 rpm and 80 % load, where it can be seen that the firing order gives no firing events in the 1st revolution of the engine cycle and two firing events in the 2nd revolution of the cycle. During the compression events the instantaneous engine torque dips to 200 Nm of negative torque, these dips correspond to the each of the compression strokes, these are each followed by expansion strokes, where all the positive crank work is generated during the cycle, and it can be seen that over 600 Nm of positive crank torque is generated during these each strokes.

The low moment of inertia of the crankshaft, generator and flywheel (located in between the two cylinders), combined with the high intra-cycle torque variations, leads to corresponding speed fluctuations. Measured intra-cycle speed fluctuations, for a cycle average speed of 2000 rpm and 80 % load, are shown in ❷, where it can be seen that when a constant load is applied by the generator there is a cyclic variation in engine speed of 740 rpm. It can be seen that the engine slows during the 1st 360 °CA of the cycle to about 1560 rpm, where no firing torque occurs, and then speeds up to 2300 rpm over the next

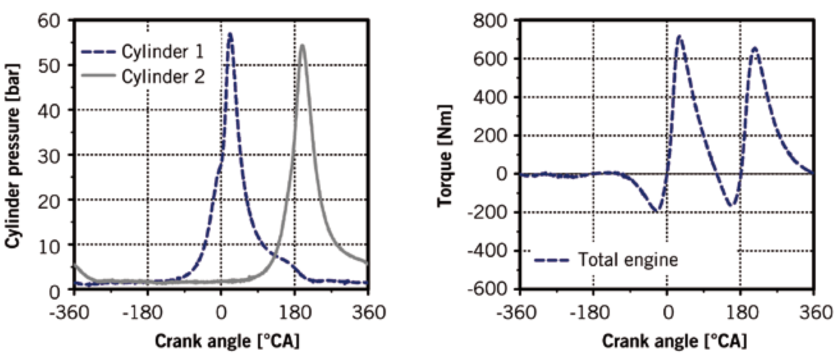

❶ Torque variations with uneven firing sequence

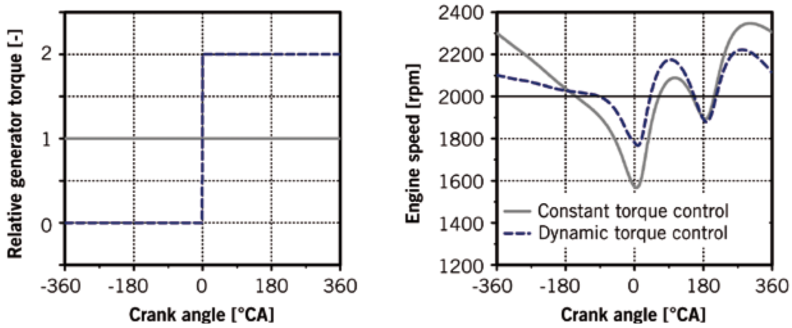

❷ Comparison of constant and dynamic generator load control

revolution in two jumps, corresponding with the two firing pulses.

These high fluctuations in crankshaft speed result in increased engine NVH. Dynamic load control strategies for the generator have been investigated, the simplest of such being to switch-off the generator during the 1st engine revolution, where the cylinder charging and compression events occur, and to double the generator load during the 2nd revolution, reducing the observed cyclic speed fluctuations considerably. Using the dynamic generator control strategy reduces the cyclic speed fluctuations of the engine across the entire speed and load operating map, ❸.

Optimisation of the reduction of the cyclic speed fluctuations, whilst not sacrificing the power output or efficiency of the Mahle range extender system at each operating point, has enabled a total system efficiency of greater than 25 % to be achieved across the entire engine operating range, and up to 31 % at the best operating point, ❹.

DEMONSTRATOR VEHICLE

In order to enable development and refinement of the NVH attributes of the range extender engine, a REEV demonstrator vehicle is being built by Mahle. It is believed that the market for REEV, of purely series-hybrid configuration, is for vehicles of compact class and smaller. This is primarily due to the lack of a direct coupling between the range extender engine and the wheels, which could enable higher high-speed cruising efficiencies in charge-sustaining mode, but adds considerably to driveline complexity.

As basis for the demonstrator vehicle it was elected to convert a conventionally powered compact class vehicle, which was converted to a full electric vehicle with a range extender. The electric powertrain was designed to enable the demonstrator vehicle performance to match, or even exceed, that of the baseline vehicle, with the exception of the absolute top speed. In addition to the 0 to 100 km/h acceleration time of 12 s, other targets were set, in particular the ability to ascend a grade of greater than 20 % and being able to attain 90 km/h on a 6 % grade, even with a completely depleted battery.

By virtue of its two cylinder configuration and fully integrated generator, the range extender unit is appreciably shorter than the 1.2-l inline four cylinder baseline engine it is replacing.

The compactness of the 55 kW (100 kW peak) traction motor and two speed transmission enable the Mahle range extender to be installed alongside them within the original engine bay of the baseline vehicle (along with the corresponding inverter units for traction motor and generator). The 14 kWh high voltage traction battery has been installed under the boot floor, without impinging upon the luggage or passenger compartments. The original 45 l fuel tank has been replaced with a 25 l tank.

The inlet system has been optimised to reduce the intake orifice noise, which had to be achieved within the tight package envelope of the demonstrator vehicle. The reduction of sound pressure level was achieved by increasing the air-filter volume and adding a quarter-wave resonator pipe to the inlet side of the air-filter volume. This led to a reduction in the sound pressure level at the intake of over 10 dB at the maximum power operating point, without negatively affecting the power output or efficiency of the engine.

VEHICLE AND ENGINE CONTROLLER

In addition to the packaging challenges presented by the integration of the electric drive components into an existing vehicle,

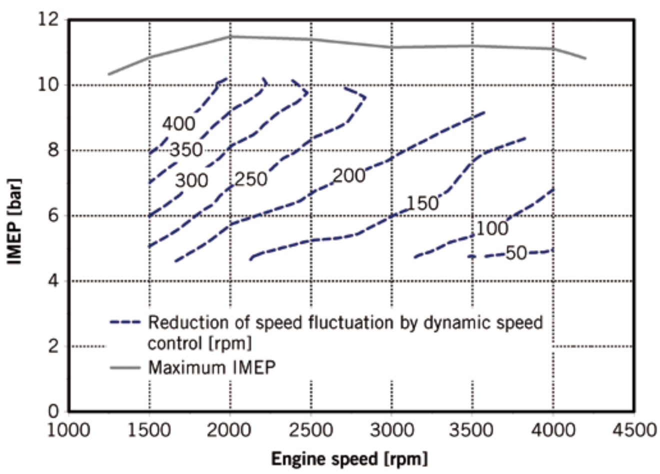

❸ Reduction of speed fluctuation by dynamic generator load control

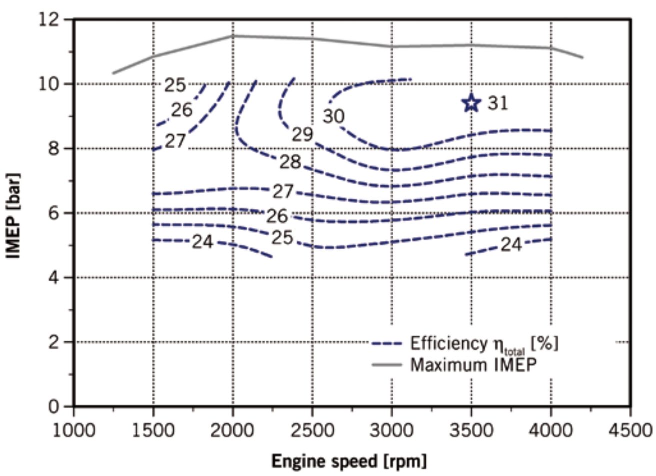

❹ Range extender system efficiency

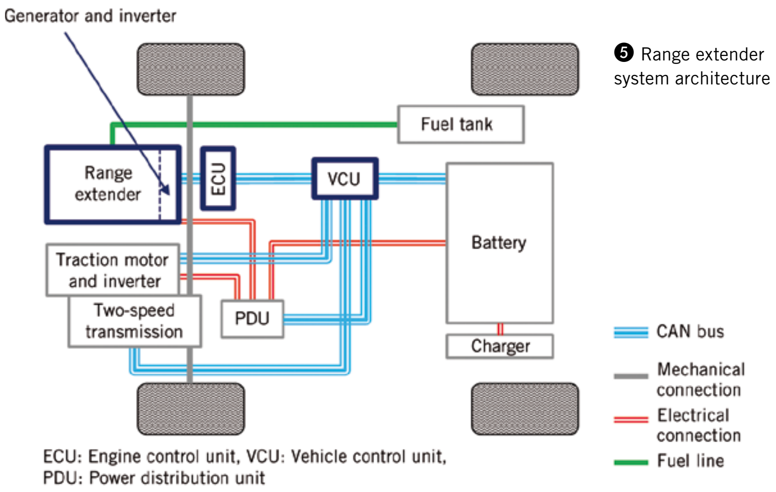

❺ Range extender system architecture

there was also the development of the control system and management of the various systems within demonstrator vehicle. The flexible engine control unit (ECU) environment developed by Mahle Powertrain proved extremely helpful here. In addition to the control of the range extender engine and generator, an open ECU was developed on the same hardware platform for the entire master vehicle control unit (VCU). The engine and vehicle control units were deliberately kept separate to enable the complete system to be a relatively simple addition to an electric vehicle, ❺. In addition to the complete drivetrain system in the VCU, the power flow between generator, battery and traction motor and voltage conversion between high-voltage and portrait and low voltage systems is performed by the power distribution unit (PDU), which is one of the central components of the REEV system architecture.

OPERATING STRATEGY

The operating strategy of the range extender engine has been devised to maximise the fuel economy of the vehicle, whilst maintaining and acceptable NVH characteristic. Additionally, intra-cycle speed fluctuations have been minimised, again for NVH reasons, by a combination of dynamic generator torque control and operating point selection. Extensive cold-start testing indicated that low load and low speed operating points were best for achieving catalyst light-off, whilst minimising the cumulative tail-pipe emissions levels prior to light-off being achieved. Testbed simulations of NEDC test cycle operation indicated that the emissions levels of the engine could be kept to around 30 % of the Euro 6 limits.

To minimise the declared vehicle CO_2 emissions based on the European test procedure it is desirable to achieve as high an electric operating range as possible and to minimise the CO_2 emissions measured in the minimum battery state of charge test. This drives a strategy that does not start the range extender unit until the battery has reached the minimum allowable state of charge (SOC), to maximise the electric only range, and also does not recharge the battery, but simply sustains it at the minimum state of charge. This is because any energy that is added to the battery during the minimum state of charge test is not credited by the test procedure, and creates additional CO_2 emissions whilst being generated.

Therefore, the proposed operating strategy for the demonstrator vehicle is to activate the range extender unit once the battery SOC falls to 0.25 and to only slightly above the instantaneous road load power requirement (of the order of 1 kW), ❻, although this would need to be modulated slightly based on instantaneous battery SOC. When battery SOC allows, it is planned to avoid range extender operation at power demands below 5 kW (or 45 km/h), however at low SOC levels the range extender unit will be activated and operated at 5 kW. This operating strategy enables the demonstrator vehicle to achieve a 70 km all-electric range. The fuel tank capacity enables a further 400 km range and the weighted tailpipe CO_2 value achieved is less than 45 g/km, and is thus under one third that of the already good baseline vehicle.

SUMMARY AND OUTLOOK

The Mahle range extender demonstrator shows conclusively that eco-friendly mobility is possible through an intelligent combination of battery electric propulsion and a combustion engine supporting on-board power generation, achieving a combination of: low-emissions, locally emission free and an almost unlimited range. Other advantages of this innovative drivetrain concept are the added thermal management capabilities for winter (energy-intensive heating) and summer (energy-intensive air conditioning) without impacting upon journey distances that can be undertaken.

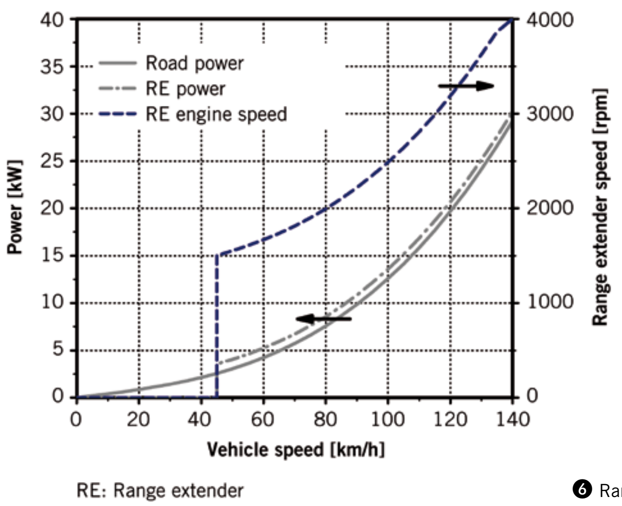

❻ Range extender operating strategy

REFERENCE

[1] Mahr, B.; Bassett, M.; Hall, J.; Warth, M.: Development of an Efficient and Compact Range Extender Engine. In: MTZ 72 (2011), No. 10

DESIGN PROCESS OF AN ELECTRIC POWERED OIL PUMP

In recent years, the increasingly tight emission standards have been driving the development of electric powered pumps whose control strategy can be optimised in order to minimise the absorbed energy. Pierburg Pump Technology anticipated the market needs and for few years has been developing a new generation of electric powered oil pumps.

AUTHORS

DR.-ING. ALESSANDRO MALVASI
is Senior Manager Product Engineering Electric Oil Pumps at Pierburg Pump Technology GmbH in Neuss (Germany).

DR.-ING. RAFFAELE SQUARCINI
is Manager Calculation and Simulation at Pierburg Pump Technology S.p.a. in Livorno (Italy).

DIPL.-ING. GIACOMO ARMENIO
is Director Product Engineering Oil Pumps & Mechanical Water Pumps at Pierburg Pump Technology S.p.a. in Livorno (Italy).

DIPL.-ING. ACHIM BRÖMMEL
is Vice President Product Engineering at Pierburg Pump Technology GmbH in Neuss (Germany).

MOTIVATION

The improvement of fuel efficiency with the main purpose of reducing emissions is currently the major driver for new developments in the automotive field.

Within this context, the electrification of the auxiliaries plays a key role because they can be driven independently from the combustion engine so as to optimise the absorbed energy.

Following this trend, electric powered oil pumps are increasingly requested due to their versatility; they can be used for lubrication, cooling, scavenge or actuation.

This flexibility makes this product suitable for a wide range of applications, from automatic transmissions to hybrid cars. The interest for engine applications is also increasing. Anticipating the needs of the market, in the last years Pierburg Pump Technology has been developing a new generation of electric powered oil pumps. In the next paragraphs, an overview of the design process for this product is described.

DEVELOPMENT STRATEGY

An electric powered oil pump is composed by three subsystems: pump, motor and electronic controller. Main driver of every new development is the integration of these modules so as to reduce the overall size and weight as well as the number of components. This goal is achievable because the company owns design and manufacturing expertise for all three subsystems. In addition, a special focus is also kept in order to achieve synergies with the electric powered water pumps so as to reduce costs and time to market while increasing reliability. Indeed, since 2003 Pierburg Pump Technology has produced more than five millions of electric powered water pumps and it is currently market leader for this product line.

DESIGN OF THE PUMPING GEARS

The main function of an electric powered oil pump is to create the required oil flow. For this reason its design, which in any case is an iterative process, starts from the pumping gears. For almost the totality of applications a volumetric pump is adopted, due to the pressure requirements usually higher than 1 or 2 bar. In particular, up to 10 or 12 bar, the Gerotor solution is the best compromise in terms of robustness, noise, friction and packaging.

The dimensioning of the gears is based on the hydraulic requirements of the oil circuit, in particular on the most demanding operating point; it consists in a given flow rate at an imposed delivery pressure for a defined oil temperature.

To generate the required flow, the rotational speed must be chosen as a compromise to have a reasonable packaging of motor and pump without running up against cavitations or noise issues. A typical speed range for continuous operation is between 1500 and 3500 rpm.

Given these assumptions, the design loop starts with the preliminary estimation of the volumetric efficiency (η_v) based on experimental results collected on similar pumps. In Eq. 1 Q is the real flow, Q_{th} is the theoretical flow and Q_{leak} is the flow wasted because of leakages.

EQ. 1

$$\eta_v = \frac{Q}{Q_{th}} = \frac{Q_{th} - Q_{leak}}{Q_{th}} = 1 - \frac{Q_{leak}}{Q_{th}}$$

Set this value, a preliminary CAD model of the gears is generated, as shown in ❶, and used to recalculate the volumetric efficiency through a Matlab routine specifically developed.

In the next step, a number of possible Gerotor designs are generated by an Amesim routine that optimises the design parameters, for example number of teeth and eccentricity, while satisfying all boundary conditions. Among the proposed Gerotors, the most suitable one is chosen by evaluating other outputs like the flow ripple.

CALCULATION OF THE ABSORBED TORQUE

The next important step is the calculation of the torque absorbed in the assigned working points. This step is crucial for the dimensioning of the electric motor. For this reason, a lumped parameters model has been developed by Simulink.

This kind of model simplifies, under certain assumptions, the behaviour of a physical system into a one-dimensional code while ineluctably losing some

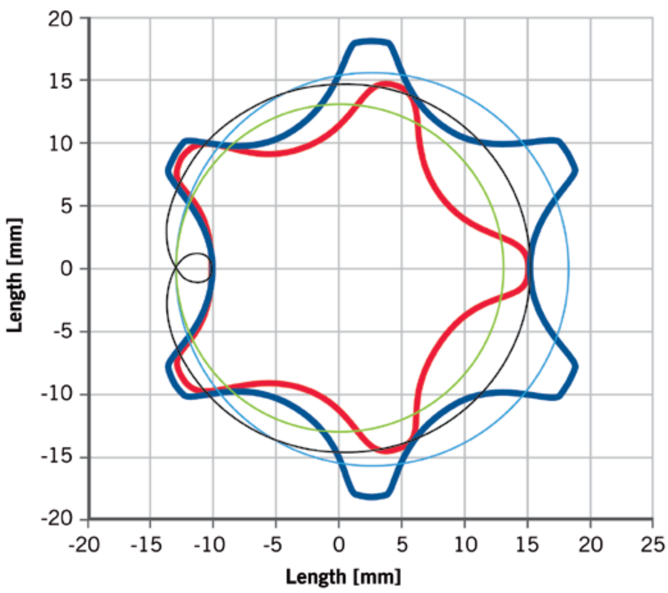

❶ Typical outcome of a Gerotor's profile calculation

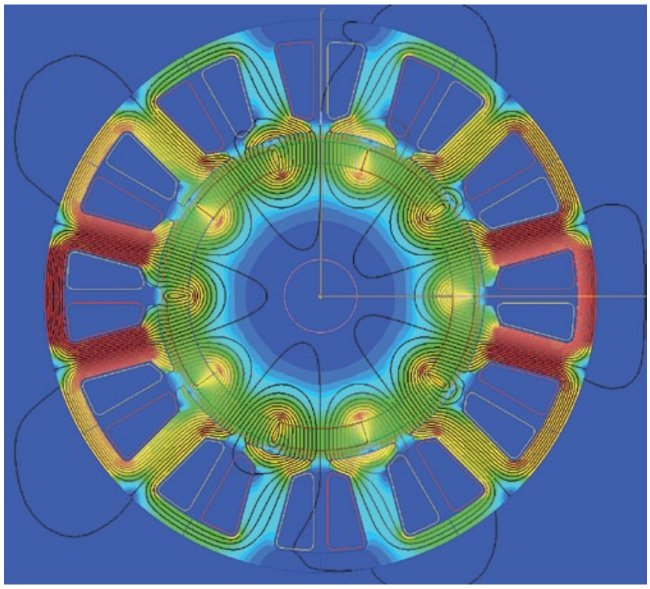

❷ Simulation of the magnet circuit for a BLDC motor

details. The code requires the use of coefficients that have to be set on the base of testing results. Thus simulation and experiment cannot be completely separated: an initial set-up of the model is necessary.

The model, described later, is composed by three macro-blocks representing the subsystems of an electric powered oil pump however, in this step of the process, only the hydraulic module is used for the torque calculation.

After implementing the geometrical features of the calculated hydraulics, the total torque is evaluated as a sum of three contributions, Eq. 2:

EQ. 2	$M_{tot} = M_T + M_{CL} + M_{\mu}$

M_H is the hydraulic torque due to the generation of required pressure and flow, M_{CL} is the coulombian contribution generated where there are dry or lubricated contacts between sliding parts and M_{μ} is the viscous contribution due to the fluid movement inside clearances.

❸ Virtual blocks-model of an electric powered oil pump

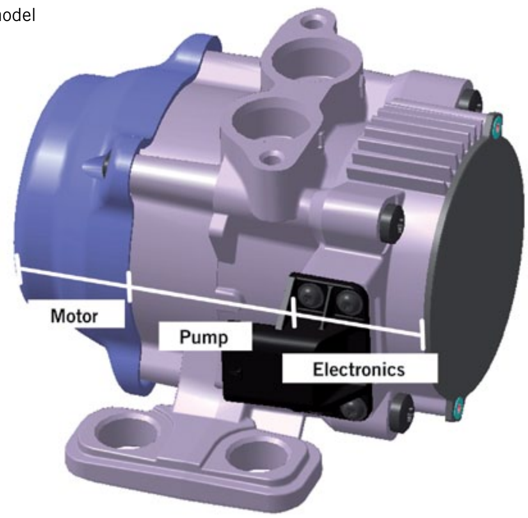

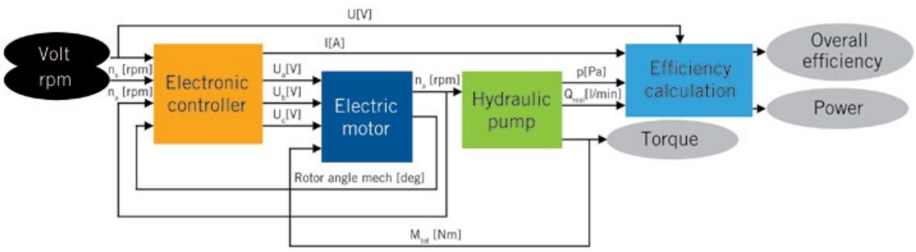

MOTOR AND ELECTRONICS DESIGN

The main function of the motor is to drive the pumping gears by generating the needed torque. For this reason, its calculation is the main prerequisite for the design of the motor. In addition, the designer needs to know temperature and speed for each working point together with some boundary conditions.

Based on these inputs, the motor is calculated making use of specific software for the design and for the optimisation of the magnetic circuit, ❷.

For the most of electric powered oil pump applications a brushless DC (BLDC) motor is used, mainly due to lifetime, noise and EMC requirements.

Radial flux and inner rotor design, to minimise the losses especially for wet running rotors, is the preferred concept. Besides, when minimising the packaging is the main driver, permanent magnets are used and the number of poles is chosen according to the needed torque and the available packaging; four poles is the most common solution, as well as a 3-phases motor is basically a standard.

The control of the rotor position can be obtained by hall-sensors or through a sensorless solution. The latter is usually the most cost-effective solution, but the former is needed when high torque level or quick dynamic response are required especially at low temperature.

The signals from hall-sensors or sensorless solutions are, together with the control signal from the car's ECU, the inputs for the electronics controller. Precisely, the bidirectional communication with the car is ensured via LIN or PWM.

The controller is build around an Integrated Circuit that, according to the need of the specific project can be a programmable one or more commonly an ASIC (Application-Specific Integrated Circuit), due to its higher cost-effectiveness in mass volume production.

Aim of this Integrated Circuit is:

: to regulate the generation of the control pulse of motor-phase
: to carry out diagnostics, for instance actual speed, temperature and current
: to apply protections against overload, over voltage and over temperature.

Notably, in terms of motor commutation, a trapezoid one is normally chosen as the best compromise between required computational workload and noise performances. From hardware point of view, the Printed Circuit Board (PCB) can be made using two technologies: FR4 or ceramic. The second solution is the state-of-the-art for high temperature applications.

INTEGRATION OF THE SUBSYSTEMS

After a pre-design of the key parts is done, the already mentioned Simulink model is used to simulate the complete system before going into a prototype phase. Notably, this activity is crucial not only for the mechanical design, but also for the presetting of the software parameters.

The model receives as main inputs voltage (V) and desired speed rotation (n_s), as shown in ❸. Given these inputs, electronics and motor blocks execute two loops modifying the electric parameters in order to find an equilibrium and obtain an actual speed (n_a) convergent to the desired one (n_s). The actual speed is used as input for the hydraulic module where the absorbed torque (M_{tot}) is calculated. The value or this resistance torque is then compared with the torque generated by the motor and, in case of discrepancies, the model updates duty cycle and actual speed so as to get to the equilibrium point.

Based on the results of this simulation, the designers work on the integration of the subsystems. Once the 3D models are finalised, further simulations are carried out to verify the design. Among the others, the simulation of the thermal management plays a crucial role. The purpose is to verify that the temperature of electronics components and electric motor does not exceed the threshold values. To this aim, the complete pump is modelled so as to have a full map of the temperature distribution, as shown in ❹.

A special care is dedicated to the modelling of details as the layers that make up the PCB because the hottest spots are usually the Mosfets of the power electronics. To fulfil this task a CFD analysis is performed with the sole solution of the energy equation; the analysis can be run either in a steady-state condition, simulating a specific operating point, or in transient condition, simulating an instantaneous thermal overload.

Other fundamental analysis for the acceptability of the design is the structural verification of the pump, both from static and dynamic point of view. To this aim, FEM and multibody analysis are carried out, often in combination, to investigate the vibration behaviour of the product and its resistance against fatigue.

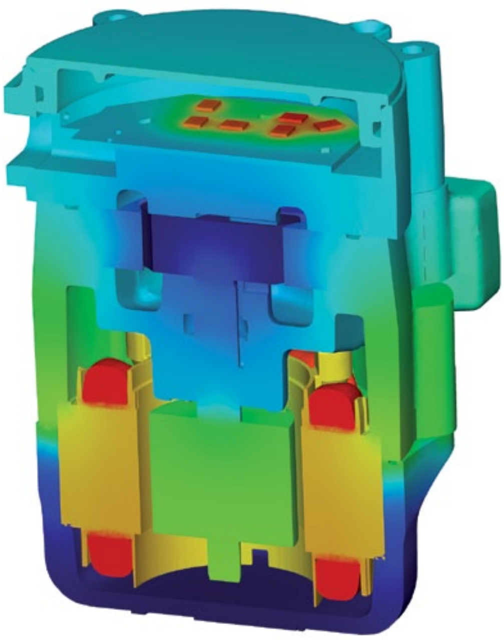

❹ CFD analysis of an electric powered oil pump: typical temperature distribution

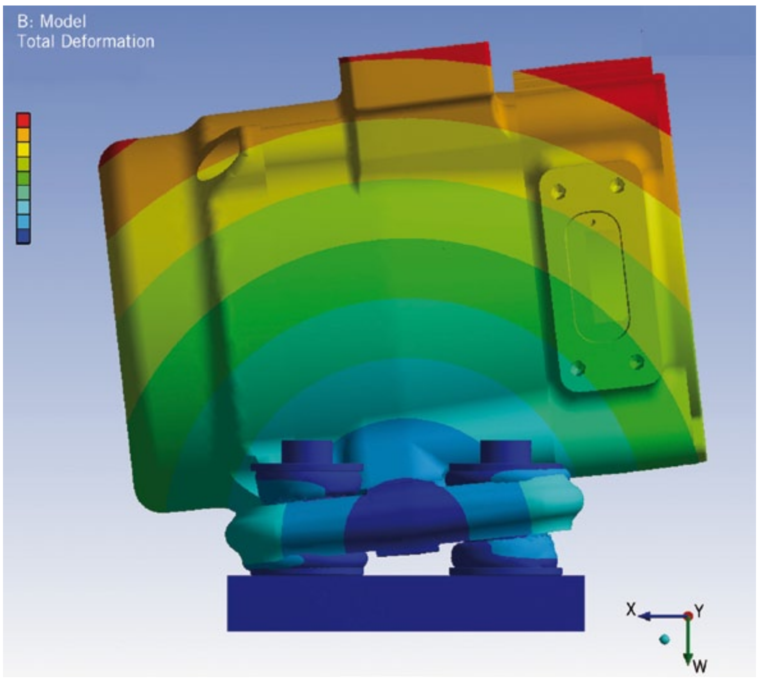

❺ Modal analysis of an electric powered oil pump: example of vibration mode

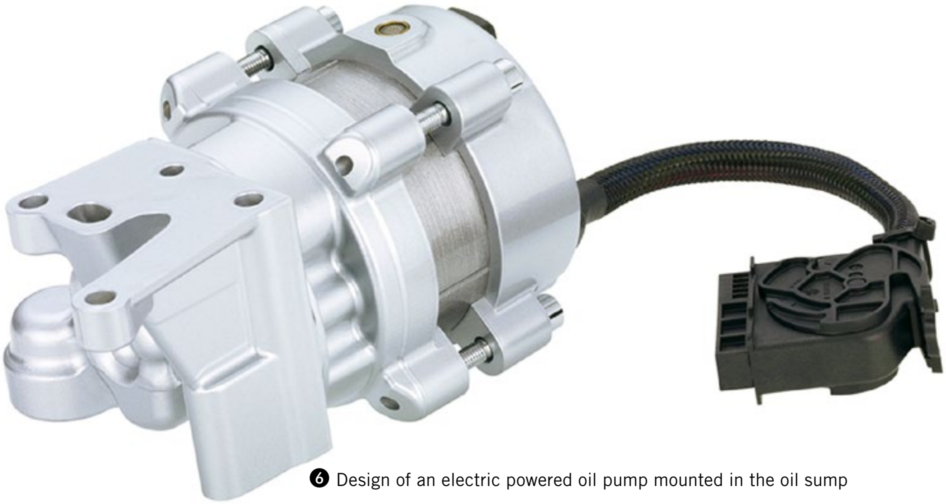

❻ Design of an electric powered oil pump mounted in the oil sump

Indeed, thanks to the increasing software and computational capabilities, also no-linear problems can be relatively easy managed as, for instance, the behaviour of rubber dampers, ❺.

As a result, through such simulations, it is possible to identify potential weak points in any component and adopt corrective actions during the early design phase.

CONCLUSIONS

The logic pattern of the design process for an electric powered oil pump has been described. Ideally, it runs from the analysis of the requirements to the definition of the design. Nevertheless, it is important to emphasise that this process is iterative and not as linear as described.

From the analysis of the market requests and following this process, two technical mainstreams have been developed respectively for pumps located inside the oil sump or mounted externally.

Both have as a common target compactness and simplicity. Nevertheless, the optimisation of the design according to the different boundary conditions led to different technical solutions for other aspects.

On the one hand, for pumps located inside the oil sump any minor leakage does not represent an issue. This feature has been exploited to simplify the design and get rid of additional sealing and motor housing, so that the stator is exposed on the outside, ❻. At the same time, a wet running rotor has been adopted and an internal oil flow created to have a cooling effect on the motor.

On the other hand, for externally mounted pumps a dry runner rotor has been preferred to avoid the creation of an internal oil circuit, more complex in the case of an external pump. Nevertheless a smart solution has been developed to cool down the power electronics using the oil.

Ultimately, although every new project has its own peculiarities, these two technical mainstreams represent a solid foundation to start any new design process.

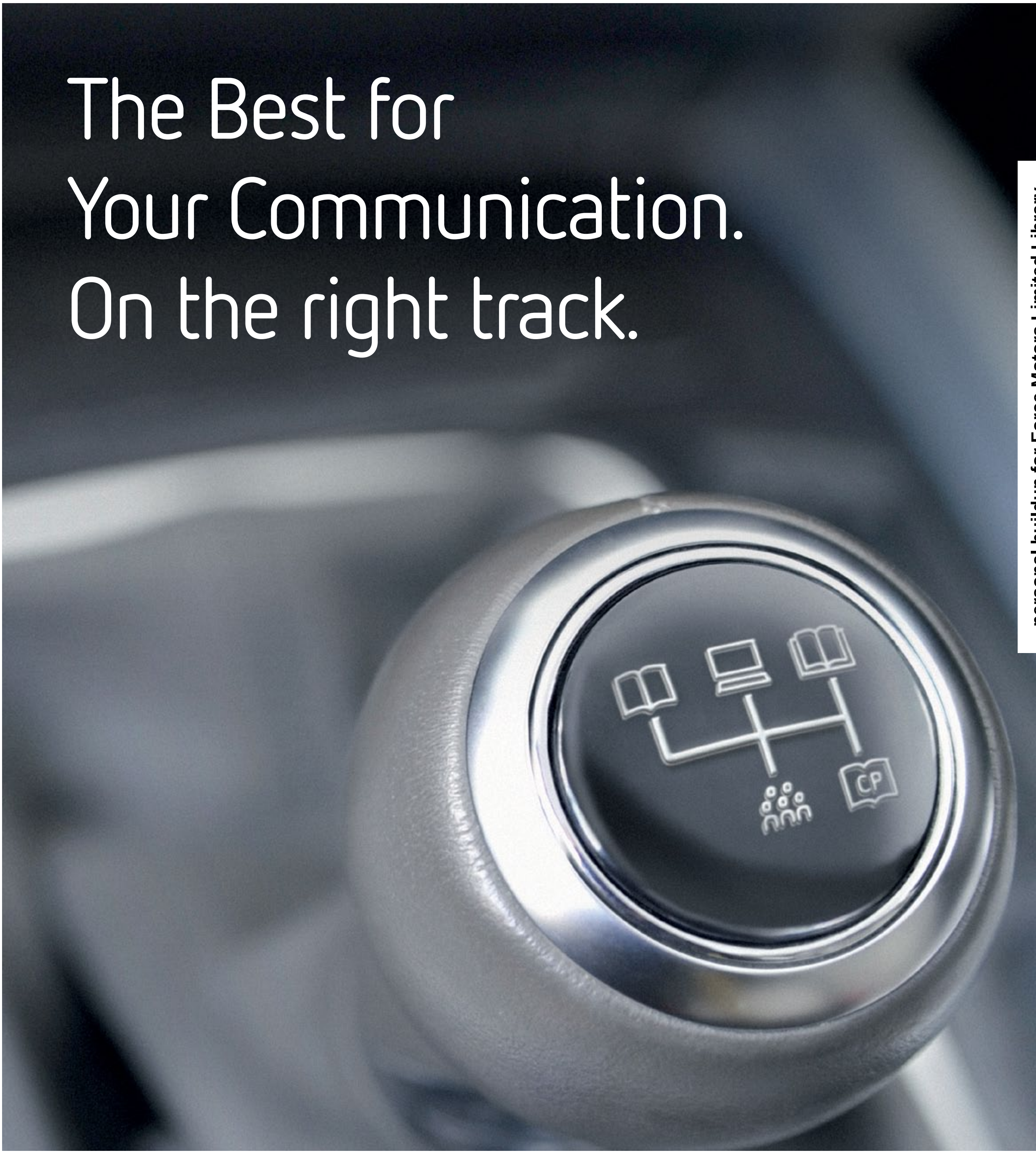
The Best for
Your Communication.
On the right track.
CP

MODULAR WATER CHARGE AIR COOLING FOR COMBUSTION ENGINES

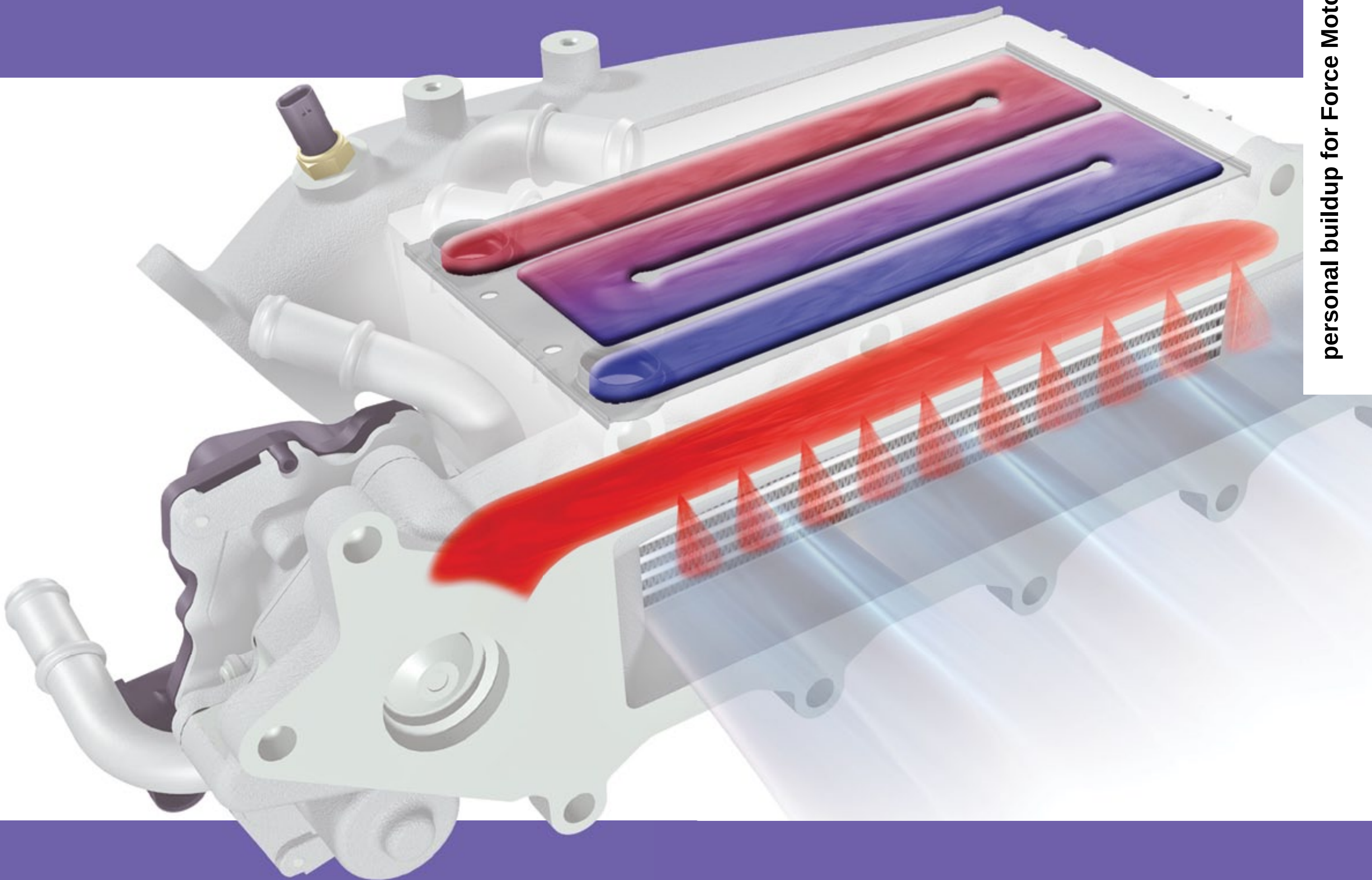

Valeo shows which considerations were taken into account with the development of a modular water charge air cooling range, such as the advantages for the engine system, the heat exchanger's material choice with respect to corrosion requirements due to exhaust gas recirculation as well as thermal and mechanical aspects due to the integration of the water charge air cooling into an intake module directly mounted onto the cylinder head.

AUTHORS

SVEN BURGOLD
is Business Development Director Air Intake at Valeo Powertrain Thermal Systems in Le Mesnil-Saint-Denis (France).

JEAN-PIERRE GALLAND
is R&D Manager Air Intake at Valeo Powertrain Thermal Systems in Le Mesnil-Saint-Denis (France).

BENJAMIN FERLAY
is Air Intake System Manager at Valeo Powertrain Thermal Systems in Le Mesnil-Saint-Denis (France).

LAURENT ODILLARD
is Air Intake System Product Engineer at Valeo Powertrain Thermal Systems in Le Mesnil-Saint-Denis (France).

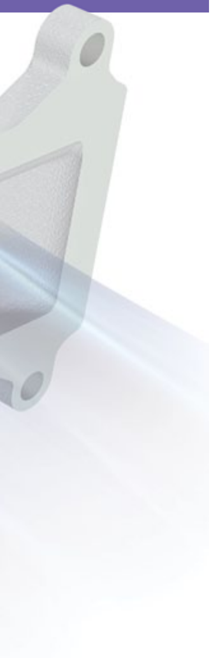

ADVANTAGES OF WATER CHARGE AIR COOLING

Indirect or water charge air cooling (WCAC) technology offers firstly the possibility of charge air thermal management by regulating the coolant flow and secondly the possibility to reduce the air volume between compressor of the turbocharger and the intake ports of the engine. This technology provides a solution between the conflicting targets of compact packaging, the achievement of the charge air cooler thermal performance target and the reduction of gas side pressure drop and in that way contributes to improved transient engine behaviour.

For over a decade, WCAC systems have been introduced on performance six-cylinder and eight-cylinder engines. A first downsized four-cylinder gasoline engine with a WCAC integrated in the air intake has been introduced in 2007, followed in 2012 by a four-cylinder diesel engine, both manufactured by VW.

The WCAC integrated in the air intake offers less architectural complexity, intake air temperature stability independent of engine load as well as improved transient behaviour of the engine due to the reduction of charge air volume and charge air side pressure drop compared to a conventional charge air path with air charge air cooling (ACAC) systems. For engines equipped with a low pressure (LP) exhaust gas recirculation (EGR) system, the charge air thermal management is enabled by regulation of the coolant flow and thus condensation effects and icing can be avoided, [1].

CHALLENGING FUTURE EMISSION REGULATIONS

The future world light-duty test cycle (WLTC) [2] will require emission homologation at higher engine loads than the current New European Driving Cycle (NEDC), ❶. Consequently for diesel engines it will require EGR also in an extended operation window compared to NEDC. For gasoline engines the map areas outside the NEDC map window will also need specific focus due to the fact that the inner engine cooling through fuel enrichment will then penalise the homologated fuel economy.

Furthermore, it is expected that engine pollutant emissions need to be certified in future at low ambient temperature (-7 °C). As a consequence, improved cold start and engine warm up will become a development target for future engine concepts.

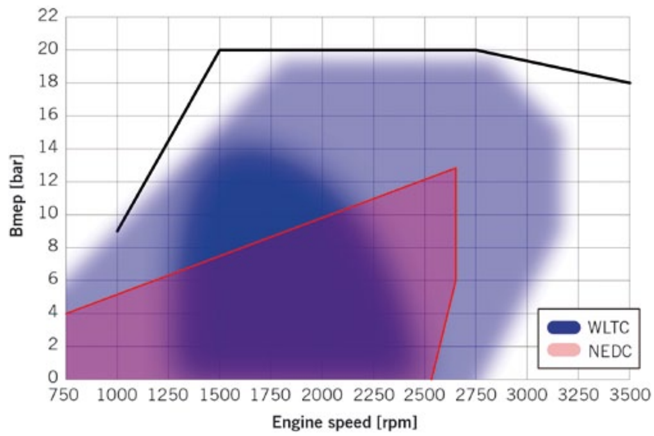

❶ Comparison: NEDC to WLTC for a diesel engine

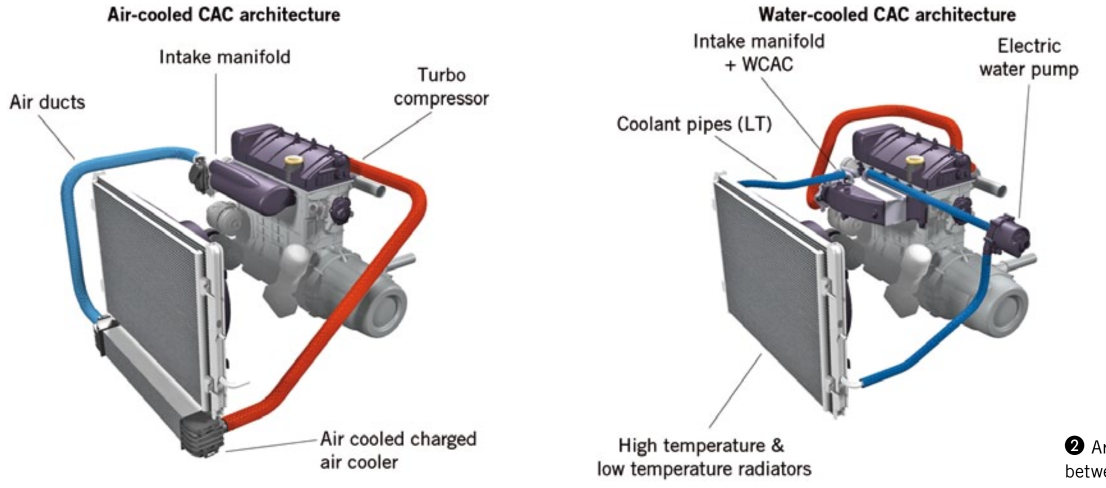

❷ Architecture comparison between ACAC and WCAC

INFLUENCES ON ENGINE PERFORMANCE

With WCAC technology, the pressure losses from turbocharger to intake port are lower. Given that water specific heat power is 3.5 times higher than air specific heat power, a liquid cooled heat exchanger is much smaller than an air cooled one for the same cooling power. Indirect charge air cooling reduces the air intake loop volume up to 50 %, charge air ducts can be shortened and in the case the WCAC is integrated into the intake manifold, one charge air duct can be eliminated, ❷. Moreover, if the WCAC is integrated into the manifold, thanks to larger inflow surface, the pressure loss of the exchanger core is also reduced as the velocities in front of the core are lower.

REDUCED PUMPING LOSSES

The pressure loss decrease allows reducing the turbine work while keeping the same boost pressure at intake valves. The airflow through the turbine can be lowered through increasing the waste gate rate, this leads to lower temperature upstream of the turbine and to reduced exhaust pressure. Without any optimisation of the turbocharger nor the engine, the pumping work is reduced by up to 5 to 10 % at high engine loads.

Considering a gasoline engine, ❸, for a constant boost pressure at full load, the upstream pressure can be decreased through waste gate discharge. The lower upstream temperature helps the turbine temperature to remain below its limit and, therefore, leads to less overfueling.

VOLUME REDUCTION AND TRANSIENT BEHAVIOUR

The air intake loop volume decrease improves the engine transient behaviour and reduces the turbocharger response time from a low engine load to a full torque demand. For a constant enthalpy at the inlet and the outlet of a given volume and for an identical heat exchange, Eq. 1 shows the impact of the air volume V on the pressure variation inside that same volume.

EQ. 1

$$\frac{dP}{dt} = \frac{\gamma}{V}(r \times Tin \times Qm_{in} - r \times Tv \times Qm_{out}) + \frac{\gamma - 1}{V}\left(\frac{dQ}{dt}\right)$$

The air intake loop volume decrease leads to a reduction of the pressure variation time and, therefore, to a faster engine response which is directly perceived by the vehicle driver. For example, a WCAC air path with a volume of 2.2 dm³ builds up a pressure variation of 5 % two times faster than the ACAC air path with a volume of 4.5 dm³.

DIMENSIONING OF THE LOW TEMPERATURE LOOP

The low temperature (LT) coolant loop in its less complex variant is composed of a WCAC, a low temperature radiator (LTR), an electrical water pump (EWP) and several coolant hoses to connect the different items. The design target is always to achieve the lowest possible charge air outlet temperature by using minimal hydraulic pump power. To achieve an optimum stable charge air outlet temperature, the heat exchanger characteristics of both, the LTR and the WCAC, need to be optimised to achieve a coolant flow

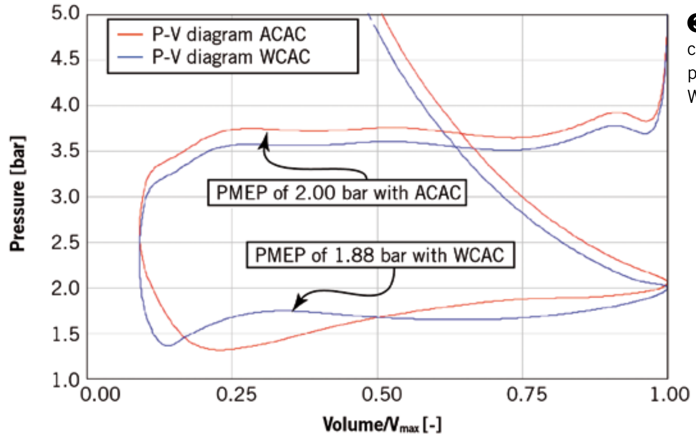

❸ P-V diagram comparison: intake air path for ACAC versus WCAC operation zone with minimum charge air outlet temperature variation. The EWP operating strategy allows controlling the charge air temperature.

LP EGR AND CONDENSATION RISK

The LP EGR gases contain gaseous liquid components. A condensation effect occurs when the compressed fresh air and EGR gas mixture is cooled down below the dew point which lies between 35 and 38 °C depending on the gas pressure and composition.

In engine bench tests, condensate quantities up to 1 to 1.5 l/h have been observed at coolant inlet temperatures of 20 °C into the WCAC and engine load equivalent to 100 km/h steady-state speed [3]. In specific vehicle driving situations favouring condensate formation – low engine load, short driving distances, gas temperature in the charged air cooler below dew point – these condensates will not be dried and then be accumulated at the lowest point of the charge air path – typically in the ACAC in the front of the vehicle.

As mentioned before, future emission homologation cycles are expected to require fulfilment of emission targets also at significantly lower ambient temperatures down to -7 °C. As a consequence, the occurrence of condensate generating engine operating points will increase, thus leading to the need to manage the charge air outlet temperature after the cooler above the dew point temperature.

A system with ACAC can be equipped with a charge air cooler by-pass valve to limit the charge air cooler thermal power for the desired conditions. The compactness of the WCAC system allows the integration into the manifold. Thus, a natural draining and drying will be achieved if condensates are generated.

HEAT EXCHANGER MATERIAL AND CORROSION REQUIREMENTS

To protect the heat exchanger against corrosion due to the condensation of LP EGR gases, a specific material combination has been developed for the coolant channel of the WCAC. The target has been to avoid an in depth corrosion attack by maintaining a superficial corrosion. The improved aluminium alloy combination, the so-called multiclad, has been compared to a reference alloy. Both went through a VDA (German association of the automotive industry) corrosion test (norm 230-214 for engine mounted components). The reference material exposed to a test solution with an pH-value of 3.5 and 10 ppm Chloride (Cl-) showed a beginning of intergranular corrosion whereas the multiclad material did not show any intergranular corrosion for both, the solution with pH 3.5 and 10 ppm Cl- as well as an even more severe solution with pH 3.5 and 1000 ppm Cl-, ❹.

THERMAL AND MECHANICAL ASPECTS

Charge air by-pass between manifold housing and WCAC core must be avoided. In case of a by-pass, a significant charge air mass flow will enter the intake ports without having been cooled down, resulting firstly in a decrease of the thermal efficiency and secondly in a local increase of the air temperature upstream of the intake valves. A 1 % by-pass mass flow leads to a 1 % loss in thermal efficiency and thus impacts the knocking limit for a gasoline engine.

WCAC INTEGRATION INTO THE INTAKE MANIFOLD

The structural WCAC aluminium module is from far the strongest concept against high temperatures and charge air pressure levels. It eliminates the by-pass leakage between manifold housing and exchanger core. Furthermore, the structural WCAC allows the integration of high pressure (HP) EGR and features like gas distribution rail into outlet tank, or EGR valve integration. Thermoplastic air intake manifolds are at that point not suitable as the temperature is much too high and they are limited for engines with low to medium specific engine power output. Furthermore, an aluminium WCAC module which becomes a manifold structural element offers the advantage against plastic manifolds as there is no need of having an envelope around it.

The dimensional advantage of the aluminium module, ❺, allows the integration of a bigger and therefore more efficient heat exchanger in a given engine packaging. Thus, such a module increases the thermal performance while reducing the charge air pressure drop by bigger

pH	Chloride [ppm]	Sample	Max. depth [µm]	Max. depth [%]	Type
3.5	10	Standard	95	17	inter
3.5	10	Multiclad	no		no
3.5	1000	Multiclad	51	12	clad

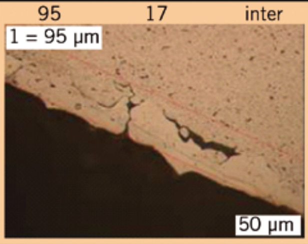

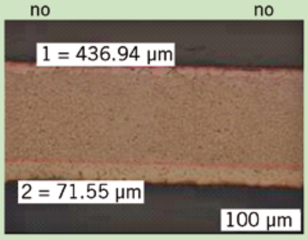

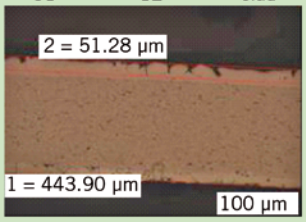

❹ Coolant channel material cut after corrosion test cross sections and the coolant pressure drop due to an increased number of coolant channels.

WCAC THERMAL SIZING

The WCAC sizing is linked to the heat dissipation and charge air side pressure loss requirements. The hydraulic power consumption of the LT coolant loop (consisting of LTR, WCAC and coolant pipes) is also an important parameter, as it determines the size of the EWP. There is a guideline how to define the necessary heat exchanger volume, ❻. Additionally to that core volume, space for coolant spigots and air guiding components must be considered. This packaging aspect must be addressed at early engine concept development stage. That way, the full WCAC benefit can be reached.

The WCAC modular range is based on heat exchangers with a depth of 60/90/120 mm and width between 160 and 320 mm corresponding to the cylinder head width of two- to four-cylinder inline engines. Typical heat exchanger heights are between 60 and 110 mm, depending on the specific engine's thermal requirements.

SUMMARY

Diesel and gasoline mass production engines with WCAC have been increasingly introduced on the market starting from 2007. In particular, the WCAC integrated into the air intake manifold offers reduction of pumping losses as well as less charge air line packaging and air path complexity.

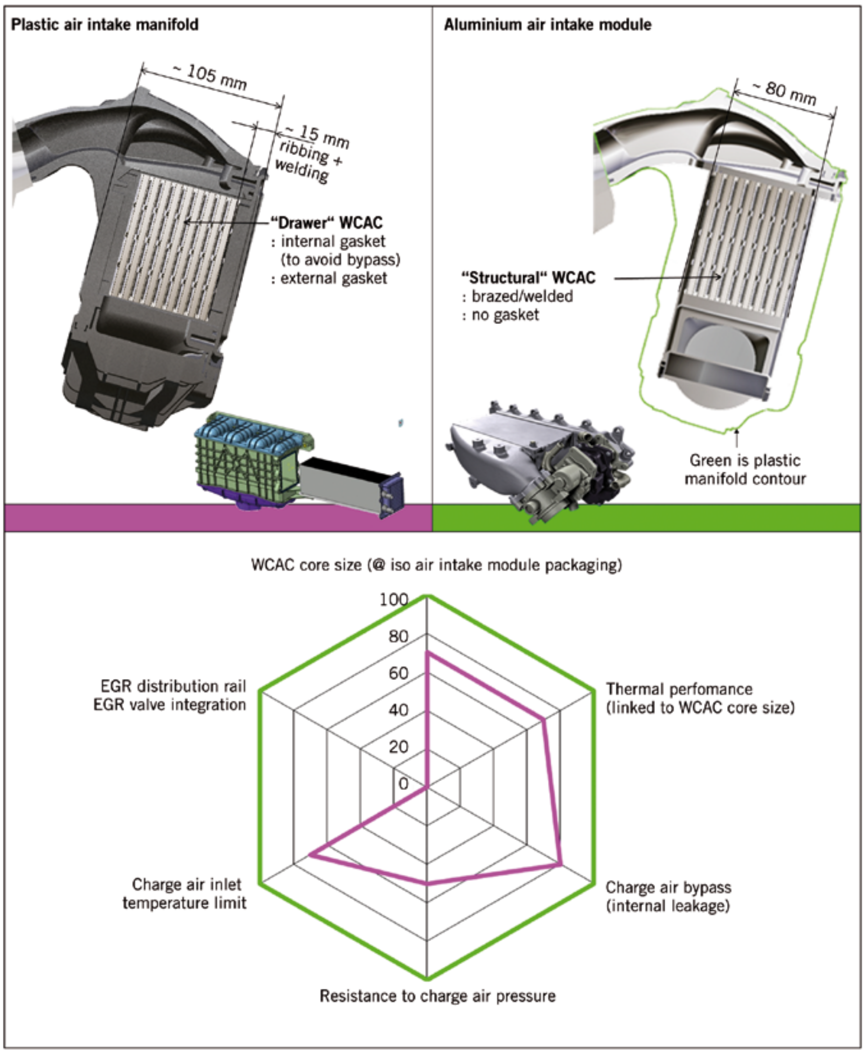

❺ Comparison of different WCAC integrations into an air intake manifold

Due to the required packaging volume in the intake manifold area, the most advantageous way is to start the integration right away from the base engine design phase. A simultaneous engineering of both the WCAC and the associated

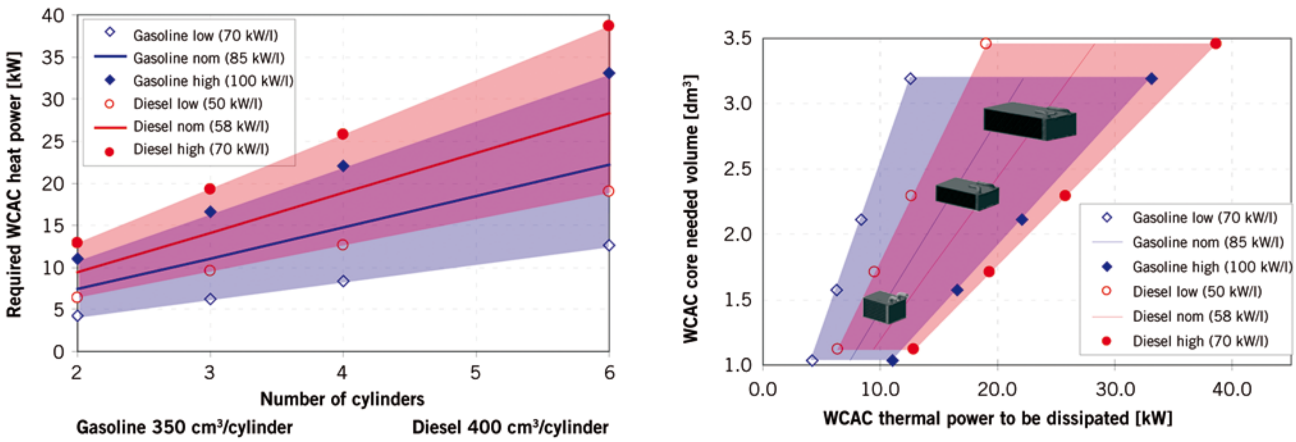

❻ Heat dissipation requirement as a function of downsizing level and engine displacement and heat exchanger core volume (dm³) as a function of thermal power vehicle front end cooling system is mandatory as the WCAC is an intake component whereas the low temperature coolant radiator is part of the vehicle front-end cooling module.

The WCAC offers the opportunity to enable thermal management of the intake air and EGR mixture and thus contributes positively to solve new problems arising through the use of LP EGR in a broader engine map window required for upcoming emission legislation. To protect the cooler against corrosion due to LP EGR gas side condensates, a new aluminium alloy with improved corrosion resistance has been developed.

The trend to higher specific engine power and to LP EGR systems leads to high gas temperatures at the inlet side of the manifold integrated charge air cooler. For high end engines, a full aluminium manifold offers the best compromise in terms of packaging and thermal performance. In case of additional flows as uncooled HP EGR will be introduced in the intake module after charge air cooler, the operating conditions lead to the selection of aluminium.

As an outlook, the intake manifold integrated WCAC will also enable further intake air thermal management functions, such as integration of a charge air by-pass for improving cold start operations. Together with the vehicle cooling system – working at multi coolant temperature levels – the vehicle cooling needs arising from engine emission compliance at cold start, very hot external temperatures, the cooling architecture compatibility with new hybrid vehicles and comfort functions can be managed in a modular way for both the engine and vehicle cooling system.

REFERENCES

[1] Neußer, H.J. et al.: Volkswagen's new modular TDI generation. Vienna Engine Symposium 04-2012
[2] WLTC (World Light-duty Test Cycle) Version 5 for Phase 2 validation (16-4-2012)
[3] Moroz, S. et al.: Adv. Cooling Systems for LP EGR in a TC Diesel Car Engine. Fisita 2008-06-152

PRESSURE PULSATION DAMPERS FOR INJECTORS

Pressure pulsations in the fuel injection system impede the formation of optimum spray properties and mixture formation. FMP Technology and KW Technologie have developed a porous body-based pulsation damper for gasoline engines that is suitable for all injectors. It suppresses opening and closing pulsations, thus allowing reproducible injection quantities to be achieved, even for short injection periods of fractions of a millisecond.

AUTHORS

PROF. DR. DR. H. C. FRANZ DURST
is Founder and Managing Director of the FMP Technology GmbH in Erlangen (Germany).

ARTHUR HANDTMANN
is Chairman of the Board of the Albert Handtmann Holding GmbH & Co. KG in Biberach (Germany).

DOMINIK HASPEL
is Development Engineer for gasoline engine injection systems, responsible for the simulation and theoretical design of injectors at the FMP Technology GmbH in Erlangen (Germany).

LARS SCHILLING
is Development Engineer for gasoline engine injection systems, responsible for the design and construction of injectors and common rail systems as well as for the development of test rigs at FMP Technology GmbH in Erlangen (Germany).

AIM OF WORK

Gasoline engines with separately operating injectors, for the direct injection of fuel in each cylinder, represent the present state-of-the-art. The injectors used in gasoline engines operate at pressures of up to 200 bar in order to provide fuel sprays with very fine droplet distributions with Sauter diameters of about 20 µm, generated by round hole nozzles. Using multiple fuel injections, combustion methods with direct injection can be realised, which would not be feasible with the intake-manifold fuel injection of conventional gasoline engines. Stratified and homogeneous combustion methods can be realised, but investigations show that further improvements of combustion methods and thus improvements of exhaust emissions are only possible when the pressure pulsations, caused by opening and closing, the injector valves can be inhibited. The latter are inherently related to the required fast opening and closing of the valves and can reach ±30 % of the mean operating pressure of an injector.

This is shown below in the time-varying pressure distribution in front of an injector, ❶. The time-varying pressure distribution in front of an injector, for example injector 2, shows that the high-frequency pressure variations caused in front of an injector by sudden velocity changes of the fuel at the beginning and at the end of an injection. Neither the influence of the pump nor the pressure loss in the common rail during injection can be recognised at first sight in the illustrated pressure profile.

Furthermore, ① shows that not only the injection of a considered injector causes pressure pulsations in front of this injector but in addition, the injections of the other injectors of an gasoline engine cause induced pressure variations. Pressure pulsations, which are caused by one of the injectors, run from this injector into the common rail and from there through the connecting pipes to the other injectors. This dependency between the injectors can only be eliminated if the pressure waves caused by the considered injector are significantly damped. The development of improved combustion methods in gasoline engines can lead to reduced emissions. The achievable improvements depend on whether the pressure pulsations, occurring in common rail injector systems, can be damped in a way that controlled fuel injections become possible. In order to achieve this goal, FMP Technology GmbH has carried out developments for the damping of pressure pulsations within the framework of a ZIM project (Pressure wave reduced, quickly operating injector valves for Otto and Diesel combustion engines) of the Federal Ministry of Economy and Technology and on behalf of KW Technologie GmbH & Co. KG. These developments are summarised in this publication and are also described in a previous publication [1].

THEORETICAL CONSIDERATIONS AND AMESIM CALCULATIONS

Porous bodies can be theoretically treated like parallel capillaries, [2]. These capillaries enable the damping of pressure pulsations, based on the relation between pressure drop and the corresponding volume flow, Eq. 1.

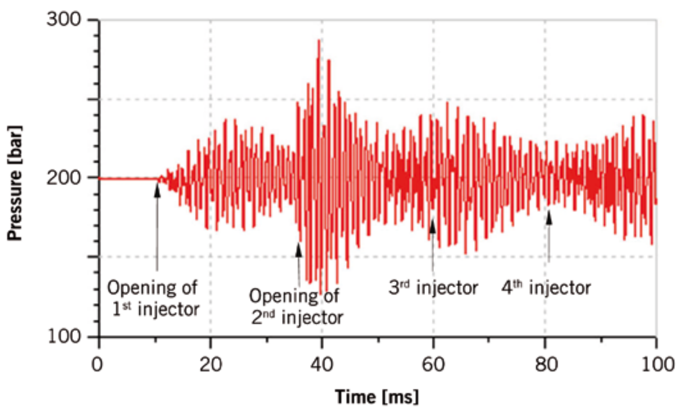

❶ Pressure pattern in front of the second injector in a common rail with four injectors

EQ. 1	$\Delta P = \frac{8\,\mu \dot{V}_c}{\pi r_c^4}\,\Delta L$

$\dot{V}$ is the total volume flow (with $\dot{V} = N\dot{V}_c$, N = number of capillaries, $\dot{V}_c$ = volume flow through one capillary), r_c is the radius of the capillaries, $\left(\frac{\Delta P}{\Delta L}\right)$ is the pressure gradient in the capillaries, μ is the viscosity of the fuel.

Thus, energy dissipation of the pulsations is the basis of pulsation damping. The flow through the individual capillaries, as shown in ❷, is the theoretical basis for the damping effect. The medium diameter of the capillaries and the number of capillaries can be calculated as in Eq. 2:

EQ. 2	$d_c = \frac{0.46 \cdot \varepsilon \cdot d_p}{1 - \varepsilon}$

d_c is the diameter of the capillaries, d_p is the grain diameter and ε the porosity of the porous material.

The Number of capillaries can be calculated as in Eq. 3:

EQ. 3	$N = \varepsilon \cdot \left(\frac{D_p}{d_c}\right)^2$

N is the number of capillaries, ε the porosity of the porous material, D_p the total diameter of the porous body and d_c is the diameter of the capillaries.

The pressure loss, caused by the employment of capillaries, can be kept low when a bundle of parallel capillaries is used. Thus, a capillary bundle, appropriately designed, represents a functional and applicable pulsation damper, ②.

For further theoretical investigations, simulations using the programme Amesim were carried out for one-dimensional problems of pulsation damping. ❸ illustrates the simulation model which was used for the investigations. It deals with an injector system, comprising a common rail, a supply pipe, and the actual injector. The latter is designed according to a pre-chamber volume and the injector nozzle for the spray generation is connected to it. An opening and closing valve induces the actual injection process. ③ clearly shows the pressure pulsations induced by the opening and closing process, which can be eliminated by the use of the suggested pulsation dampers based on porous bodies. An optimisation of the parameters of the porous bodies results in very good damping of the pressure pulsations. The pressure changes, obtained in the injection system during injection while the common rail was closed, can be clearly seen.

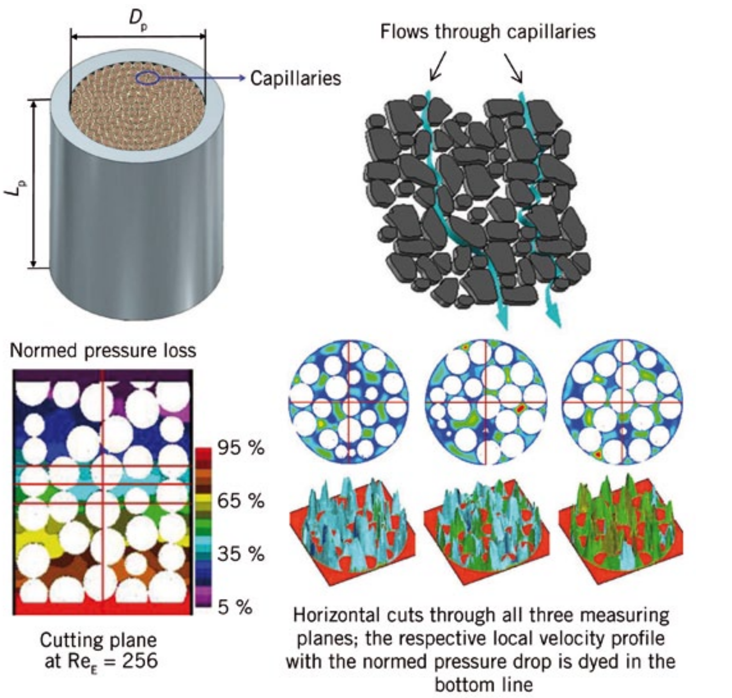

❷ Numerical treatment of flows through porous media and illustration by means of capillary flows

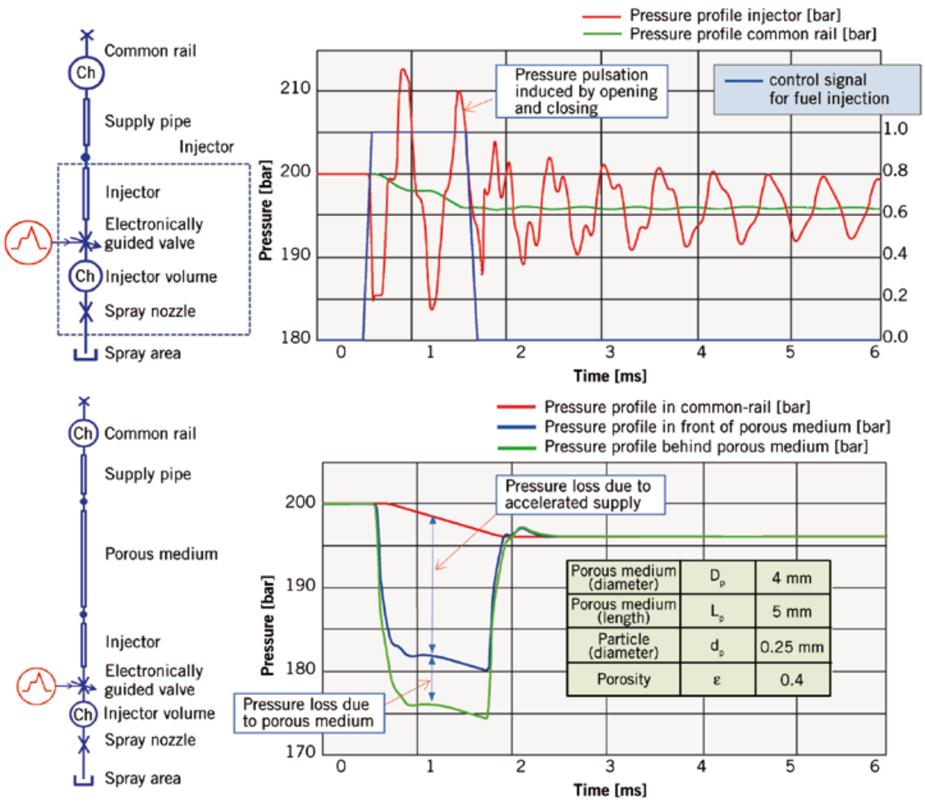

❸ Simulation of included pressure pulsations with the Amesin calculation method

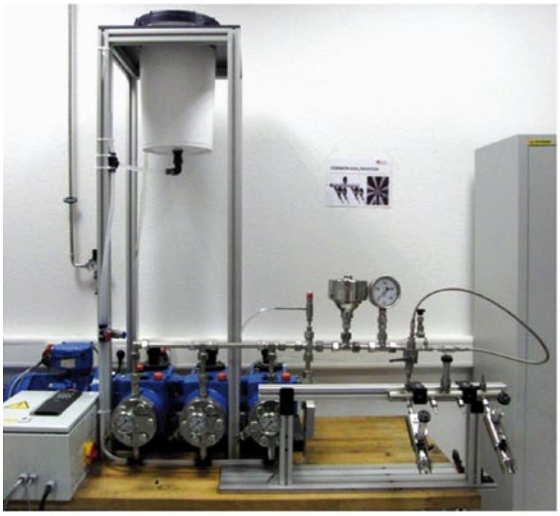

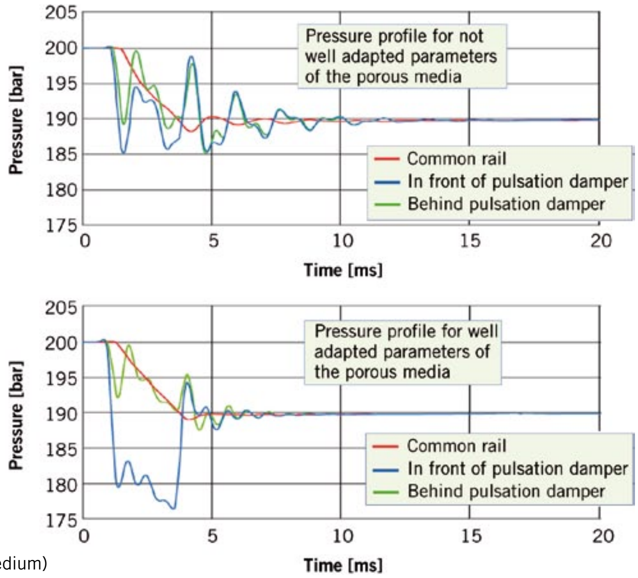

❹ Test rig and measurement results for various pore geometries (right above: non-suitable porous medium, right below: suitable porous medium)

EXPERIMENTAL INVESTIGATIONS

The results of the system behaviour simulation showed how pressure pulsation dampers based on porous media need to be designed, manufactured and applied in order to be used in injection systems for gasoline engines. The appropriate porous body inserts were manufactured and integrated into the supply pipes of a common rail for four injectors. In order to test the effect of the porous body inserts on the pressure pulsations caused by the operation of the valve, a test rig was set up, which is shown in ❹. This test rig enabled the performance of a series of experiments to adapt the properties of the applied porous bodies, such as the sphere diameter d_p, the length L_p and the porosity ε, in a way that the desired damping of the pressure pulsations started. Results are also shown in ❺. For the measurements, the common rail was loaded to a determined pressure and subsequently separated from the pump. When a suitable porous medium was chosen, very good damping properties were achieved in the investigated injection systems. The functioning of the designed pulsation dampers was verified in extensive experiments at the high-pressure test rig.

In summary, it is evident that the pulsation damper enabled the total elimination of the interaction of the injectors. When the injector marked in green, ⑤, was operated without pulsation damper, the passive injector, marked in blue, showed significant pulsations. This is shown in the diagram on the left. On the right it is shown that the injector, marked in blue, is not affected by pulsations when the injectors are equipped with pulsation dampers. It shall be pointed out that fast injections are possible, to which the developed pulsation damper can react, as shown in the diagram on the right. The results presented in the illustration above correspond to a pre-injection of 0.5 ms, a main injection of 2 ms and an after injection of a further 0.5 ms. With the current system, pre-injections are also possible in the range of 0.25 ms if the actuator and its electronics allow this.

The exemplary results presented above clearly show that the development of a pulsation damper, which reacts to fast injections with its whole damping effect, has been a success. Pulsation damping could be realised technically because of theoretical investigations concerning the damping effect of capillaries. As calculations using the Amesim programme showed, high frequencies can be dampened well while low frequencies can only be dampened poorly. As the pressure pulsations during the opening and closing of injection valves are high-frequency, it is possible to dampen them. Therefore, combustion processes in gasoline engines as well as fuel consumption and CO_2 emissions can be much better controlled.

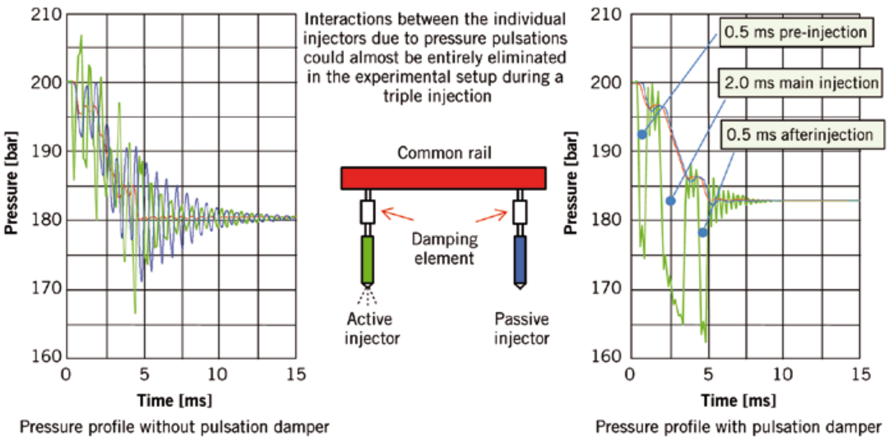

❺ Schematic of the test rig and measurement results for injectors without (left) and with (right) pulsation dampers

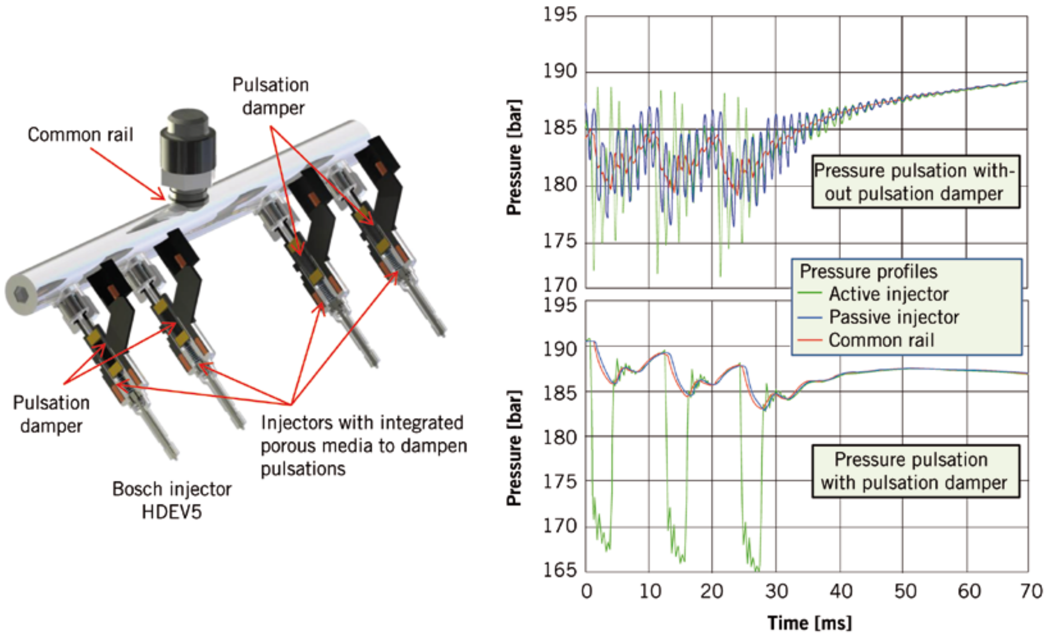

❻ Common rail with Bosch injectors (HDEV5) with integrated pulsation damper and illustration of pressure pattern with and without dampers

PULSATION DAMPERS FOR GASOLINE ENGINES

The illustrated developments resulted in a method for damping pressure pulsations and integrating the damper into injector systems. As shown in ❻, injectors of this type can be integrated into a conventional common rail system without having to adapt the existing system any further. The developed pressure pulsation damper is installed between the common rail and the actual injector. Again, the comparison of the pressure profiles in the damped and un-damped system clearly shows the positive influence of the damping elements on the pressure profile. The results obtained within the framework of the author's work regarding the damping effect of porous bodies for the reduction of pressure pulsations in injection systems were compared to other methods described in the literature. The methods examined comprised classical methods, such as the use of orifices for partial reflection and the resulting overlay of pressure waves for the elimination of pulsations, as well as novel methods such as a "mini common rail" inside the injector where the damping is reached through the volume or the bypass injector system described by the authors of this publication, see [1], which can almost entirely avoid the emergence of pressure pulsations.

In summary, from all examined systems, only the bypass injector was able to achieve a fuel reduction in pressure pulsations comparable to the system with porous media. As the bypass injector has to pump a large amount of fuel continuously due to its functionality whereas the dampers based on porous media do not need any additional components, the concept of damping pressure waves by means of porous media seems to be the best and the most suitable method for gasoline engines. In addition, it is transferable to diesel engines.

Combined with twin-jet spray generators [4], the pulsation dampers described here can be applied to create injection systems which have outstanding properties for the well-controlled combustion in engines. The work described here provides a significant contribution to a more controlled combustion in gasoline engines. Thus, the preconditions for the reduction of emissions and the further development of engines for the future are fulfilled.

REFERENCES

[1] Durst, F.; Haspel, D.; Ünsal, B.; Resch, R.: Schnell schaltende Einspritzventile mit praktisch druckwellenfreien Kraftstoff-Zuführleitungen. In: MTZ 68, (2007), No. 10, pp. 86-92

[2] Bird, R. B.; Stewart, W. E.; Lightfoot, E. N.: Transport Phenomena. Wiley & Sons: Hoboken/USA, 2002

[3] Zeiser, T.: Simulation und Analyse von durchströmten Kugelschüttungen in engen Rohren unter Verwendung von Hochleistungsrechnern. Verlag Dr. Hut: München, 2008

[4] Durst, F.; Handtmann, A.; Weber, M.; Schmid, F.: Injektoren mit Doppelstrahldüsen für Ottomotoren. In: MTZ 73 (2012), No. 6, pp. 484-491

RAPID CONTROL PROTOTYPING FOR CYLINDER PRESSURE INDICATION

Cylinder-pressure-based controls that allow cycle-synchronous reactions to events in the combustion chamber are a particularly promising possibility further optimising engine combustion processes. However, the requirements of real-time cylinder indication are fast pushing today's systems up against their limits. The Institute for Combustion Engines at RWTH Aachen University and dSpace together developed a high-performance prototype for online indication with cycle-synchronous combustion control.

AUTHORS

DIPL.-WIRT.-ING. JAN PFLUGER
is a research associate at the Institute for Combustion Engines at RWTH Aachen University (Germany).

DR.-ING. JAKOB ANDERT
is Project Manager for Vehicle Electronics and E-Mobility at FEV GmbH in Aachen (Germany).

DIPL.-ING. HOLGER ROSS
is Product Manager for Rapid Control Prototyping Systems at dSpace GmbH in Paderborn (Germany).

DIPL.-ING. FRANK MERTENS
is Lead Product Manager for Rapid Control Prototyping Systems at dSpace GmbH in Paderborn (Germany) .

MOTIVATION

To save fossil fuel resources and further reduce toxic emissions, new methods of optimising are necessary in addition to hybridisation and electrification. One particularly promising possibility is cylinder-pressure-based controls that allow cycle-synchronous reactions to events in the combustion chamber. These require that the cylinder pressure is measured and the characteristics are calculated in real time so that they can be processed in engine management [1].

Developing innovative, cylinder-pressure-driven combustion processes requires powerful hardware and software. Rapid control prototyping (RCP) systems are a well-established method with OEM and suppliers. With powerful hardware and support from the model-based development process, developers can very quickly determine the potential of any new approach. RCP platforms are used at an early development phase to replace engine ECU that is not yet available. They are based on powerful embedded processors with PowerPC or x86 architectures and on operating systems that ensure real-time behaviour, fast boot times and reliable, autonomous, in-vehicle operation. However, the requirements of real-time cylinder indication are fast pushing today's systems up against their limits. To capture cylinder pressure data, compute the relevant characteristics, and feed them back into the closed-loop engine management, high processing power and minimum response times and latencies are necessary. For example, a processor in a current RCP system uses, on average, 60 % of its capacity to calculate the indicated mean pressure and the centre of combustion for one cylinder in only a 0.1 ms task [2]. This resolution is insufficient for complex controls, and at the same time the processing capacity available for further algorithms is considerably restricted. This is why a new system approach is being used for RCP in combustion process development.

In a cooperation project, the Institute for Combustion Engines at RWTH Aachen University and dSpace together developed a high-performance prototype for online indication with cycle-synchronous combustion control. The main focus of this is to combine, in dSpace's Micro Auto Box II RCP system, a processor and a field-programmable gate array (FPGA) that can be programmed via a model-based tool chain. This enables users to distribute algorithms flexibly on the processor and the FPGA, and results in considerably increased performance compared with purely processor-based RCP systems. In addition, a set of basic functions for indication was developed for the FPGA.

HARDWARE ARCHITECTURE AND DEVELOPMENT ENVIRONMENT

With its hardware architecture and parallel processing ability, the programmable FPGA provides ideal conditions for the online analysis of complex cylinder pressure data, ❶. This can significantly reduce the load on the processor, and additional processing capacity can be used for the control and the actual engine management. With the FPGA, signal preprocessing can be performed for different I/O channels, and individual functions for cylinder pressure anal-

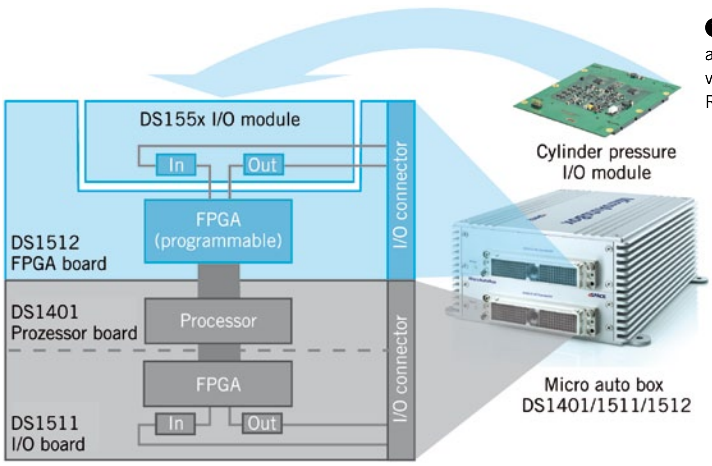

❶ FPGA processor architecture for a vehicle-capable RCP system

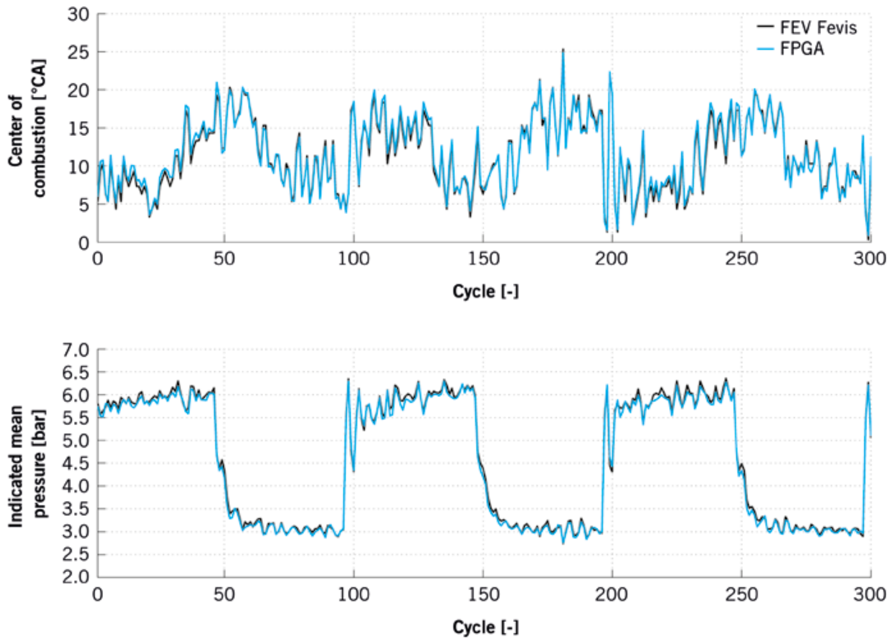

❷ Comparison of the indicated mean pressure and centre of combustion of the FPGA blockset with the results of the FEV reference system

ysis can be executed in parallel independently of one another. This speeds up computation and enables deterministic time behaviour. It is these properties that also make the FPGA ideal for designing fast, cascaded controllers with the underlying controller part implemented on the FPGA, where cycle times of a few microseconds are easily achievable.

The FPGA is connected to the main processor via a bus system that is specially designed for RCP use. This guarantees very short response times and latencies so that even complex engine management models can be implemented with the typical 10-kHz sampling rate.

The I/O converters – such as ADC, DAC or digital I/O for connecting sensors and actuators to the FPGA – are located on separate plug-on I/O modules and can be replaced to suit different application scenarios and requirements. In addition to the real-time indication interfaces, other sensor/actuator interfaces are also available via the I/O Board of the RCP-System or via a modular signal conditioning and power stage platform with which the RCP-System can be extended.

FPGA DEVELOPMENT WITH MODEL-BASED SYSTEM DESIGN

With RCP systems, model-based system design based on Matlab/Simulink allows fast iteration cycles for optimisation without requiring specialist knowledge of any particular programming language. In contrast, FPGA are traditionally programmed with hardware description languages such as VHDL or Verilog. This allows all the resources on the FPGA to be accessed and the functions to be optimised. In the RCP system environment with processor-FPGA architecture, the Xilinx System Generator (XSG) Blockset is used for model-based FPGA programming. This makes it possible to develop functions model-based and implement them directly on the FPGA without any intermediate manual steps. Users can continue working in their familiar development environment and concentrate completely on designing functions and algorithms.

FPGA BLOCKSET FOR INDICATION

The entire indication functionality that was developed is implemented on the FPGA, and the engine management that builds on it is computed on the processor. Signal preprocessing, including position encoder evaluation and drift compensation for the cylinder pressure signal, is integrated into the FPGA functionality to ensure high temporal resolution for the input signals.

The evaluation provided by the FPGA blockset also includes computation of the indicated mean pressure, the heat released by fuel conversion, and the resulting combustion behaviour including the start, centre and end of combustion. Wall heat transfer can also be included, but to make parameterisation easy, it is not integrated as standard. The blockset also calculates the maximum pressure and maximum pressure gradient, as well as the associated crank angle in the work cycle. All the implemented functions run in real time with a resolution of 0.1 crank angle degrees, and the FPGA also allows the algorithms to be processed at temporal resolutions of up to 12.5 ns without using extra resources. Calculation of the centre of combustion has also usually completed within 0.1 crank angle degrees after the end of combustion.

The algorithms developed in this cooperation project are designed to evaluate a single-cylinder engine and are now being transferred to a four-cylinder engine. The available FPGA resources will also be able to support six- and eight-cylinder engines in future development steps.

VALIDATION BY TEST BENCH MEASUREMENTS

The developed system was validated on a HIL test bench and also on a single-cylinder SI engine and compared with a

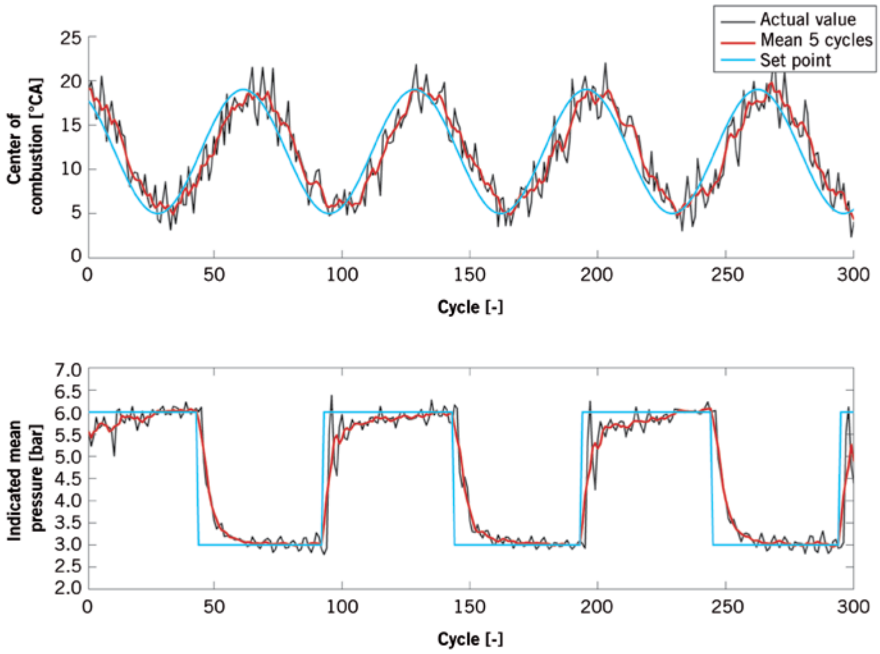

❸ Simultaneous control of the centre of combustion and mean pressure based on evaluation by the FPGA blockset

commercial real-time analysis system from FEV GmbH, as a reference. ❷ shows the results of both systems for mean pressure and centre of combustion across 300 work cycles with varying loads and ignition times.

The results of computing the centre of combustion show a good match across the entire operating range, with a mean deviation of 0.52 crank angle degrees. The indicated mean pressure also shows slight deviation of only 0.057 bar, and the remaining deviations can be explained by the different calibration of the crankshaft position.

In the second step, the cycle-synchronous combustion control was implemented by means of FPGA indication. This involved implementing an engine management system and a control on the processor part of the RCP-system that adjusts the valve control times, the injection quantity and the ignition time. ❸ shows an example of the behaviour of the two variables.

The graph demonstrates the successful use of the software within the closed control loop without prior parameterisation. The actual values follow the curve of the reference values with only a few work cycles' delay, which is due to the integrative part of the PI controller used. Cycle-synchronous evaluation makes it possible to react to a control deviation in the very next work cycle and therefore to optimise the control behaviour in transient operation.

APPLICATION FIELDS FOR THE BASIC BLOCKSET

The basic blockset that was developed allows indication values to be used at an early point in the process of developing combustion engines and combustion processes. The values can be used directly within the engine management with little effort. This makes it possible to replace complex modelling of the current torque by highly precise measurement.

The commissioning and measurement of the combustion engine can be significantly accelerated. Because indication values are available, the load and centre of combustion can be controlled within the engine management without additional hardware or software. The combustion process can easily be adapted by means of indication, for example, to different fuel grades or alternative fuels. Easy integration of controller limits and switch-off thresholds based on indication values contributes to safe operation, both on the test bench and in the vehicle.

By integrating engine management and indication in a single device, a minimum controller latency is achieved. The indication values are available 0.1 crank angle degrees after completion of the combustion cycle, allowing cycle-synchronous intervention for maximum system dynamics. Control applications that make tough demands on real-time capability and precision, such as controlled auto ignition (CAI), can especially benefit from the advantages of the basic blockset. The vehicle-capable hardware means that such innovative approaches can also be tried out and measured in the vehicle.

POTENTIAL OF FPGA-BASED CONTROL

In addition to the functions of the basic blockset, users can also implement their own functions in the FPGA via a programming interface. They can therefore model combustion chamber process such as wall heat transfer or the varying gas composition in greater detail. This supports further adaptation to the specific requirements of a particular application case.

Using indication signals is also recommended for acoustic evaluation of the combustion process. For example, a highly dynamic, closed loop control can be implemented to optimise the acoustic behaviour of diesel engines, ❹.

There is further potential for combustion control if control interventions can be initiated within one cycle, ❺.

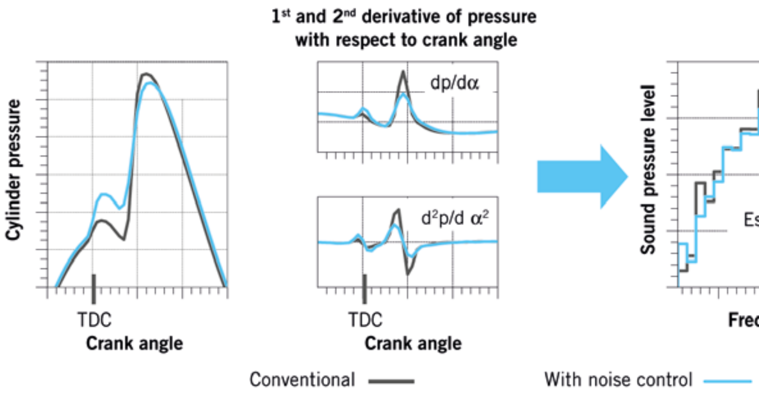

❹ Possible real-time control of diesel engine acoustics by using indication (schematic)

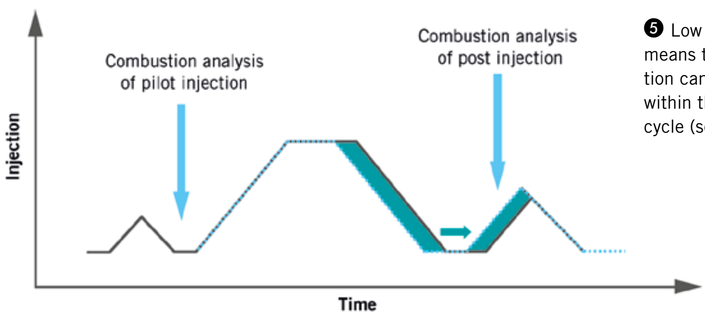

❺ Low system latencies means that control intervention can be performed within the ongoing work cycle (schematic)

For example, the combustion behaviour of the pre-injection can be evaluated, and subsequent injections can be suitably adjusted, in the same cycle. This provides promising options that can hardly be represented with conventional methods, especially for optimising diesel engines [3].

CONCLUSION

The project involved developing an application-specific I/O interface module for the FPGA of the RCP-system from dSpace and a basic blockset of indication functions. The functionality allows innovative, cycle-synchronous control approaches to be implemented. The FPGA's performance makes it possible to significantly speed up the functions used, with minimum system latencies. The extensibility of the FPGA provides the necessary degrees of freedom for future applications to meet the ever more complex demands of combustion process development.

REFERENCES

[1] Zhao, H.: HCCI and CAI engines for the automotive industry. Woodhead Pub., 2007
Andert, J.: Modellbasierte Echtzeitoptimierung der ottomotorischen Selbstzündung. RWTH Aachen University, Dissertation, 2012
Schnorbus, T.: Zylinderdruckgeführtes Einspritzmanagement beim Dieselmotor. RWTH Aachen University, Dissertation, 2010

THANKS

This report is the result of research cooperation between dSpace GmbH and the Institute for Combustion Engines at RWTH Aachen University under the direction of Prof. Dr.-Ing. S. Pischinger. The authors would like to express their thanks for the funding received under ZIM, the central innovation program for small and medium-sized businesses. Thanks are also due to Dr.-Ing. Martin Nijs, Dipl.-Ing. Peter Sternberg and Dipl.-Ing. Rene Savelsberg for their cooperation on the project.

SPRINGER-VIEWEG.DE

Including more than 160,000 technical terms for handling construction projects abroad

Klaus Lange

Elektronisches Wörterbuch Auslandsprojekte Deutsch-Englisch, Englisch-Deutsch; Electronic Dictionary of Projects Abroad English-German, German-English

Vertrag, Planung und Ausführung; Contracting, Planning, Design and Execution

2010. EUR 169,95

ISBN 978-3-8348-0883-7

The electronic technical dictionary „Projects Abroad" is indispensable for all those communicating and negotiating with contractors, clients or engineers in English in the context of construction projects abroad.

With some 84,000 English-German and 76,000 German-English entries it is one of the most comprehensive reference works on the market, covering engineering, operations and legislation in the construction sector - a reliable companion to help you successfully handle construction projects abroad.

The UniLex Pro user interface includes many search features including a pop-up search option that automatically displays translations in a pop-up window - regardless of the program being used at the time.

System requirements:

- Windows 7, XP
- Available hard disk space: min. 200 MB
- Core memory: min. 512 MB
- CD-ROM drive

About the Author

He has worked together with international partners to offer numerous seminars preparing students for construction projects abroad.

Yes, please send me

Fax +49(0)6221 / 345 – 4229

___ Copies
Elektronisches Wörterbuch Auslandsprojekte Deutsch-Englisch, Englisch-Deutsch; Electronic Dictionary of Projects Abroad English-German, German-English
ISBN 978-3-8348-0883-7
EUR 169.95

Company ______ Surname, First Name ______

Department ______

Street (no P.O. boxes, please) ______ Postal Code | City ______

Date | Signature ______

Springer Vieweg

Ordering is easy at: SpringerDE-service@springer.com Phone +49 (0)6221 / 345 – 4301

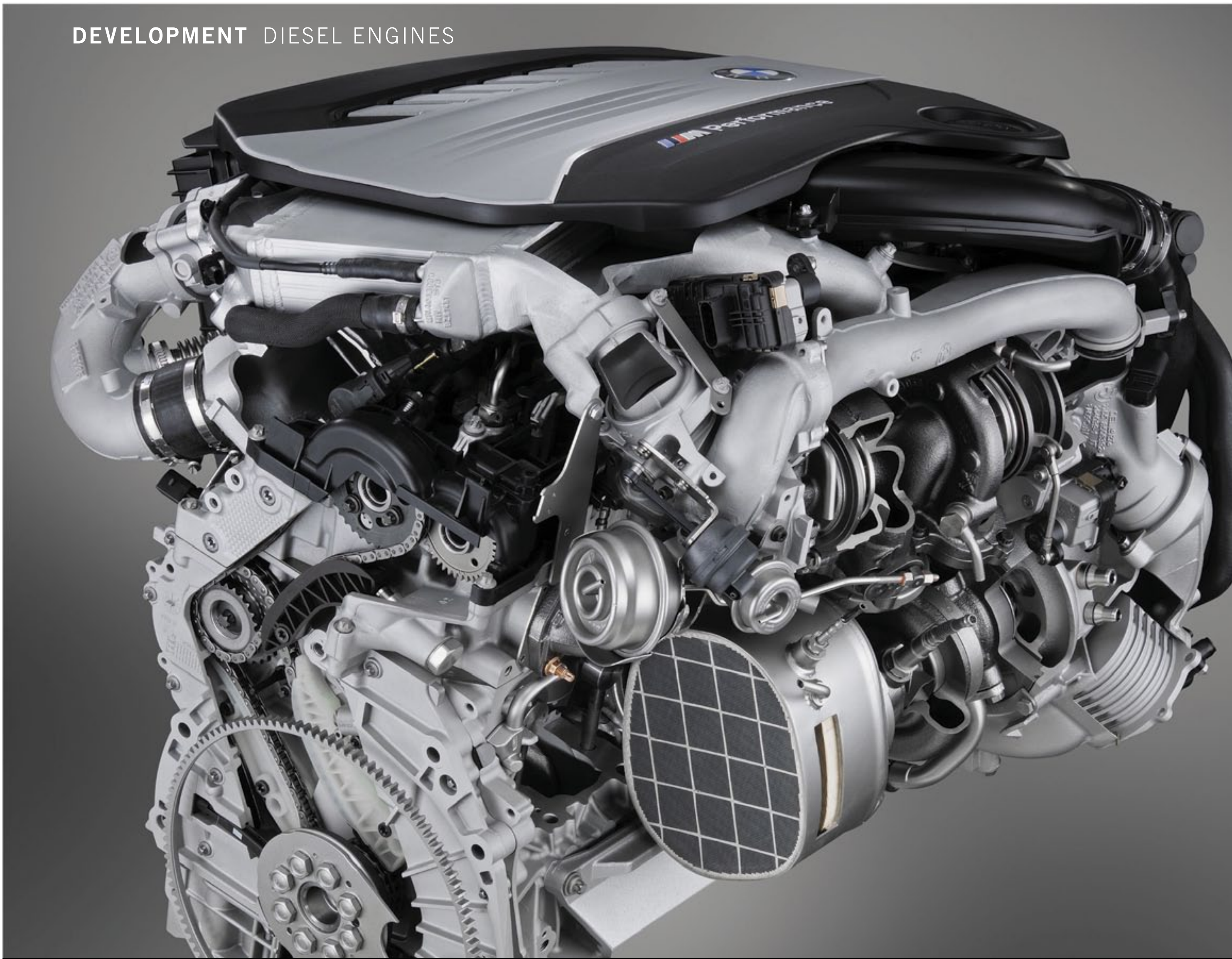

THE NEW BMW SIX-CYLINDER DIESEL ENGINE WITH THREE TURBOCHARGERS

PART 2: INTAKE, COOLING AND EXHAUST

BMW is presenting a further milestone in diesel engine development, the newly developed TwinPowerTurbo version of its 3.0-l six-cylinder engine for M Performance vehicles. The new engine, which is a consistent expansion of BMW's proven modular engine family, develops a specific power output of 93 kW/l and torque of 247 Nm/l, putting it in a leading position among passenger car diesel engines. Achieving these figures demanded more than a combination of an innovative turbocharger system and a highly stress-resistant base engine alone. In addition to a high-performance intercooler, it also required an optimum design of the intake and exhaust system specifically for high levels of turbocharging. The development of these components and the results achieved in the vehicles are described in this second part of the report.

AUTHORS

DIPL.-ING. JOHANNES DWORSCHAK
is Project Manager for diesel engines at the BMW Group in Steyr (Austria).

DIPL.-ING. ROLF FELTES
is Head of the engine peripherals for diesel engines department at the BMW Group in Steyr (Austria).

DIPL.-ING. THOMAS FORTNER
is Head of the exhaust re-treatment for diesel engines department at the BMW Group in Steyr (Austria).

DIPL.-ING. WERNER MALLINGER
is Head of the mechanical systems and cooling for diesel engines department at the BMW Group in Steyr (Austria).

OBJECTIVE

The vehicle integration – and thus the layout of the air intake, cooling, and exhaust systems on the new BMW six-cylinder TwinPowerTurbo engine – led to challenges similar to those encountered during the initial implementation of the two-stage turbocharging concept on the BMW six-cylinder diesel engine in the year 2004 [1]. As long ago as 2004, it was possible to show the full performance potential of the two-stage turbocharging concept with more efficient use of existing components of the cooling and exhaust systems. In view of the virtually doubled values for air flow rate and required cooling output, the objectives to be achieved with the new top diesel engine system from BMW were no less challenging.

Deployment of the engine in the vehicles of the 5 series, 7 series, X5 and X6 series was another declared project objective. The planned deployment in a number of vehicle series meant that the complex and costly development of engine-specific body variants was eliminated as a possible solution approach. Instead, the aim was to create a dual system: On one hand, components from existing modular systems have been used. On the other hand, all engine-specific functions to be newly developed have been designed in such a way that they can be used unchanged over all vehicle series. This approach represents a maximum of efficient development work requiring no compromises whatsoever with regard to engine output.

AIR INTAKE SYSTEM

For all the air ducts, care was taken to ensure that conceptual synergies to existing BMW diesel engine modular systems were achieved. From the intake muffler to the entry point of the low-pressure stage, it was possible to design the engine-mounted air intake channel as a common part across the different vehicle derivatives, ❶. The intake muffler arrangement to the side of the engine can also be found in a similar form on the BMW six-cylinder basic engine; the filter cartridge is even a common part across all current six-cylinder diesel engines. The two-way unfiltered air intake for the X5 and X6 vehicle models is above the cooling module; on the 5 series and 7 series it is in front of the cooling module to the side.

Lowering the intake pressure loss was a key issue during the entire development. A number of measures ensure that the air mass flow through-rate of 1400 kg/h results in negative intake pressure that is as low as possible. Restricting development to the BMW 5 series, 7 series, X5 and X6 models led to greater freedoms in designing the intake muffler and fresh air ducts, making it possible to achieve additional enlargements in the cross section. The geometry of the clean air flow was also improved by means of numerical optimisation [2]. In total, this made it possible to reduce the pressure loss by more than 20 % relative to comparable versions of BMW diesel vehicles. Particular attention was paid here to the direct flow-on area of the low-pressure stage, ❷.

Despite very aerodynamic design, there are no acoustic irregularities in the outlet area. The pressure pulses triggered by the intermittent air induction are effectively reduced primarily by the multi-stage turbocharger system, an effect produced by the many impedance jumps and compressor wheels functioning as throttle points.

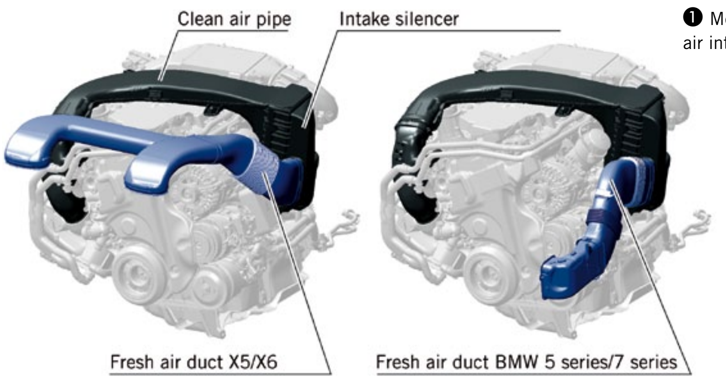

❶ Modular structure of air intake system

CHARGE AIR COOLING

The newly developed system must control the following boundary conditions:
: heat quantities of up to 50 kW to be dissipated
: air masses up to 1400 kg/h with minimum pressure loss
: charge-air pressure up to 4000 mbar (absolute).

High charge pressures, high air mass flow through-rates and high heat levels to be dissipated – the charge air cooling of the new high-performance engine has to meet these demanding requirements. The solution was found in a two stage indirect charge air cooling system, a first in BMW diesel engines. The first stage is integrated into the compressor housing of the low-pressure stage and serves as intercooling for the compressed charge air between the low-pressure stage and the two high-pressure stages. The second stage forms the classical part of the charge air cooling and is arranged directly in front of the throttle valve horizontally above the engine, ❸.

A major advantage of indirect charge air cooling is the possibility for a more or less rigid connection between exhaust turbochargers and intercoolers. Only when this requirement is met it can be ensured that sealing of up to 4 bar absolute pressure is kept under control with minimal pressure losses. Connection to vehicle-fixed components such as cooler and auxiliary water pump requires only hoses of small cross section.

In the shown charge air cooler branch of the coolant circuit, coolant flows through the main radiator and intercooler in parallel. In the vehicle, the low-temperature radiator and the auxiliary electric water pump of the eight-cylinder BMW TwinPowerTurbo gasoline engine have been adopted. The flow-optimised water circuit for the charge air cooling is connected via venting and filling lines to the main coolant circuit, which means that no additional expansion tank for the low temperature circuit was required. The combined effect of the individual partial circuits is shown in a diagram in ❹.

In order to provide optimal charge-air temperature in all operating states of the engine, the charge-air temperature and coolant temperature are continuously monitored. The determined values are used to regulate the water pump and electric fan.

At a charging pressure of up to 4 bar and not inconsiderable dynamic load, the strength requirement of the charge air cooling system demands the maximum from the geometric dimensioning of the intercoolers. This is why the intercooler boxes as well as all charge air lines on the pressure side were not made of plastic but of cast aluminium. This design also achieves excellent acoustic properties. On one hand, the aluminium tubes prevent the emission of high-frequency flow noise. On the other hand, the compact design means that the charge air duct components are located almost completely underneath the engine cover that is padded with absorption material. Indirect charge air cooling has an additional advantage: Vibrations of the engine are not transferred to the cooling module via the charge air hoses, which are very rigid during operation, and therefore not transferred to the vehicle.

The charge air cooling system that has been developed meets the package requirements of all vehicles in which the new high-performance diesel engine is deployed. It will be adopted into the vehicles of the 5 series, 7 series, X5 and X6 series unchanged on the engine side.

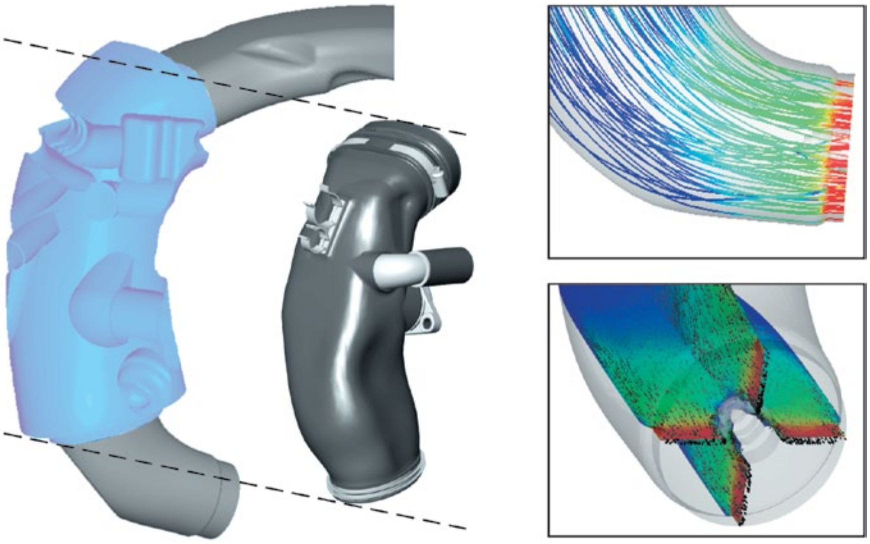

❷ Numerical optimisation of the clean air pipe

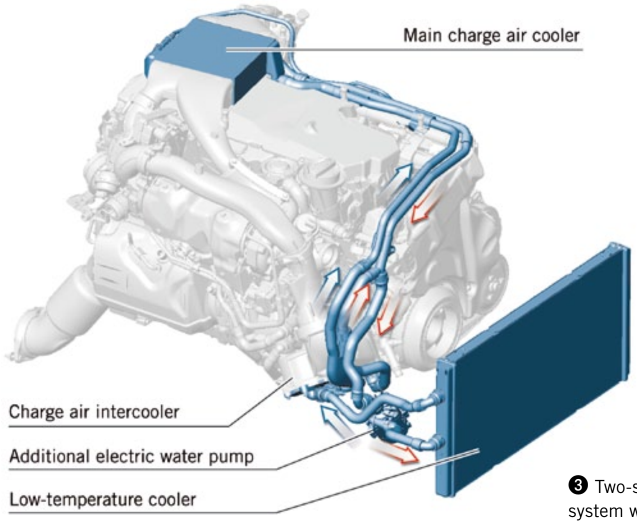

❸ Two-stage charge air cooling system with air ducts

VEHICLE COOLING SYSTEM

Alongside the layout of the charge air cooling, providing the corresponding cooling output in the high-temperature

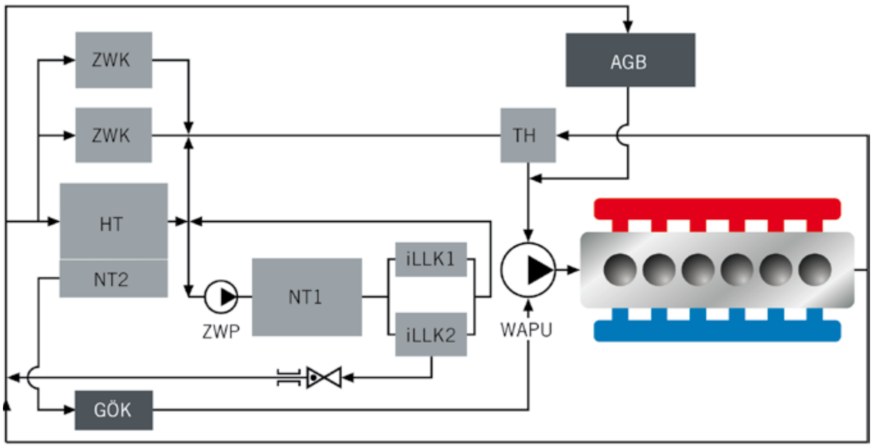

AGB	Expansion tank	**GÖK**	Transmission oil cooler
TH	Thermostat	**iLLK1**	Charge air cooler
ZWK	Additional radiator	**iLLK2**	Charge air main cooler
HT	High-temperature cooler	**ZWP**	Additional water pump
NT1	Low-temperature cooler for transmission oil	**WAPU**	Water pump
NT2	Low-temperature cooler for charge air		

❹ Diagram layout of cooling circuit

circuit also involved extensive challenges during development of the TwinPowerTurbo diesel engine. In the maximum engine output range, heat quantities of more than 170 kW have to be dissipated in the components of the cooling system in the vehicle, including charge air cooling. The components of the cooling module shown are a high-temperature cooling radiator with integrated under cooling section to cool the transmission oil, an air-conditioning condenser, a low-temperature cooling radiator for the indirect charge-air cooling, a power steering oil cooler and an electric suction fan with 850 W output.

In addition to the components arranged in the main field, up to two additional coolant radiators are deployed. These are positioned in front of the wheel arches and ensure outstanding thermal stability in all operating states. ❺ shows the arrangement applied in the vehicle with the 5 series as an example.

A mechanical water pump is used to deliver the coolant in the main circuit. This is already used in other BMW six-cylinder diesel engines and was adopted unchanged. The recourse to existing modular systems applies to most of the components – and to all vehicles in which the new high-performance engine will be deployed.

EXHAUST SYSTEM

In order to meet the power output targets, the exhaust mass flow had to be increased over the existing engine with two turbochargers to over 1400 kg/h. The systematic optimisation of the exhaust system and the reduction of the exhaust backpressure were therefore preconditions for producing the power output of the new variant with three chargers. The starting point is the optimised functional concept for an engine-proximate arrangement of the catalytic converter and diesel particulate filter (DPF) in a common housing, ❻. This is typical of all BMW diesel vehicles.

Thanks to simulation of the pressure loss at the individual components of the exhaust system, it was possible to implement suitable measures and achieve the target value of 500 mbar. One measure to reduce the exhaust backpressure was an enlargement of the DPF cross-section by approximately 14 %, whereby a uniform geometry across all vehicle derivatives was implemented with the new engine.

The DPF is made of SiC (Silicium Carbid) material and has a catalytic coating that is zoned in the direction of flow. The outside of the common housing for the particle filter and catalytic converter has acoustic-thermal insulation consisting of a fleece covered with a perforated metal foil. This design reduces the acoustic noise emitted by the component itself and absorbs airborne sound in the engine compartment [3]. The sensor sys-

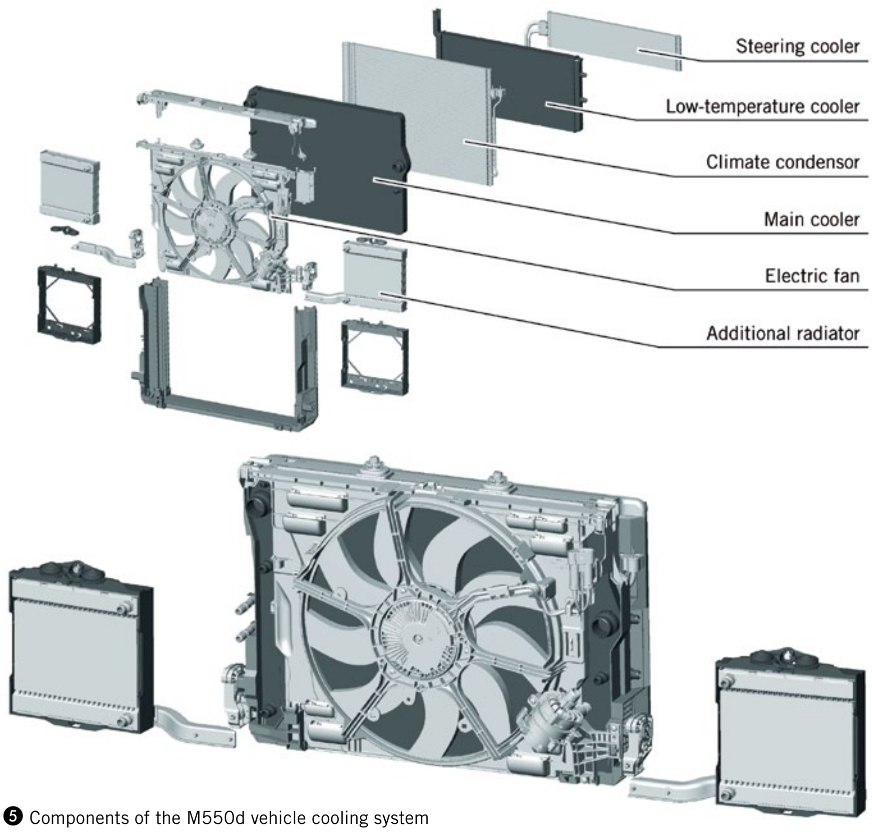

❺ Components of the M550d vehicle cooling system

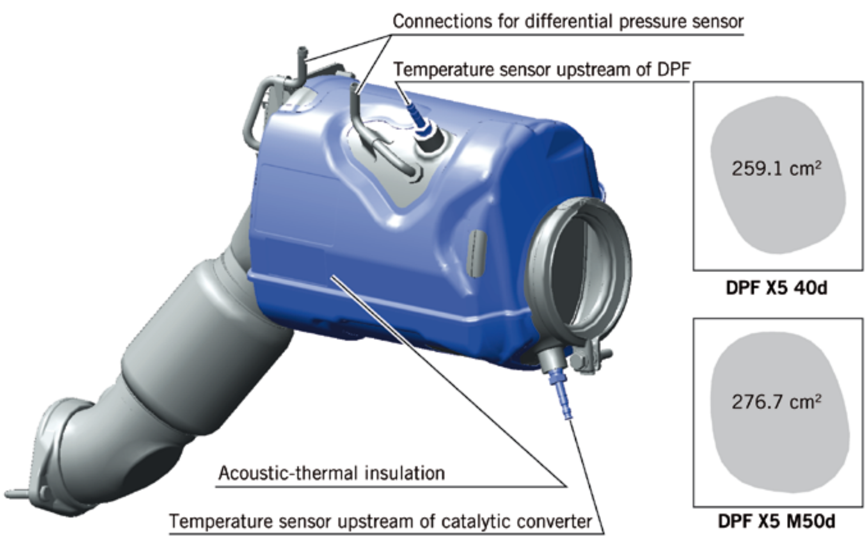

❻ Hot end with acoustic-thermal insulation

tem of the exhaust re-treatment system consists of a differential pressure sensor upstream/ downstream of the DPF, a lambda oxygen sensor upstream of the catalytic converter (integrated in the low pressure turbocharger), temperature sensors upstream and downstream of the catalytic converter, as well as a lambda oxygen sensor downstream of the DPF (Euro 6 only). A set of metal bellows, configured for a wide frequency range, separates the vibrations between the engine-mounted front and rear exhaust systems. The twin-channel exhaust system of the eight-cylinder gasoline engine is used in the vehicles of the X series in the rear area of the cold-end components to optimise the exhaust backpressure, ❼. In the 5 series and 7 series, the series-standard BMW so-called BluePerformance technology [4] enables pre-compliance with the future emission level Euro 6. The catalytic converter used here is designed as a NO_x storage catalytic converter.

The rear part of the exhaust system is two-way and contains a centre silencer as well as a rear silencer each on the left and right. The tailpipe trims have been specially designed for the new BMW top diesel engine versions with regard to shape and colour assignment. The reduction in the wall thickness of the pipes and mufflers to 1.5 mm achieves an optimal compromise between acoustic characteristics and weight. The increased exhaust mass flow rates meant that, compared to the 535d, the diameter of the pipes had to be enlarged from 65 to 70 mm. The associated increased noise development is essentially compensated for by a centre silencer that is designed as an absorber. Alongside the acoustic efficiency, particular attention was paid to the aerodynamic design of the absorber. The resonator end mufflers made using shell molding technology with integrated absorbers are configured for the 3rd engine order in the engine speed range of 1300 to 1800 rpm. They reduce the humming noise that occurs in the regeneration mode of the diesel particle filter to a level that is subjectively no longer perceptible. The high-frequency noise elements are reduced by the absorption cartridge. The design of the entire exhaust system is shown in ❽ with the BMW 5 series as an example.

RESULTS FOR THE COMPLETE VEHICLE

With the market launch of the 750d xDrive models in September 2012, the model family of the newly developed BMW 3.0-l six-cylinder engine is complete. ❾ summarises the vehicle performance and fuel consumption figures of all variants. Sports car performances, coupled with the low fuel consumption of a 3.0-l diesel engine, are the outstanding characteristics of all models. Thanks to the BMW typical xDrive all-wheel drive system that is typical of BMW and deployed as series standard in each type of vehicle, acceleration values that are on equal terms with turbocharged eight-cylinder gasoline engines are achieved. In the BMW 5 series and 7 series model, the exhaust re-treatment system BMW BluePerformance, which is also deployed as series standard, already ensures pre-compliance with the Euro 6 exhaust emission standard.

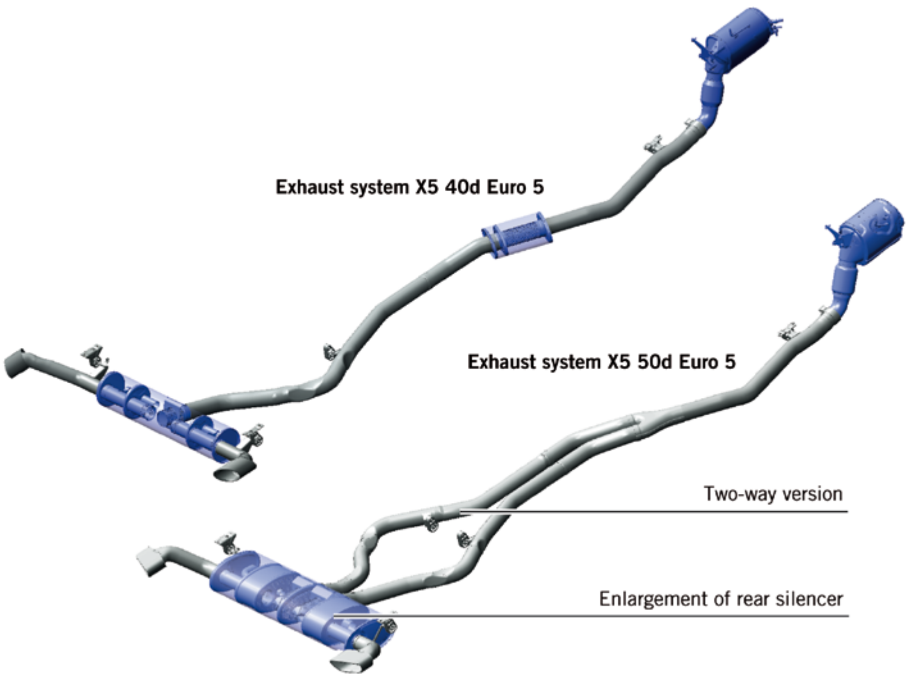

❼ Comparison of the exhaust systems X5 40d and X5 M50d

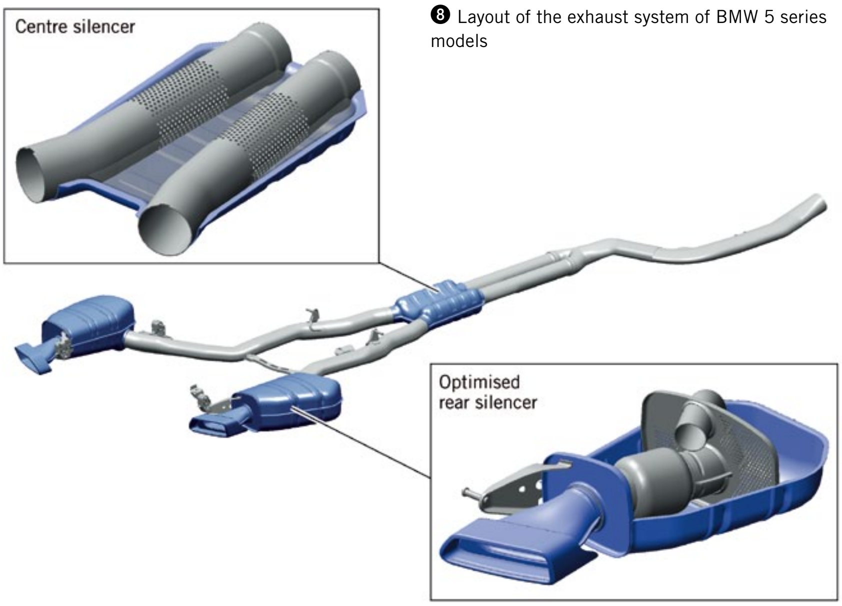

❽ Layout of the exhaust system of BMW 5 series models

	M550d xDrive saloon	M550d xDrive touring	750d xDrive	750Ld xDrive	X5 M50d	X6 M50d
Max. output [kW]	280					
Max. torque [Nm]	740					
0-100 km/h [s]	4.7	4.9	4.9		5.4	5.3
Top speed [km/h]	250 (limited)					
CO_2 [g/km]	165	169	169		199	204
Emission level	Euro 6				Euro 5	

❾ Vehicle performance and fuel consumption figures of all model variants

SUMMARY

The new BMW TwinPowerTurbo diesel engine is the youngest member of the BMW diesel engine family and at the same time is the top model in that family. Integration into the different vehicle product lines was a special challenge during development. The two-part strategy applied as the solution enables the intelligent combination of existing components of the vehicle modules with newly developed components that can be deployed across all model series. This procedure ensured development in line with the BMW EfficientDynamics strategy [5].

Particular highlights here are the two-stage indirect charge air cooling and the exhaust systems of the 5 series and 7 series. The latter permit the low exhaust back pressures while simultaneously complying with the Euro 6 exhaust emission standard.

Thanks to the performance capability of the air intake, cooling and exhaust systems, the peak power output of 280 kW can also be achieved in vehicles of the BMW 5 series. Furthermore, a maximum road speed of 250 km/h can be achieved for the first time in a vehicle of the BMW X5 and X6 series with a diesel engine system.

REFERENCES

[1] Kratowill, H.; Mattes, W.; Steinparzer, F.; Stütz, W.: Two-stage exhaust turbocharger on the BMW 3.0-liter 6-cylinder diesel engine. 13th Aachen Colloquium on Vehicle and Engine Technology, 2004
[2] Giovannini, A.; Haider, B.; Nefischer, P.: Optimization Methods in the Product Development Process of High Performance Diesel Engines. 2nd Conference on Applied Optimization, Karlsruhe, 2008
[3] Feltes, R.; Peuker, R.; Weber, F.: Complete vehicle and drive acoustics of the new BMW 525d. In: ATZ 114 (2012), No. 1
[4] Dworschak, J.; Neuhauser, W.; Rechberger, E.; Stastny, J.: The new BMW 6-cylinder diesel engine. In: MTZ 70 (2009), No. 2
[5] Langen, P.; Nehse, W.: BMW EfficientDynamics – a look to the future. 30th International Vienna Engine Symposium, 2009

THANKS

Dipl.-Ing. Erwin Rechberger, Head of the acoustics and vibrations for diesel engines department at the BMW Group in Steyr (Austria), also assisted in the production of this article.

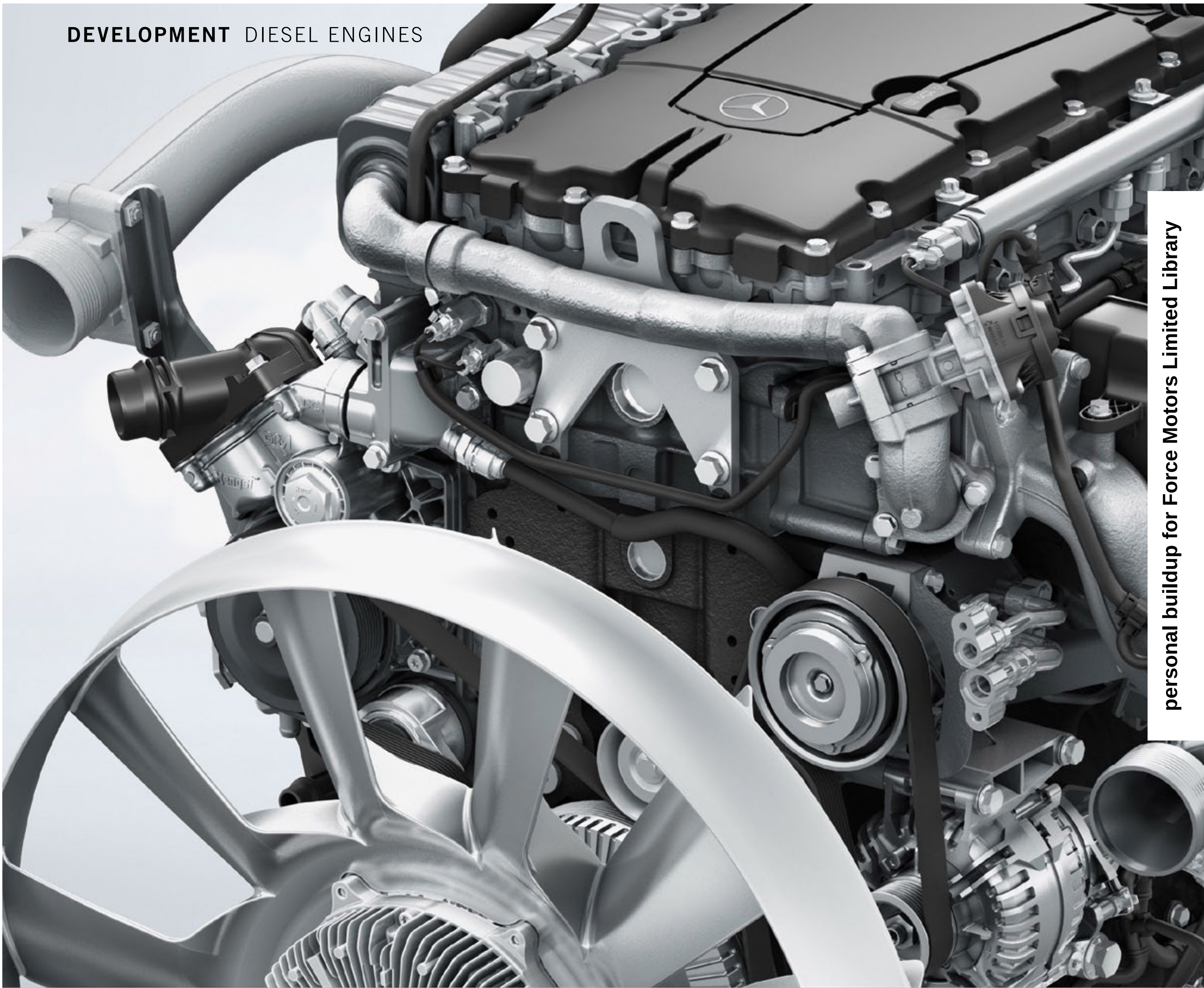

MERCEDES-BENZ MEDIUM-DUTY COMMERCIAL ENGINES

PART 2: APPLICATION AND DEVELOPMENT PROCESS

Daimler Trucks has launched a generation of all-new Mercedes-Benz diesel engines for medium-duty commercial vehicles with the coming into effect of the Euro VI emission standard. The concept of the new OM 93x model series was introduced in the first part of this article in MTZ 10. In the following, the second part covers the underlying operating strategies and the development process.

AUTHORS

DIPL.-ING. (BA) BÖRGE NIELSEN
is Senior Manager Testing OM 93x and was the R&D Project Leader for the new engine generation at Daimler AG in Stuttgart (Germany).

DIPL.-ING. HARALD HUTTENLOCHER
is Manager FEA and was Sub Project Leader CAE for the OM 93x at Daimler AG in Stuttgart (Germany).

DR.-ING. VOLKER SCHWARZ
is Manager Development Functions and Emissons Exhaust Gas Aftertreatment Systems and Sub Project Leader for the Euro VI aftertreatment systems OM 93x at Daimler AG in Stuttgart (Germany).

DIPL.-ING. MARKUS DIETRICH
is Manager Design Core Engine and Circuits at Daimler AG in Stuttgart (Germany) and was already in charge for the very first concept drafts of the new model series.

COMPLIANCE WITH EURO VI REQUIREMENTS

The introduction of the Euro VI emissions standard brings with it stricter legal limits for NO_x mass and particulate mass (77 and 67 %, respectively). A closed particulate filter becomes necessary due to the additional limitation of the particulate count to 6 x 10^{11}/kWh.

With respect to NO_x aftertreatment via an SCR catalytic converter, implementing and weighing a cold test in the transient WHTC test cycle translates into an additional key challenge. The optimum engine-out emissions level for operating costs as they relate to diesel fuel and AdBlue was determined to range between 3.0 and 4.0 g NO_x/kWh. The SCR catalytic converter designed for this engine-out emissions level then reliably reduces NO_x to below the legal limit. When a cold engine start is carried out, high exhaust gas recirculation rates keep NO_x emissions compliant before the exhaust gas aftertreatment system is fully operative.

CONTROL CONCEPT FOR THE ENGINE AND EXHAUST GAS AFTERTREATMENT SYSTEM

The control concept for the new OM 93x engine model series was designed from the beginning as an integrated system that integrates the engine and exhaust gas aftertreatment (ATS) [1]. The software structure for the engine and ATS electronics is the result of internal development work carried out at Daimler Trucks and safeguards full compliance with the relevant requirements.

New requirements are especially placed on the control concept of the engine with regard to different load states of the particulate filter. The exhaust gas backpressure at full engine load varies depending on the amount of ash and soot in the filter over a range of more than 200 hPa. The exhaust gas recirculation rate required must be regulated precisely and independently of this backpressure. A cascade governor is therefore used on engines of the OM 93x model series. This device first regulates the boost pressure defined by the engine control unit and then maintains the appropriate EGR rate via the EGR valve. The EGR rate is determined indirectly by way of a signal sent by a wideband lambda oxygen sensor mounted at the outlet of the turbine in the exhaust gas turbocharger. This, in turn, ensures a consistent engine-out emissions level, even if the exhaust gas backpressure and ambient conditions fluctuate.

To optimise the correlation between engine and exhaust gas aftertreatment in terms of emissions and operating costs, the engine is operated in different modes, ❶. Transitions occur as a factor of ambient conditions and the current state of exhaust gas aftertreatment. After the cold start, the engine is in operating Mode 1, which focuses on quickly heating the SCR catalytic converter. When operating temperature is reached, Mode 2 is activated to transition to Mode 5, or standard operating mode. When the exhaust gas aftertreatment control unit requires an active regeneration of the diesel particulate filter (DPF), the engine switches to operating mode Mode 3 or Mode 4 as dictated by the state of the exhaust aftertreatment system. These modes allow the exhaust camshaft adjuster to quickly and reliably heat the exhaust gas.

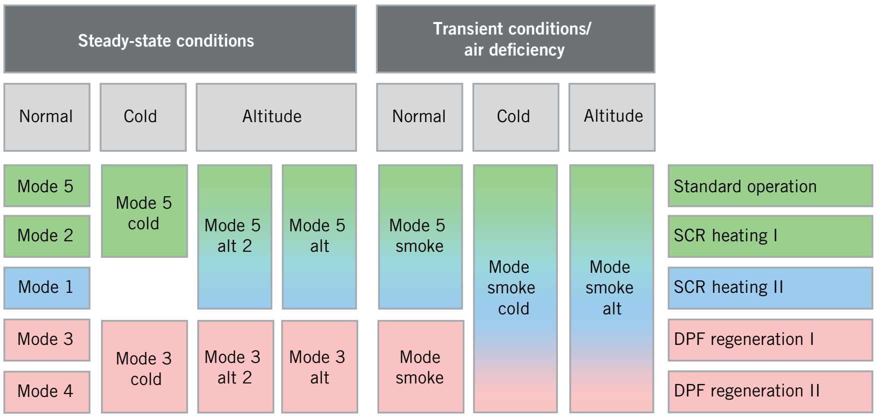

❶ Control concept: possible operating modes of the engine

ON-BOARD DIAGNOSTICS

The Euro VI emissions standard has not only further restricted the limit values and testing procedures for exhaust emissions, but also drastically increased the self-diagnosis requirements for the on-board system. All emissions-relevant components and subsystems must be monitored. Three on-board diagnostics (OBD) monitors used for this purpose will now be explained. The effect of the EGR cooler is monitored by measuring the temperature of the boost air combined with the recirculated exhaust gas. If this temperature exceeds the limit values that apply to the engine in relation to ambient and load conditions, it can be assumed that the cooling effect is insufficient as sensed by the OBD monitor.

The monitor must also detect possible dilution of the diesel exhaust fluid (DEF), which would lead to NO_x emissions of more than 0.9 g/kWh in the WHTC certification cycle. To this end, the signals of both NO_x sensors are used to monitor current NO_x conversion of the exhaust aftertreatment system during operation. If this volume undershoots the relevant threshold value, a software routine carries out a plausibility check for both NO_x sensor signals and evaluates system response to fluctuations in DEF injection quantities to determine whether the decrease in volume can be attributed to componentry (e.g. substrate aging, malfunction of the DEF injection unit) or dilution of the diesel exhaust fluid.

Legislation also requires a function that detects mechanical damage to the DPF (e.g. cracks) leading to a defined loss of pressure drop through the unit. The signals from the pressure sensor

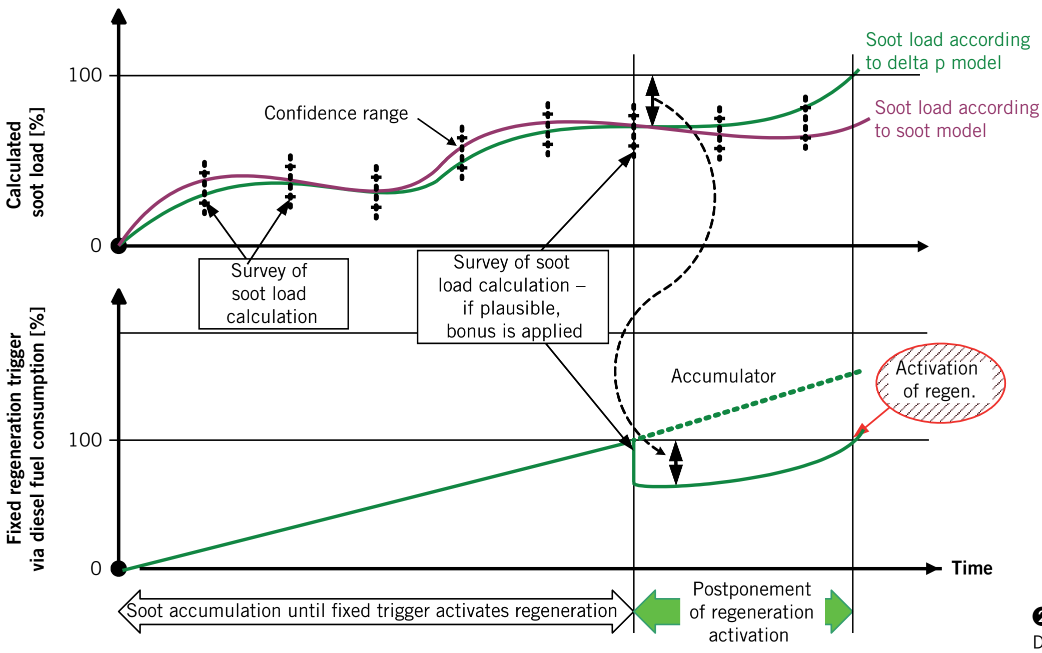

❷ Determination of soot load in the DPF (schematic view)

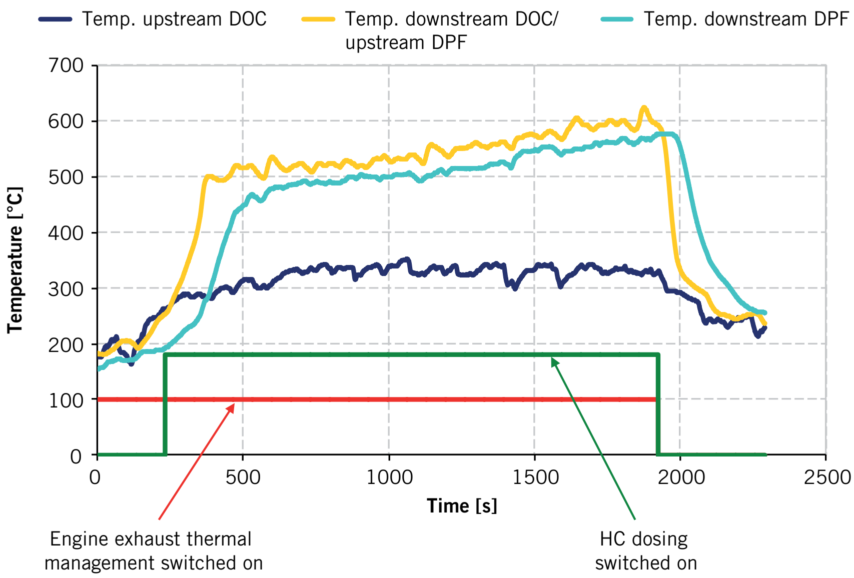

❸ Process of an active DPF regeneration

upstream and downstream of the DPF are leveraged for this purpose, whereby noise from the signals is eliminated by a specially developed software function that is based on the Kalman filter. The usable data that result then serve as a reference point for detecting a problematic filter as mandated.

DPF REGENERATION

Active or forced DPF regeneration should occur as seldomly as possible to optimise fuel consumption and minimise the wear and tear placed on the components of the exhaust aftertreatment system and engine. At the same time, however, steps must be taken to ensure that the DPF is never overloaded with soot in any dynamic load collective. The newly developed regeneration strategy employs three models that work together to determine the level of soot loading in the filter as shown schematically in ❷. The base model calculates the soot accumulation in the DPF as a function of the engine's fuel consumption and does not take into account passive soot burn-off effects. The second model (soot model) factors in the soot emission values relayed by the engine control unit respective of operating conditions involving passive regeneration. The third model (soot delta P) calculates soot loading based on the increase in back pressure created by the DPF.

When the soot estimated by the second and third model lies within a defined confidence interval, a regeneration is only triggered if the result of one of the models exceeds the soot load threshold. Should this load never be exceeded, the purging cycle is automatically triggered after a defined time of operation to pack the ash at the rear of the filter. This is the case with the OM 936 in many common dynamic load collectives and in the WHTC test bench cycle. If the second and third model do not coincide, purging is triggered based on the fuel consumption model.

The engine then switches to an operating mode that increases the exhaust temperature via the light-off temperature of the diesel oxidation catalyst (DOC) under almost all conditions. The HC dosing unit injects diesel fuel into the exhaust flow downstream of the engine to increase the exhaust temperature at the DOC to the level required for soot burn-off.

The regeneration process not only ensures that all soot is incinerated even when the DPF has a high accumulation of the material, but does this while maintaining the applicable limit values for maximum temperatures and gradients. To accomplish this, a model (soot unload model) is used to determine the current level of soot present during active regeneration so that the target regeneration temperature can be adapted as required in real time. The soot burn-off rate varies depending on the temperature, exhaust mass flow rate, and oxygen in the exhaust gas. Combined with different driving profiles, these variables mean that regeneration times are rarely identical. ❸ illustrates the progression of a DPF regeneration cycle in conjunction with the regulated exhaust gas temperature curves.

DEVELOPMENT PROCESS

In order to optimally handle the increasing complexity of the product and achieve excellent reliability (starting with the very first vehicle delivered to a customer) without exceeding planned outlay and scheduling dates, the methods and tools used in the product creation process were also developed further. These efforts paid off, since the new development methods made it possible to optimise the product in a way that had not been possible before.

Orchestrating the complex intricacies of the engine and exhaust aftertreatment system in a target-oriented manner meant that the development procedure had to ensure a high level of accuracy when it came to answering "classic" engine development questions pertaining to the long-term reliability of the base engine and the design of the circulation systems used, for example. The product creation process for the OM 93x model series was based on an evolved, standardised project procedure used at Daimler Trucks. The following highlights those elements that proved to be key success factors as the project was underway.

A-SAMPLE PHASE

Early design concepts were accompanied by broad, iterative use of simulation tools (FEM, MBS, CFD), and the main dimensions established at this time (bore, stroke, cylinder spacing, cylinder head bolting concept, bearing dimensions, arrangement/configuration of the camshafts, layout of the coolant and oil circuits) still apply today.

As initial drafts took shape, extensive outlay was expended to coordinate activities with all vehicle divisions around the world that were planning to use the engine or foresaw application at some point. Technical specifications were then drawn and mutually agreed. Based on these specifications, the CAE front-loading based design work "from the inside out" was supplemented with an opposing draft "from the outside in", which

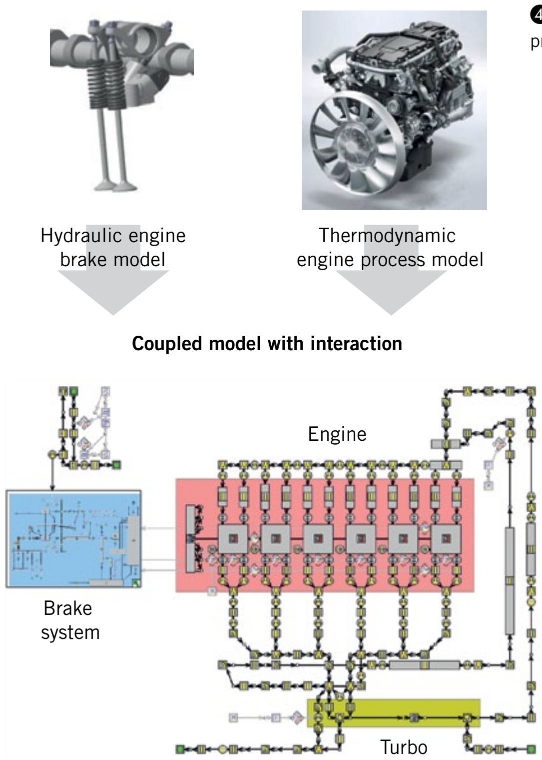

❹ Coupled hydraulics/engine process model

continues to ensure a high usage rate of common parts across a wide range of vehicle applications.

The rigorously pursued CAE front-loading concept, but also the selective usage of A-sample prototype engines allowed the first concepts to be transformed into a stable component design at an early stage. In this context, working with single-cylinder engines proved to be essential to combustion development. Multi-cylinder engines were then used to configure and define overall air management. These activities were also accompanied by 1-D engine process simulations, allowing for a strict limitation of the number of prototype engines. With this approach, combustion-relevant geometry characteristics were already finally established as input parameters for the subsequent sample phase.

B-SAMPLE PHASE

CAE-assisted optimisation was then carried out for all parts to develop a geometrical configuration that largely approaches the level of maturity required for the series product. At this time, the results of initial simultaneous engineering were already factored in (design optimisation with respect to product costs, manufacturing, assembly, servicing, and repair).

The B-samples that crystallised were subsequently tested with a focus on data record application, functional measurements, and verification of the product performance required. Endurance testing of B-sample engines was only carried out to a minimal extent.

C-SAMPLE PHASE

This phase was characterised by safeguarding reliability and durability. Off-tool parts were therefore tested as far as possible. All diecast aluminium components, for example, were already produced with this manufacturing process. The same applied to injection-molded plastic components. Adopting this approach was possible thanks to the binding geometrical stability established with the B-samples. This, in turn, eliminated the need to place further focus on endurance testing in the D-sample phase and greatly reduced the outlay expended at this stage.

D-SAMPLE PHASE

Parts procurement was already handled using production plant processes and was based on parts finally released by product engineering. The D-sample engines assembled under production-like conditions in the engine plant are regarded as “customer-ready”. The D-sample thus primarily serves to promote familiarity with series processes in production and assembly environments. Product engineering tasks are limited to conducting final

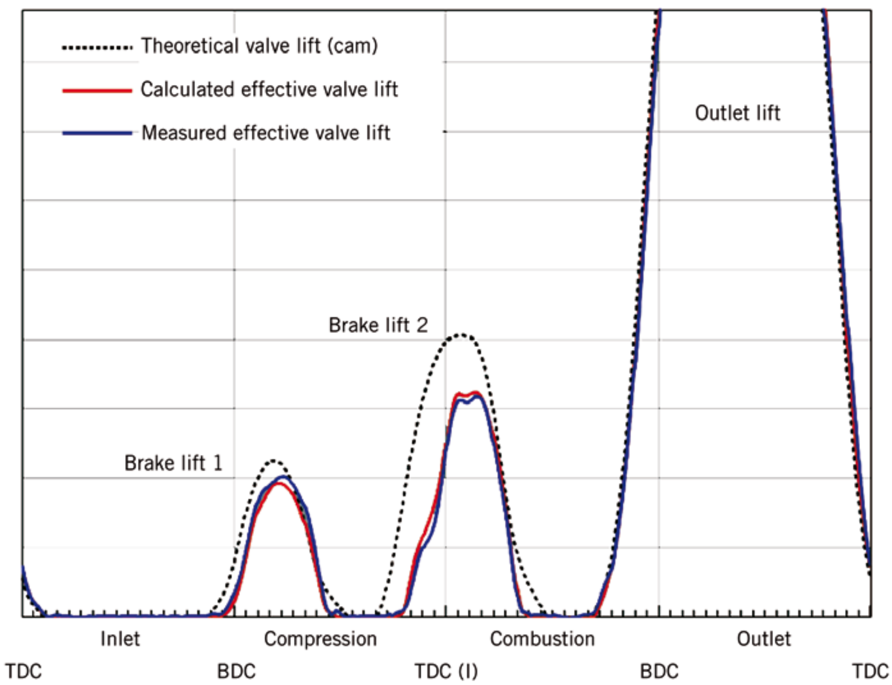

❺ Simulation of the effective outlet valve lift: comparison of numeric analysis and measurement

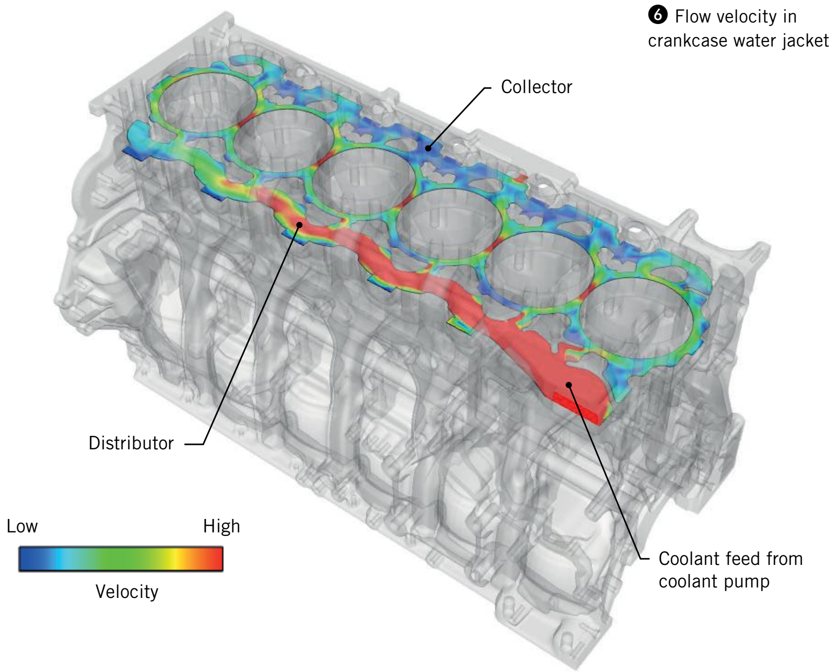

❻ Flow velocity in crankcase water jacket

endurance tests with a few characteristic samples to merely safeguard and confirm the previous results obtained for parts and engines that were made using series processes. The following sections exemplify how the key elements of this procedure were implemented in the development process.

DEVELOPMENT OF THE ENGINE BRAKE SYSTEM

The way the internally developed braking system operates was introduced in [1]. Determining the concept to employ for this system immediately involved quantifying target braking performance in conjunction with the four different turbocharging variants of the engine. To assess also the load-bearing capabilities of the base engine components and to establish the foundation for a regulation concept, a simulation coupling gas dynamics with hydraulics was carried out, ❹. Extensive collaboration between computation, design and testing/application staff allowed a high degree of behavioural accuracy to be determined using this model, ❺. The cam shape was optimised on the computer only and provided for excellent engine braking while maintaining the design limits for in-cylinder pressure.

Based on comprehensive CAE sensitivity studies for the actuating components (waste gate, EGR valve, and exhaust camshaft phaser) the control concept was developed. For this purpose, not only steady-state but also transient situations, such as those in which the engine brake is activated and deactivated, were modelled. The model quality finally allowed populating the calibration maps with data for further turbocharging variants upfront engine testing.

In order to optimise machining tolerances in light of product costs and robust system behaviour, the coupled simulation model was used for assessing the impact of these tolerances. By means of fractional factorial variant matrices and statistical evaluation of the results (DoE method, Design of Experiments) it was possible to investigate a high number of parameters regarding their impact on engine brake power and in-cylinder pressure with limited effort.

COOLING CONCEPT AND DURABILITY OF THE CYLINDER HEAD

The coolant circuit should provide consistent cooling of all cylinders to minimise cylinder distortion and maintain temperature limits for the GJL (standard grey cast iron) cylinder head in particular while using as little power from driving the coolant pump as possible. To this end, concepts were compared and contrasted and a final concept was chosen and subsequently optimised using 3-D flow simulations only. The layout favoured could thus be finalised early on, at the end of the A-sample phase.

The water jacket of the crankcase comprises a distribution and collection facility whose geometry was configured based on CFD simulations, ❻. Transfer ducts on both sides allow the coolant to flow from the crankcase to the cylinder head with two-piece water jacket. The lower water jacket, ❼, has the smallest cross sections near the outlet valve land to achieve high heat convection in this area. The heat dissipation was additionally improved by

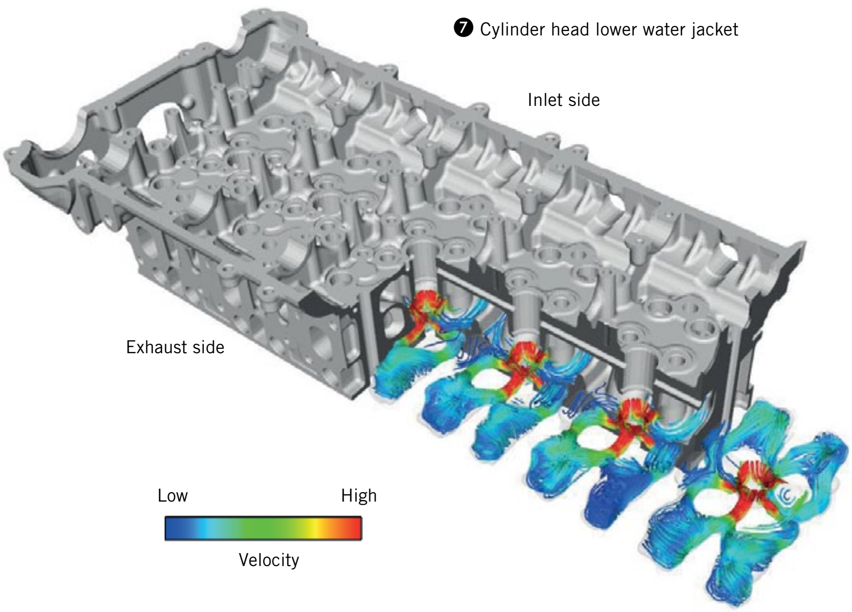

❼ Cylinder head lower water jacket

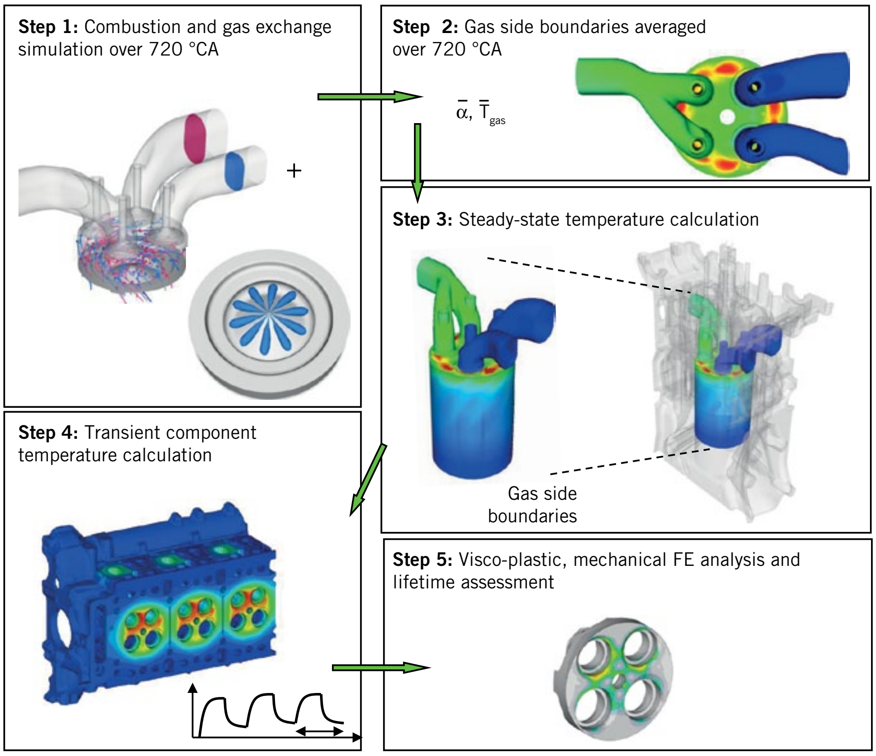

❽ Simulation process of thermo-mechanical strength

allowing nucleate boiling to occur here under full-load conditions.

Coolant then flows along the injector into the upper water jacket, which has large cross sections to realise low pressure loss while functioning as a water-collection facility. At this point, the coolant divides to supply the EGR cooler and the external coolant collection facility of the cylinder head to minimise overall pressure loss.

The maximum temperature of the cylinder barrels was reduced by up to 60 K as compared to the predecessor model series with the help of CFD optimisations. This makes a noteworthy contribution to engine durability. Better, more consistent cooling of the cylinders could also be achieved.

Making a cylinder head able to reliably withstand thermomechanical fatigue (TMF) is a challenge when designing engines with high specific outputs. To verify the durability of a cylinder head, a complex computation method was used, ❽. The first step is to conduct a combustion analysis to calculate the transient gas-specific constraints in the cylinder, which are cycle averaged (step 2 in ⑧) and used together with the heat transfer rates from the aforementioned simulation of the coolant circuit to determine component temperatures in steady-state operating points (step 3 in ⑧). These temperatures are then calculated in transient fashion for the test cycle defined (step 4). Finally, a viscoplastic mechanical FE analysis of the head is carried out with conclusive evaluation of durability.

Reducing the temperature of the cylinder head base plate had the greatest effect on counteracting cracks. The temperatures calculated were validated in a B-sample engine with corresponding instrumentation and optimised on the computer. By minimising the thickness of the base plate and the seat ring, a 30 K reduction of maximum temperatures was achieved. Reducing restraints against thermal expansion further improved durability. The target durability obtained on the computer was subsequently confirmed in endurance thermal shock testing.

DATASET CALIBRATION

The considerable increase in complexity of the new engines and exhaust aftertreatment systems as compared to those of the Euro V era has resulted in control units that monitor ten times the number of applicable parameters. Development times and allocated resources have only increased by a fraction of this magnitude, however. The practice of using DoE test bench software for steady-state mapping has been established for some time. This method was broadly applied to develop the Euro VI systems. Further advanced DoE tools were also used to automatically calibrate functions in transient operation. In the process, standardised, recurring transient states of operation are used to automate a parameter variation and map this to characteristic quantities, which in turn can be optimised using existing DoE techniques for steady-state operation.

For the exhaust aftertreatment system, making optimal use of potentials also requires comprehensive application work. A new strategy was therefore devised to reduce development costs and time. The datasets for the exhaust aftertreatment control unit were populated using a simulation tool developed internally at Daimler AG. Engine test bench operation was then only carried out to validate these records.

❾ exemplifies the simulation results of the temperature gradient in the DPF substrate for the critical moment when the engine drops to idle speed shortly after an active regeneration is triggered with respect to soot loading and the period of time from part-load operation with HC dosing to idling mode. On the test bench,

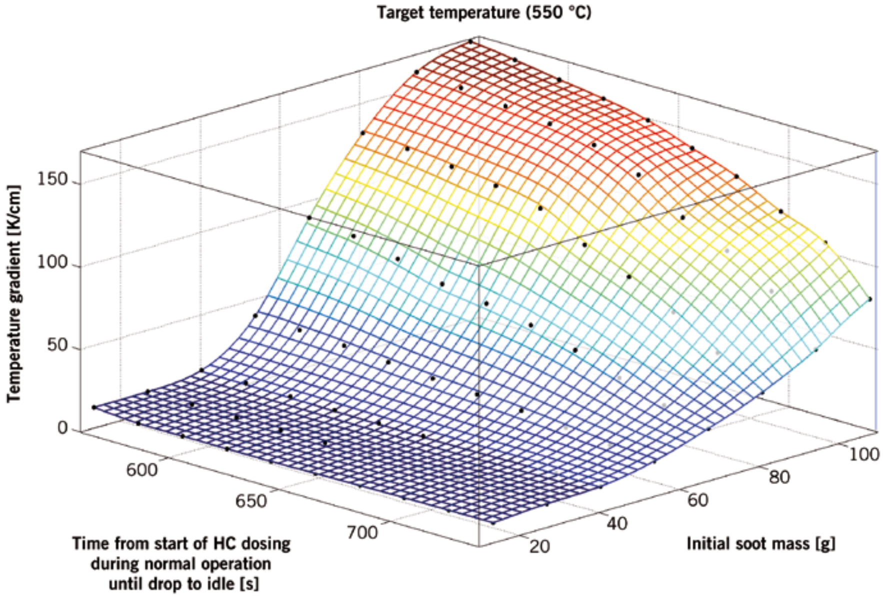

❾ Simulation results drop to idle

the datasets thus created were only validated for compliant soot loading. The same simulation tool was also used for creating the AdBlue dosing pilot control maps and for ageing-related NO_2 formation maps.

SUMMARY

The new OM 93x engine model series was developed by making broad use of modern and newly developed tools and processes. This is exemplified in the engine braking system, cooling circuit and dataset application. A high level of product maturity was reached at production start-up. Success factors that made a key contribution to this outcome include the readiness and openness to engage in productive, interdisciplinary collaboration and the broad application of CAE tools. These enable highly accurate predictions to be made based on experience gained in previous projects and pinpoint comparisons with test results. Further factors leading to success were the targeted further development of CAE tools to answer new questions that arose from the development tasks as well as the early creation of solid design plans and a high level of commitment among everyone involved. On this basis, it was possible to order the production tools at an early stage in order to reach the endurance test fleet (test bench and vehicle) with off-tool parts.

REFERENCE

[1] Herrmann, H.-O.; Nielsen, B.; Gropp, C.; Lehmann, J.: Mercedes-Benz Medium-Duty Commercial Engines – Part 1: Engine Concept and Exhaust Aftertreatment. In: MTZ 73 (2012), No. 10, pp. 4-11

IMPRINT

MTZ WORLDWIDE

www.MTZonline.com

Founded 1939 by Prof. Dr.-Ing. E. h. Heinrich Buschmann and Dr.-Ing. E. h. Prosper L'Orange

Organ of the Fachverband Motoren und Systeme im VDMA, Verband Deutscher Maschinen- und Anlagenbau e.V., Frankfurt/Main, for the areas combustion engines and gas turbines
Organ of the Forschungsvereinigung Verbrennungskraftmaschinen e.V. (FVV)
Organ of the Wissenschaftliche Gesellschaft für Kraftfahrzeug- und Motorentechnik e.V. (WKM)
Organ of the Österreichischer Verein für Kraftfahrzeugtechnik (ÖVK)
Cooperation with the STG, Schiffbautechnische Gesellschaft e.V., Hamburg, in the area of ship drives by combustion engine

11 I 2012 _ November 2012 _ Volume 73
Springer Vieweg I Springer Fachmedien Wiesbaden GmbH
P. O. Box 15 46 · 65173 Wiesbaden · Germany I Abraham-Lincoln-Straße 46 · 65189 Wiesbaden · Germany
Amtsgericht Wiesbaden, HRB 9754, USt-IdNr. DE811148419

Managing Directors Dr. Ralf Birkelbach (Chairman), Armin Gross, Albrecht Schirmacher I **Director Corporate Publishing, Corporate Content & Ad Sales** Armin Gross
Director Marketing & Direct Sales Rolf-Günther Hobbeling I **Director Production** Christian Staral

EDITORS IN CHARGE
Dr. Johannes Liebl, Wolfgang Siebenpfeiffer

EDITOR IN CHIEF
Dr. Alexander Heintzel
phone +49 611 7878-342 · fax +49 611 7878-462
alexander.heintzel@springer.com

VICE EDITOR IN CHIEF
Dipl.-Ing. (FH) Richard Backhaus
phone +49 611 5045-982 · fax +49 611 5045-983
richard.backhaus@rb-communications.de

MANAGING EDITOR
Kirsten Beckmann M. A.
phone +49 611 7878-343 · fax +49 611 7878-462
kirsten.beckmann@springer.com

EDITORIAL STAFF
Dipl.-Ing. (FH) Andreas Fuchs
phone +49 6146 837-056 · fax +49 6146 837-058
fuchs@fachjournalist-fuchs.de
Dipl.-Ing. Michael Reichenbach
phone +49 611 7878-341 · fax +49 611 7878-462
michael.reichenbach@springer.com
Stefan Schlott
phone +49 8726 9675-972
redaktion_schlott@gmx.net
Markus Schöttle
phone +49 611 7878-257 · fax +49 611 7878-462
markus.schoettle@springer.com
Martina Schraad
phone +49 611 7878-276 · fax +49 611 7878-462
martina.schraad@springer.com

PERMANENT CONTRIBUTORS
Andreas Burkert, Prof. Dr.-Ing. Stefan Breuer, Hartmut Hammer, Dipl.-Ing. Ulrich Knorra, Prof. Dr.-Ing. Fred Schäfer, Roland Schedel

ENGLISH LANGUAGE CONSULTANT
Paul Willin

ONLINE I ELECTRONIC MEDIA
Portal Manager Automotive
Christiane Brünglinghaus
phone +49 611 7878-136 · fax +49 611 7878-462
christiane.bruenglinghaus@springer.com
Editorial Staff
Katrin Pudenz M. A.
phone +49 6172 301-288 · fax +49 6172 301-299
redaktion@kpz-publishing.com

SPECIAL PROJECTS
Managing Editorial Journalist
Markus Bereszewski
phone +49 611 7878-122 · fax +49 611 7878-462
markus.bereszewski@springer.com

ASSISTANCE
Christiane Imhof
phone +49 611 7878-154 · fax +49 611 7878-462
christiane.imhof@springer.com
Marlena Strugala
phone +49 611 7878-180 · fax +49 611 7878-462
marlena.strugala@springer.com

ADDRESS
Abraham-Lincoln-Straße 46 · 65189 Wiesbaden
P. O. Box 1546 · 65173 Wiesbaden, Germany
redaktion@ATZonline.de

ADVERTISING

HEAD OF KEY ACCOUNT MANAGEMENT
Tanja Pfisterer

HEAD OF SALES MANAGEMENT
Britta Dolch

SALES MANAGEMENT
Volker Hesedenz
phone +49 611 7878-269 · fax +49 611 7878-78269
volker.hesedenz@best-ad-media.de

MEDIA SALES
Frank Nagel
phone +49 611 7878-395 · fax +49 611 7878-78395
frank.nagel@best-ad-media.de

KEY ACCOUNT MANAGEMENT
Rouwen Bastian
phone +49 611 7878-399 · fax +49 611 7878-78399
rouwen.bastian@best-ad-media.de

DISPLAY AD MANAGER
Petra Steffen-Munsberg
phone +49 611 7878-164 · fax +49 611 7878-443
petra.steffen-munsberg@best-ad-media.de

AD PRICES
Advertising ratecard from October 2011

MARKETING I OFFPRINTS

PRODUCT MANAGEMENT AUTOMOTIVE MEDIA
Sabrina Brokopp
phone +49 611 7878-192 · fax +49 611 7878-407
sabrina.brokopp@springer.com

OFFPRINTS
Martin Leopold
phone +49 2642 907-596 · fax +49 2642 907-597
leopold@medien-kontor.de

PRODUCTION I LAYOUT
Heiko Köllner
phone +49 611 7878-177 · fax +49 611 7878-78177
heiko.koellner@springer.com

SUBSCRIPTIONS
Springer Customer Service Center GmbH
Haberstraße 7 · 69126 Heidelberg · Germany
phone +49 6221 3454-303 · fax +49 6221 3454-229
Monday to Friday, 8 a.m. to 6 p.m.
springervieweg-service@springer.com

SUBSCRIPTION CONDITIONS
The eMagazine appears 11 times a year at an annual subscription rate 199 € for private persons and 299 € for companies. Special rate for students on proof of status in the form of current registration certificate 98 €. Special rate for VDI/ÖVK members on proof of status in the form of current member certificate 172 €. Special rate for studying VDI members on proof of status in the form of current registration and member certificate 71 €. Annual subscription rate for combination MTZworldwide (eMagazine) and MTZ (print) 398 €. All prices include VAT at 7%. Every subscription comes with access to the ATZonline archive. However, access is only available for the individual subscription holder. To obtain access for your entire company/library/organisation, please contact Rüdiger Schwenk (ruediger.schwenk@springer.com or phone +49 611 7878-357).

YOUR HOTLINE TO MTZ

Editorial Staff
☎ +49 611 5045982
Customer Service
☎ +49 6221 3454-303
Advertising
☎ +49 611 7878-395

The subscription can be cancelled in written form at any time with effect from the next available issue.

HINTS FOR AUTHORS
All manuscripts should be sent directly to the editors. By submitting photographs and drawings the sender releases the publishers from claims by third parties. Only works not yet published in Germany or abroad can generally be accepted for publication. The manuscripts must not be offered for publication to other journals simultaneously. In accepting the manuscript the publisher acquires the right to produce royalty-free offprints. The journal and all articles and figures are protected by copyright. Any utilisation beyond the strict limits of the copyright law without permission of the publisher is illegal. This applies particularly to duplications, translations, microfilming and storage and processing in electronic systems.

PEER REVIEW

PEER REVIEW PROCESS FOR RESEARCH ARTICLES IN ATZ, MTZ AND ATZ ELEKTRONIK

Scientific articles of universities in ATZ Automobiltechnische Zeitschrift, MTZ Motortechnische Zeitschrift and ATZelektronik are subject to a proofing method, the so-called peer review process. Articles accepted by the editors are reviewed by experts from research and industry before publication. For the reader, the peer review process further enhances the quality of the magazines' content on a national and international level. For authors in the institutes, it provides a scientifically recognised publication platform.

In the Peer Review Process, once the editors has received an article, it is reviewed by two experts from the Advisory Board. If these experts do not reach a unanimous agreement, a member of the Steering Committee acts as an arbitrator. Following the experts' recommended corrections and subsequent editing by the author, the article is accepted.

In 2008, the peer review process utilised by ATZ and MTZ was presented by the WKM (Wissenschaftliche Gesellschaft für Kraftfahrzeug- und Motorentechnik e. V./German Professional Association for Automotive and Motor Engineering) to the DFG (Deutsche Forschungsgemeinschaft/German Research Foundation) for official recognition. ATZelektronik participates in the Peer Review since 2011.

AUTHORS

DR. CHRISTIAN GERHART
is Coordinator of the Project Nora in the Division New Business at AlzChem AG in Trostberg (Germany).

DR. BERND SCHULZ
is Head of the Laboratory Research & Development at NIGU Chemie GmbH in Waldkraiburg (Germany).

DR. OLIVER KRÖCHER
is Head of the Laboratory for Bioenergy and Catalysis at the Paul Scherrer Institute in Villigen (Switzerland).

DIPL. CHEM. DANIEL PEITZ
is Research Fellow at the Laboratory for Bioenergy and Catalysis at the Paul ScherrerInstitut in Villigen (Switzerland).

DR. RER. NAT. EBERHARD JACOB
is Managing Director of Emissionskonzepte Motoren in Krailling (Germany).

SELECTIVE CATALYTIC REDUCTION OF NITROGEN OXIDE – PART 1: FORMATES AS AMMONIA STORAGE COMPOUNDS

The application of selective catalytic reduction (SCR) technology found unexpectedly broad diffusion in the exhaust gas after-treatment of lean-burning engines due to the potential advantage in fuel economy. However, a shadow is falling on the most frequently employed reducing agent aqueous urea solution (AUS): insufficient low temperature stability, limited shelf-life and the formation of solid decomposition products hamper its utilisation. At the Paul Scherrer Institute, alternatives to urea were investigated and, using a novel bifunctional gold-catalyst on TiO_2-basis, decisive improvements were made concerning their application.

THE SEAL OF APPROVAL FOR SCIENTIFIC ARTICLES IN MTZ.
MTZ
PEER REVIEW
RECEIVED 2011-12-28
REVIEWED 2012-02-02
ACCEPTED 2012-08-13
REVIEWED BY EXPERTS FROM RESEARCH AND INDUSTRY.

1 COMPARISON OF DIFFERENT AMMONIA STORAGE COMPOUNDS

1.1 UREA-DERIVATIVES

Eutectic mixture of aqueous urea solution (AUS 32.5 %) is commonly used in SCR applications.Worldwide supply chain is well established for the standardised versions AdBlue (Europe), DEF (North America) or ARLA32 (Brazil) – but unfortunately with some restrictions for practical use specially concerning solid residues from decomposition and cold and warm stability of the formulation from ISO 22241. Solid residues in the exhaust system could be avoided by the use of a hydrolysis catalyst, as for the extension of the working temperature range alternatives are still under development. The most prominent alternatives are summarised in ❶ and are widely described [1].

To increase the freezing stability of AUS32.5, a commercial formulation of aqueous urea solution with additive of ammonium formate (AmFo) is available known as Denoxium. This solution is out of spec due to ISO 22241 but lower freezing temperatures could be achieved and therefore it better fits to winter conditions. Unfortunately, AmFo is corrosive. It heavily corrodes ferritic chrome steel in a very short period. This is due to the fact that AmFo easily decomposes to ammonia (NH_3) and formic acid (HCOOH). HCOOH is highly corrosive by destruction of passivating layers on metal surfaces.

Replacing NH_3 by a very strong base, such as Guanidine $(NH_2)2C{=}NH$, results in a stable, highly soluble and non-toxic salt, ① (top right). Tests with aqueous Guanidinium Formate (GuFo) solution have shown no corrosive activity such as on ferritic chrome steel (1.4509 und 1.4512), used for dosing units and exhaust systems. In a long-term test different stainless steel samples had been exposed twelve month to solution of GuFo60 (60 % GuFo in water) at 50 °C. At the probe,neither an optical change at the surface nor a mass reduction could be monitored. Additionally no components of the alloy could be detected in the solution. As expected, no corrosion could be found at austenite chrome steel.

1.2 FORMULATIONS

The solubility of GuFo is extraordinary with about 6.2 kg per 1 l in water at room temperature. Moreover, crystallisation behaviour by drying AUS32 could not be seen for GuFo. Hygroscopicity of dry GuFo is very high, therefore originally dried GuFo salt will get liquid again just by uptake of ambient humidity, ❷ (left).

GuFo could also be mixed in a wide range with aqueous urea. The resulting ternary formulation of GuFo, urea and water could be trimmed to different cold stabilities. Less water in the solution and therefore increased total concentration result in a relatively high NH_3 release potential per litre. ② (right) shows an overview of different mixtures with each freezing point and NH_3 release potential. In the same manner by 1:1 mixture of AUS32.5 with a kind of antifreezing additive – high concentrated GuFo74/3 formulation (74 % GuFo, 3 % urea) – a freezing stable mixture of GuFo37/18 for winter application could be formulated. Additionally the NH_3 release potential would be increased by 65 % in comparison to AdBlue.

Unlike AUS32.5, GuFo solutions could be extremely supercooled, far below the thermodynamically stable point of freezing without showing crystals. That is why a new method for detection of cold stability has been developed. The measurement of the cold stability of fuels for winter applications is done classical by CFPP test (Cold Filter Plugging Point, due to DIN EN 116) showing -40 °C for a GuFo41/16 (41 % GuFo, 16 % urea) solution. The thermodynamically stable crystallisation point for this mixture is already at -18 °C. The potential for supercooling is also shown by measurements with dynamic scanning calorimetry (DSC) resulting in a freezing point

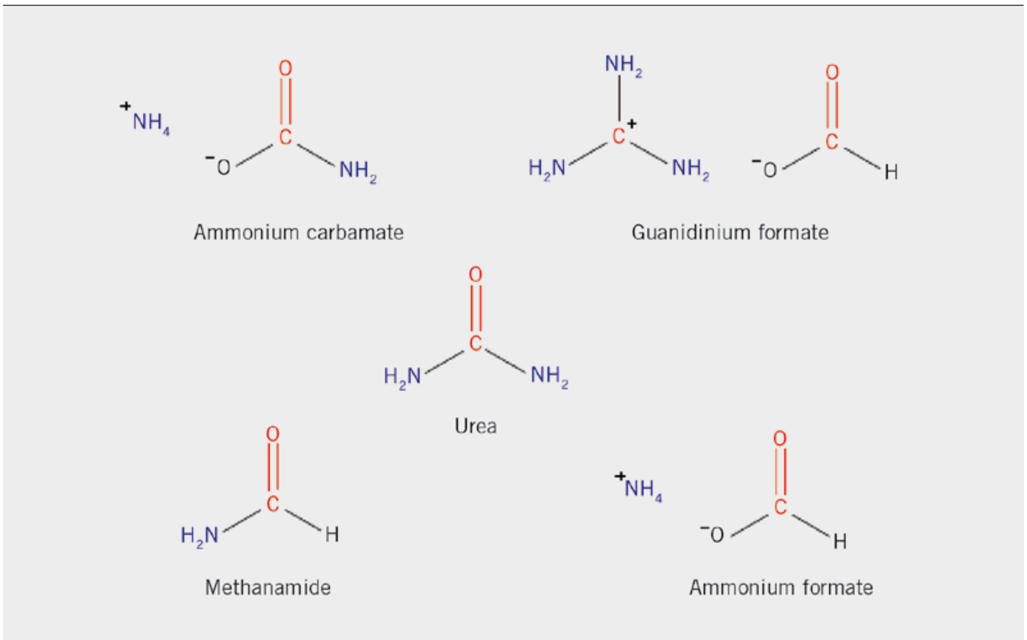

❶ Ammonia precursor for SCR-Applications with different molecular structure and N-content (the molecular part for ammonia storage is blue, carbon structure is red)

FORMULATION	MIXTURE [%]			TEMPERATURE STABILITY		NH_3–CAPACITY	
	UREA	GUFO	H_2O	MELTING POINT [°C]	BOILING POINT [°C]	KG/KG	KG/L
AUS32.5/ADBLUE	32.5	–	67.5	-11.5	Decomposition	0.18	0.20
GUFO60	–	60	40	-5	~105	0.29	0.34
GUFO37/18	18	37	45	-28		0.28	0.33
GUFO43/19	19	43	38	-11		0.32	0.38

❷ Humidity uptake of Guanidinium Formate (GuFo) from left to right within 3 h just (left) and comparison of different ASC formulations from aqueous urea and guanidinium formate (right)

of -46.2 °C for GuFo60 and a melting point of -19.08 °C. The stable crystallisation point for GuFo60 is actually around -5 °C.

For detecting the thermodynamically stable crystallisation point specific actions have to be taken. Shaking, stirring or scratching at the walls or even some solid contaminations do not lead in any case to a stable crystallisation in GuFo solutions. That is why only additionally seeding with crystals from an in advance frozen solution of the same concentration will be applied as a secure method. Only in this case crystallisation under all circumstances could be achieved. A solution had been defined as "frozen" if optically a first clouding could be detected. All results for freezing point in ② (right) are temperatures achieved by autologous seeding at the point of first undissolving crystals in the solution. The melting point is defined analogue as temperature at the point of last crystals totally dissolved. This is the fixed maximum criteria for cold stability or freezing point. By this method, a Denoxium-30 formulation has a freezing point of -25 °C.

Another advantage of GuFo solutions is the stability at elevated temperatures. ❸ shows a comparison between a GuFo60 solution and a classical AUS32.5. To simulate long-term stability within a few days – in a typical deterioration test –, for both solutions the pressure at elevated temperature (80 °C) has been measured. GuFo60 shows clearly a less steeper increase in pressure than AUS32.5 and therefore a clearly improved warm stability.

1.3 FURTHER PROPERTIES

Further differences between aqueous AUS32.5 and GuFo solutions could be found in ❹. Dilation at freezing of GuFo solution is

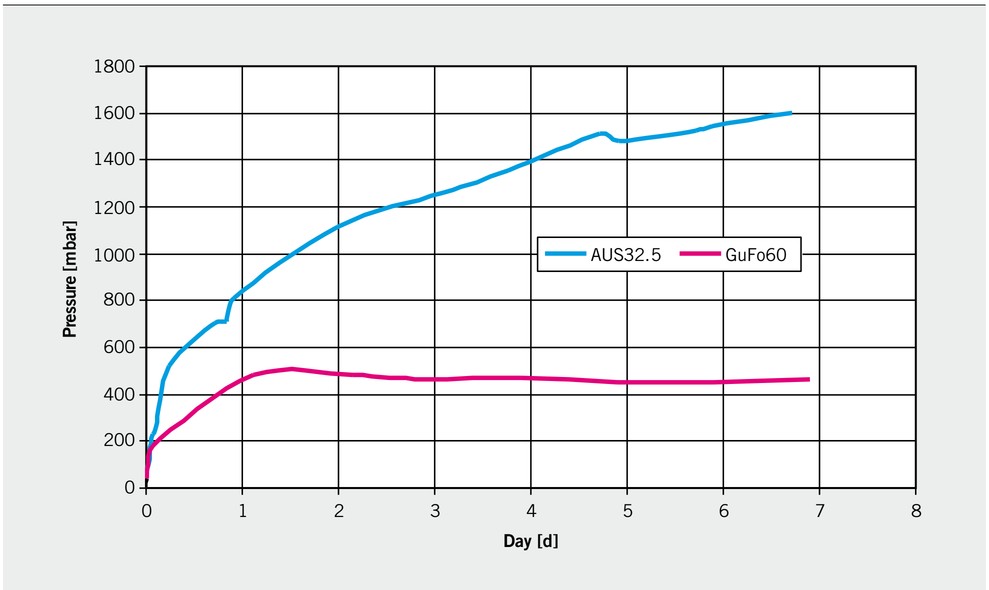

❸ Long-term stability of AUS32.5 and GuFo60 at 80°C for several days

PARAMETER	GUFO60	GUFO38/15	AUS32.5
Volume dilation factor at 30 °C [1/K]	0.000473079	0.0004788	0.0004705
Volume dilation factor phase change	-2 %	+2 %	+7 %
Viscosity [cP] at 20 °C	5	4	1.4
Surface tension [10-3 N/m] at 20 °C	64.7	61.7	65
Electrical conductivity [mS/cm]	117	105	1.97
Specifi heat capacity Cp (*T*) at 20 °C [J/g K]	2.7	2.87	3.5
Melting enthalpy [J/g]	210.7	203.5	270
Vapour pressure [hPa] at 40 °C	40	47	70

❹ Physical properties of GuFo solutions in comparison with AUS32.5. (GuFo38/15 = 38 % Guanidinium Formate with 15 % urea)

less due to the lower water content. In comparison with AUS32.5, containing non-dissociated urea, the high conductivity of aqueous GuFo salt is remarkable. Additionally the vapour pressure of GuFo60 is clearly below AUS32.5. The required enthalpy for total decomposition of GuFo60 respectively AUS32.5 to ammonia gas is a sum of energy changes by heating up from ambient temperature inclusive phase change and the actual reaction enthalpy. Due to less water content in GuFo60, the required total enthalpy is clearly below the one of AUS32.5, ❺. However for complete, residue-free decomposition a higher temperature level is required.

2 INVESTIGATIONS CONCERNING THE RELEASE OF NH_3 FROM ASC

Aqueous solutions of formats or formulations with urea have obviously benefits compared to urea solutions, due to a higher release potential of NH_3 and a better stability of the solution at low or high temperature [1]. However, besides the physicochemical properties of the solutions, the side-product free release of NH_3 in the target application remains one of the most important criteria for the application of ASC. The nitrogen bound in ASC should be released as NH_3, while the carbon should be released as harmless CO_2.

2.1 EXPERIMENTAL SETUP

For the investigation of the catalytic decomposition of formate-based ASC, a laboratory scale test rig was utilised [2]. In this setup, solutions of ASC were sprayed on decomposition catalysts by a micro-two-fluid nozzle. Experiments were performed with model gases, whose composition could be changed according to the later application, and which was heated to the desired temperature. The gaseous decomposition products released during decomposition were continuously analysed via a Fourier-transform infrared-spectrometer. In addition, aerosols and higher-molecular compounds could be washed out with an absorption solution and quantified by means of high-pressure liquid chromatography. An overview of the experimental setup is shown in ❻.

2.2 RESULTS AND DISCUSSION

In formate compounds like AmFo or GuFo, NH_3 is completely released from the ammonium- or guanidinium-cation. After the release of NH_3, formic acid (HCOOH) results from the formate-anion [3]. It thermolyses to CO and H_2O or catalytically decomposes to CO_2 and H_2. HCOOH can react with NH_3, releasing water, to yield methanamide (MA, common name: formamide), which is teratogenic and, therefore, classified as toxic. MA can further dehydrate to hydrogen cyanide (HCN), which is a very toxic compound. The described chemical reactions are depicted in, ❼ [4].

Around 180 °C at the latest, AmFo will be completely decomposed into its dissociation products NH_3 and HCOOH [5]. While this is advantageous for the release of the stored NH_3 from the ASC, all the reactants for the side reactions depicted in ⑦ are thereby provided. As AmFo is injected into the main exhaust gas flow upstream of the SCR catalyst, the decomposition can only be performed on the SCR catalyst. As the catalyst is not active for HCOOH decomposition, the reaction does not proceed catalytically but solely thermal. At temperatures above 300 °C at the latest, HCOOH will completely decompose to CO and H_2O, but below this temperature the decomposition will be increasingly incomplete. As a result, one can measure emissions of MA and HCN below 300 °C [6].

In general, GuFo behaves similarly to AmFo,so the complete decomposition without residues of GuFo was only investigated on hydrolysis and not on SCR catalysts [7]. In ❽ (top left and right) the temperature-dependent decomposition of GuFo60 on titaniumdioxide (anatase) is shown. At temperatures above 260 °C and low *GHSV*< 20,000/h, the guanidinium-cation released more than 98 % of the stored NH_3. It can also be observed that HCOOH is not yet fully decomposed to CO at 260 °C. Insufficiently decomposed HCOOH in combination with the high concentrations of NH_3 leads to the formation of MA and HCN [6]. Ideally, HCOOH should be decomposed on the catalyst before it could react with NH_3.

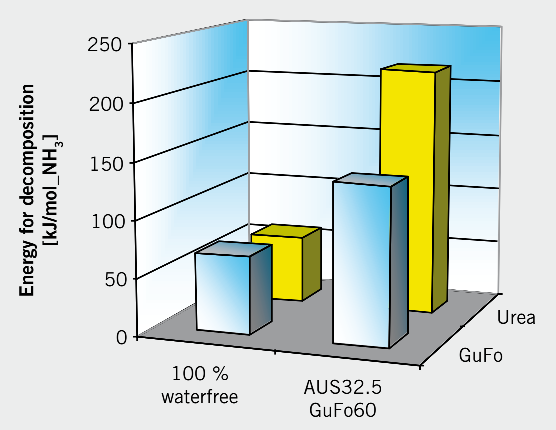

❺ Enthalpy per generated mol NH_3 for total decomposition of the precursor to ammonia inclusive heating up to reaction temperature

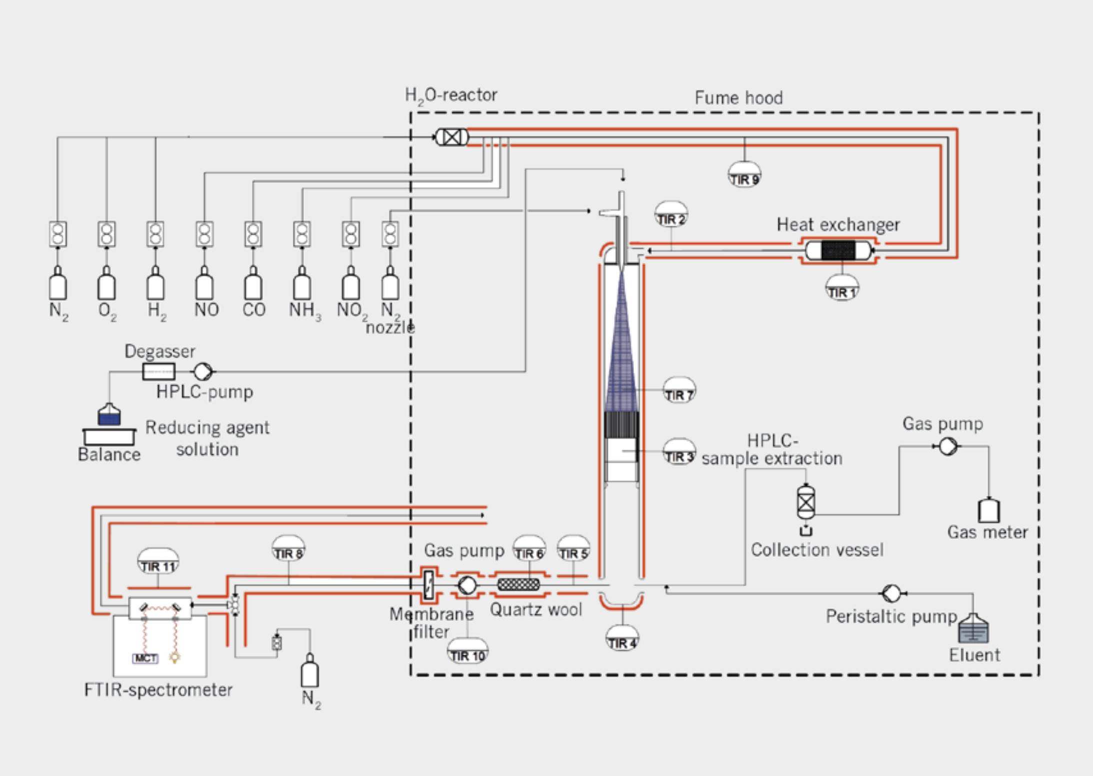

❻ Experimental setup for the investigation of different ASC regarding their decomposition on hydrolysis catalysts

This would eliminate the emission of corrosive HCOOH and its undesired side products. Optimally, HCOOH decomposition would lead to CO_2 rather than CO. Indeed, several catalysts for the conversion of HCOOH to CO_2 are known in [8, 9], amongst others, even typical oxidation catalysts could be used. However, such catalysts would also oxidise the released NH_3. A suited decomposition catalyst must selectively decompose HCOOH, without showing activity for the NH_3 oxidation. Regarding these special requirements, gold, supported on TiO_2 (anatase) proved to be surprisingly well suited. The TiO_2 support enabled hydrolysis of the guanidinium-cation to NH_3, while the additional noble metal gold catalysed the formate decomposition in order to avoid HCOOH and its side products.

In ⑧ (bottom) the reaction products of the decomposition of GuFo60 on a 1.5 % Au/TiO_2 catalyst are shown in dependency of the temperature. This time, the NH_3 yield reached a value of above 98 % already beginning at 250 °C. Much more striking was the absence of CO and HCOOH, as those were completely converted to CO_2. As expected, this led to a complete suppression of MA and HCN formation down to 220 °C. The theoretically possible oxidation of NH_3 by gold was negligible, as the NH_3 yield was practically 100 %. At temperatures >220 °C the observed results of the

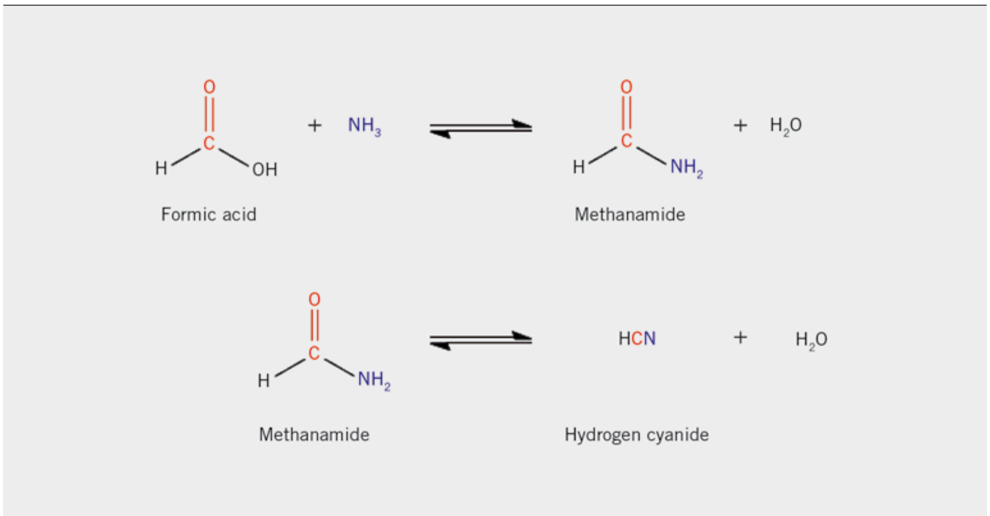

❼ Formation of methanamide and hydrogen cyanide from formic acid and ammonia catalytic decomposition of GuFo can be described by the reaction Eq. 1:

EQ. 1

$$C(NH_2)_3HCO_2 + 2\ H_2O \rightarrow 2\ CO_2\ +\ 3\ NH_3 + H_2$$

The primarily produced hydrogen is probably oxidised on the gold catalyst to yield H_2O. For real-life applications, besides the activity also the long-term stability of the catalyst is important. Thus, the two most important aging mechanisms in exhaust gas aftertreatment systems were evaluated – hydrothermal aging and catalyst poisoning by sulfatisation. Since long-term tests could not be conducted, hydrothermal aging procedures with subsequent experiments were performed instead. In ❾ the results of the measurements are compared.

At first sight, ⑨ shows that unlike TiO_2 the Au-doped catalyst does not produce CO, HCOOH, MA or HCN even in its aged state. Additionally, possible oxidation products of NH_3 are plotted. The sum of NO, NO_2 and N_2O emissions was less than 0.5 % of the expected NH_3 yield, and, thus, comparable to the results with TiO_2. In summary, the catalyst showed an extraordinary high stability towards hydrothermal aging at an operation temperature of 250 °C.The stability versus sulfatisation was tested by exposing the catalyst to a gas flow containing 200 ppm of SO_2 at a temperature of 400 °C for 6 h. Afterwards, the conversion of GuFo60 was determined again, ❿. The results show that the NH_3 yield at 250 °C remained above 98 %, whereas the CO_2 yield decreased in this temperature range. At high temperatures, HCOOH was preferably dehydrated to CO, but at low temperatures, HCOOH could be monitored.

3 SUMMARY AND OUTLOOK

Both, GuFo and AmFo are completely decomposable to NH_3 in an exhaust gas side stream at moderate space velocities and at a temperature of 250 °C on an Au/TiO_2 catalyst, without the formation of undesired side products. A complete and residue-free decomposition is possible under controlled and with these investigations defined conditions in a thermal stabilised side-stream reactor. The gained catalyst knowhow was transferred within the

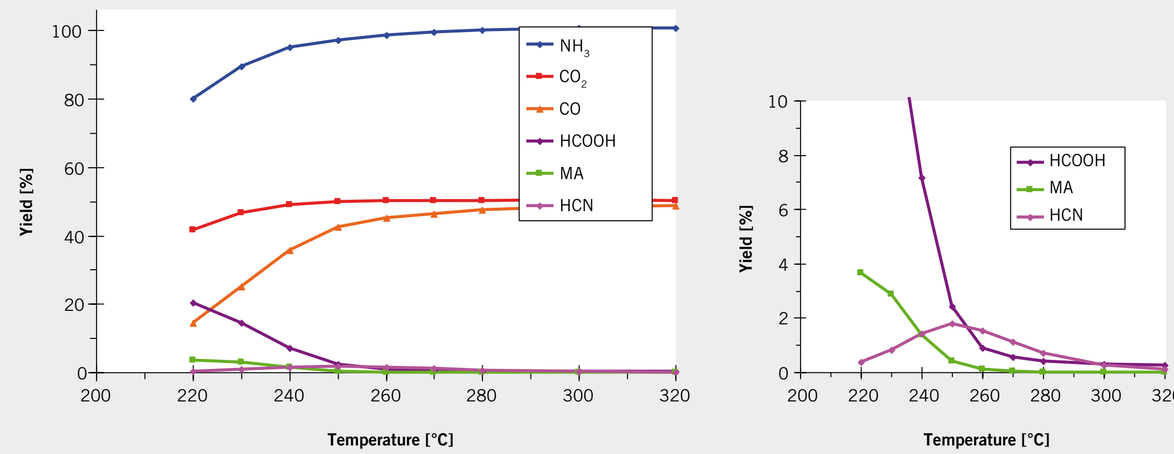

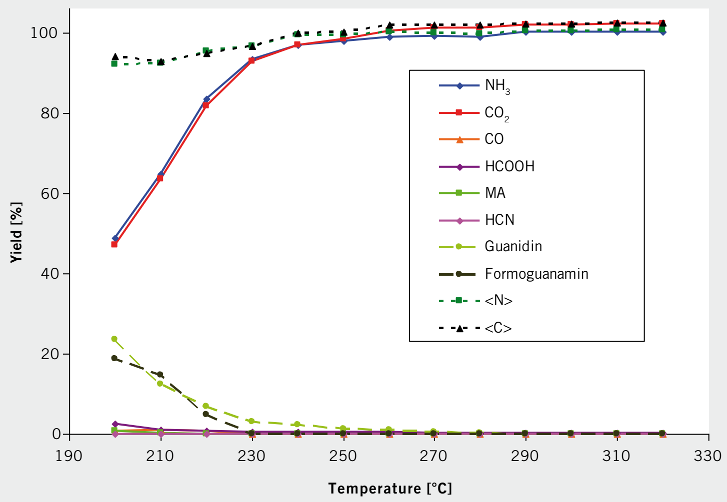

❽ GuFo60 decomposition (top left and right) on a TiO_2 (anatase) catalyst (GHSV = 15,900/h; carrier gas: 5 % H_2O, 10 % O_2, 85 % N_2; feed rate GuFo60: 3 g/h); GuFo60 decomposition (bottom) on a 1.5 % Au/TiO_2 catalyst (GHSV = 14,900/h; carrier gas: 5 % H_2O, 10 % O_2, 85 % N_2; feed rate GuFo60: 3 g/h)

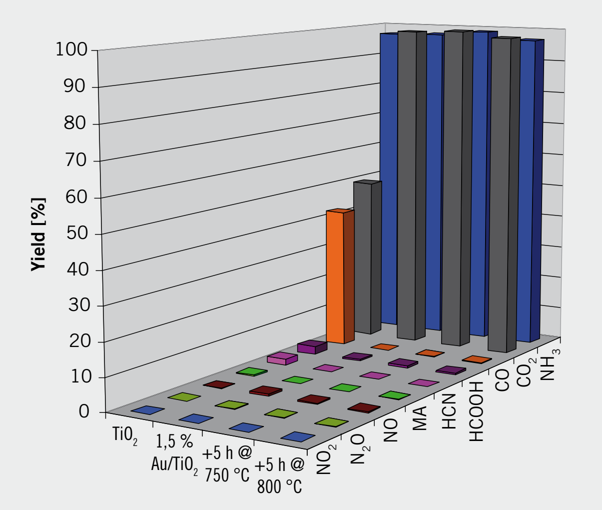

❾ Yields of gaseous reaction products at 250 °C during decomposition of GuFo60 on TiO_2, same conditions as in ⑧ (bottom) – Au/TiO_2, Au/TiO_2 aged at 750 °C for 5 h and Au/TiO_2 additionally aged at 800 °C for 5 h

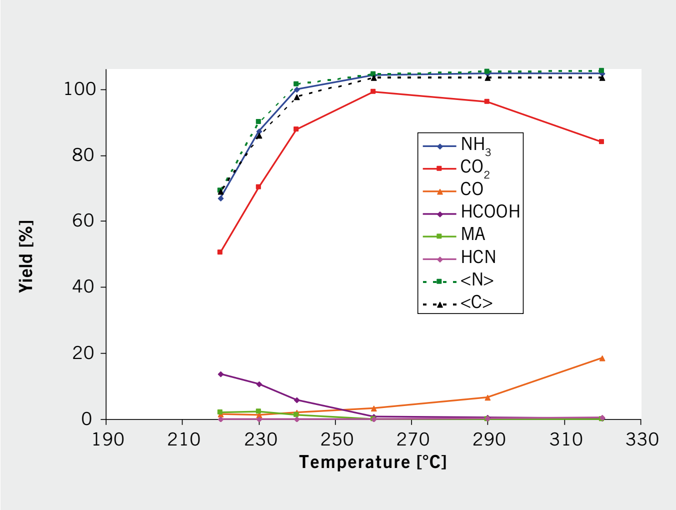

❿ GuFo60 decomposition on a 1.0 % Au/TiO_2 catalyst after aging with 200 ppm SO_2 at 400 °C for 6 h (GHSV = 19,100/h;carrier gas: 5 % H_2O, 10 % O_2, 85 % N_2, feed rate GuFo60: 3 g/h)

research project to the TU Munich, where it was used to set up a practice-relevant ammonia generator. This system will be presented in the second part of this report in MTZ 12/2012.

REFERENCES

[1] Kröcher, O.; Elsener, M.; Jacob, E.: New reducing agents for the low-NO_x SCR technology. 5th International Exhaust Gas and Particulate Emissions Forum, 19./20. February 2008, Ludwigsburg

[2] Peitz, D.; Bernhard, A.; Elsener, M.; Kröcher, O.: Laboratory test reactor for the investigation of liquid reducing agents in the selective catalytic reduction of NO_x. In: Rev. Sci. Inst. (2011), no. 82, 084101

[3] Todorova, T.; Peitz, D.; Kröcher, O.; Wokaun, A.;Delley, B.: Guanidinium Formate Decomposition on the (101) TiO_2-Anatase Surface: Combined Minimum Energy Reaction Pathway Calculations and Temperature-Programmed Decomposition Experiments. In: J. Phys. Chem. C (2011), no. 115, pp. 1195-1203

[4] Kröcher, O.; Elsener M.: Hydrolysis and oxidation of gaseous HCN over heterogeneous catalysts. In: Appl. Catal. B 2009, no. 92, pp. 75-89

[5] N. N.: PubChem database of NCBI. CAS-Nr. 540-69-4, http://pubchem.ncbi.nlm.nih.gov

[6] Kröcher, O.; Elsener, M.; Jacob, E.: A model gas study of ammonium formate, methanamide and guanidinium formate as alternative ammonia precursor compounds for the selective catalytic reduction of nitrogen oxides in diesel exhaust gas. In: Appl. Catal. B (2009), no. 88, p. 6682

[7] Kröcher, O.; Elsener, M.; Jacob, E.: Neue Reduktionsmittel für die LowNO_x-SCR-Technik. 5. Int. Forum Abgas- und Partikel-Emissionen, 19./20. February 2008, Ludwigsburg

[8] Boddien, A.; Mellmann, D.; Gartner, F.; Jackstell, R.; Junge, H.; Dyson, P. J.; Laurenczy, G.; Ludwig, R.; Beller, M.: Efficient Dehydrogenation of Formic Acid Using an Iron Catalyst. In: Science (2011), no. 333, pp. 1733-1736

[9] Bulushev, D. A.; Beloshapkin, S.; Ross, J.R.H.: Hydrogen from formic acid decomposition over Pd and Au catalysts Catal. In: Today (2010), no. 154, pp. 7-12

THANKS

The results of this work were obtained within the framework of the BFS research project Nora (NO_x reduction in engine exhaust gas using guanidiniumsalts). The Bavarian Research Foundation is gratefully acknowledged for their generous funding of the Nora project for three years. In addition, the work was supported with catalysts and coatings of the companies Cristal Global, Emitec, Alantum, Interkat and Süd-Chemie, which are hereby also acknowledged.This system will be presented in the part II of these article.